ISTANBUL TECHNICAL UNIVERSITY ★ GRADUATE SCHOOL OF SCIENCE ENGINEERING AND TECHNOLOGY

LONG TERM DEFORMATION AND EARTHQUAKE HISTORY OF THE OVACIK FAULT (EASTERN TURKEY): IMPLICATIONS AND CONTRIBUTIONS TO THE INTRA-PLATE DEFORMATION OF ANATOLIA

M.Sc. THESIS

Müge YAZICI

Department of Geological Engineering

Geological Engineering Programme

JUNE, 2018

ISTANBUL TECHNICAL UNIVERSITY ★ GRADUATE SCHOOL OF SCIENCE ENGINEERING AND TECHNOLOGY

LONG TERM DEFORMATION AND EARTHQUAKE HISTORY OF THE OVACIK FAULT (EASTERN TURKEY): IMPLICATIONS AND CONTRIBUTIONS TO THE INTRA-PLATE DEFORMATION OF ANATOLIA

M.Sc. THESIS

Müge YAZICI
505151313

Department of Geological Engineering

Geological Engineering Programme

Thesis Advisors: Prof. Dr. Boris A. NATALIN
Thesis Co-Advisor: Dr. Öğr. Üyesi Cengiz ZABCI

JUNE, 2018

ISTANBUL TEKNİK ÜNİVERSİTESİ ★ FEN BİLİMLERİ ENSTİTÜSÜ

OVACIK FAYI'NIN UZUN SÜRELİ DEFORMASYONU VE DEPREM TARİHÇESİ: ANADOLUNUN LEVHA-İÇİ DEFORMASYONUNA ETKİSİ VE KATKISI

YÜKSEK LİSANS TEZİ

Müge YAZICI
505151313

Jeoloji Mühendisliği Anabilim Dalı

Jeoloji Mühendisliği Programı

Tez Danışmanları: Prof.Dr. Boris A. NATALIN
Eş Danışman: Dr. Öğr. Üyesi Cengiz ZABCI

HAZİRAN 2018

Müge YAZICI, a M.Sc student of İTÜ Graduate School of Science Engineering and Technology student ID 505151313, successfully defended the thesis/dissertation entitled "LONG TERM DEFORMATION AND EARTHQUAKE HISTORY OF THE OVACIK FAULT (TURKEY): IMPLICATIONS AND CONTRIBUTIONS TO THE INTRA-PLATE DEFORMATION OF ANATOLIA", which she prepared after fulfilling the requirements specified in the associated legislations, before the jury whose signatures are below.

Thesis Advisor :	**Prof.Dr. Boris A. NATALIN** ISTANBUL Technical University	.....
Co-advisor :	**Dr.Öğr.Üy. Cengiz ZABCI** ISTANBUL Technical University	.....
Jury Members :	**Prof.Dr. H. Serdar AKYÜZ**	.....
	Prof.Dr. Erhan Altunel Osmangazi University	.....
	Dr.Öğr.Üy. Mehmet Korhan Erturaç Sakarya Universty	.....

Date of Submission : 3 May 2018

Date of Defense : 5 June 2018

FOREWORD

Since 2010, when I start to learn geology at ITU, my cruosity to natural sciences has continuously increased. Geology has become one of the most important part of my life, as not only a prosession but also its contributions to intellectual point of view and philosophy.

First, I would like to express my gratitude to my supervisors Prof. Dr. Boris A. Natalin and Dr. Cengiz Zabcı for their invaluable guidance, critisim and encouragements through out my research. I also thank to, Dr. Taylan Sançar, Prof.Dr. H. Serdar Akyüz, Assoc. Prof.Dr. Gürsel Sunal, Prof.Dr. Gültekin Topuz and Dr. Gönenç Göçmengil for their support and help for various parts of my thesis.

I also thank my friends Yetkin Egi, Mehran Basmenji, Ali Osman Yücel, Nurettin Yakupoğlu and my sister Merve Yazıcı for their help and support during last three years.

I am grateful to local authorities of Ocak (Kemaliye), Yeşilyurt (Kemaliye) and Arapgir who provide support during my field studies.

Finally, I would especially like to thank to my parents Nevin Yazıcı and Hüseyin Yazıcı for their great support and motivation.

This study is supported by TÜBİTAK Project tilted “Ovacık Fayı (Malatya-Ovacık Fay Zonu) üzerinde morfokronolojik ve paleosismolojik çalışmalar: Jeolojik kayma hızı ve eski deprem tarihçesinin araştırılması” No.114Y227 and BAP MYL-2017-40833 “Ovacık Fayı'nın kısa ve uzun dönem deformasyonu ve deprem tarihçesi: Türkiye'nin levha içi deformasyonu haKkında fikirler” projects. However, some of results of this study include major revisions and changes from the TÜBİTAK report of the project.

May 2018

Müge YAZICI
Geologist

TABLE OF CONTENTS

Page

ABBREVIATIONS

App : Appendix
BCE : Before Common Era
CAFZ : Central Anatolian Fault Zone
CAP : Central Anatolian ‘ova’ Province
DBs : Drainage Basins
EASZ : East Anatolian Shear Zone
EAPS : Eastern Anatolia Province of Shortening
EB : Erzincan Basin
EM : Electro Magnetic waves
E-MORB : Enriched Mid Ocean Ridge Basalts
Fig : Figure
fs : Fault segment
KTJ : Karlıova Triple Junction
MF : Malatya Fault
MOFZ : Malatya – Ovacık Fault Zone
NASZ : North Anatolian Shear Zone
NTP : North Turkish Province
OB : Ovacık Basin
OF : Ovacik Fault
OIB : Ocean Island Basalts
REE : Rare Earth Elements
TZF : Tuz Gölü Fault
UV : Ultraviole waves
Vp : Valley profile
WAEP : Western Anatolia Extentional Province

SYMBOLS

al **:** Alluvium

COp **:** Cretaceous Ophiolitic melange

g **:** Çöpler granitoid

HI **:** Hypsometric Integral

Kk **:** Kemaliye Formation

ksn **:** Normalized steepness index

Lmf **:** Total length of mountain front

Ls **:** Straight length of mountain front

Mzm **:** Munzur Limestone

PzMzk **:** Keban Metamorphics

Smf **:** Mountain front sinuosity

Tc **:** Tertiary cover deposits

Ty **:** Yamadağ Volcanic Complex

Qaf **:** Quaternary Alluvial fan

Qd **:** Quaternary debris flow

Qm **:** Quaternary morain

Θ **:** Concavity index

LIST OF TABLES

Page

LIST OF FIGURES

Page

LONG TERM DEFORMATION AND EARTHQUAKE HISTORY OF THE OVACIK FAULT (EASTERN TURKEY): IMPLICATIONS AND CONTRIBUTIONS TO THE INTRA-PLATE DEFORMATION OF ANATOLIA

SUMMARY

The post-collisional convergence between the Eurasian and the Arabian plates and the subduction along the Hellenic Trench (the Eurasian and the African plates) lead to the deformation of Anatolia. The Anatolian Block in which the westward escape tectonics with respect to Eurasia is accommodated along the North and East Anatolian shear zones (NASZ and EASZ). Anatolia incorporate almost all kind of structural elements from strike-slip dominated (especially in the Central Anatolian 'ova' Province) to extensional (the Western Anatolia Extensional Province) and compressional (the Eastern Anatolia Province of Shortening) tectonic features within this complex tectonic regime. In addition to plate boundary elements, the NASZ and the EASZ, Anatolia is internally deformed by many NE-striking sinistral and NW-striking dextral faults. Moreover, all tectonic elements in the Anatolian Block, which all carry certain amount of deformation, give an opportunity to study the intra-plate deformation of this particular place. Microseismisity also indicates that the interior of the Anatolian Block has a considerable degree of deformation. The instrumental seismicity represents spatially a detailed, but only a screenshot of the earth's dynamics when we consider the long history of faults. Therefore, any data about palaeoearthquakes provide a temporal control on the behaviour of active tectonic structures, which is important on understanding the long-term deformation of intra-plate regions.

The Ovacık Fault (OF), which is the northeastern member of the Malatya-Ovacık Fault Zone (MOFZ), is close to the eastern boundary of the Anatolian Block. Although the tectonic geomorphology is very impressive along the OF, this fault is just poorly known in terms of active tectonics except geodetic and geologic slip rate estimates. This study covers geology, tectonic geomorphology along the strike of the fault and a palaeoseismological study to understand the distribution and character of the deformation along and around this particular structure. The geology of the region starts with the Keban metamorphics (PzMzk) at the bottom of the stratigraphy, which is unconformably overlaid by olistostromal facies of the Kemaliye Formation (Kk). The Munzur Limestone (Mzm) is thrusted over to both of these units while it is overlain by the south vergence thrust of the Cretaceous ophiolites (Cop). The Tertiary cover deposits (Tc), which include mainly limestones and fine grain clastic rocks, unconformably overlies all older units. All of these units are cut by the intrusion of the Çöpler granitoids (g). The Yamadağ Volcanic Complex (Ty), which widely spreads at the southwestern part of the study region, is composed of basalts, andesites and dolerites (Fig. 3.2). The Quaternary sediments such as debris flow deposits (Qd), alluvial fan deposits (Qaf), morains (Qm) and alluvium (Qal) have best exposures in the Ovacık Basin. The region is affected by polyphase deformation processes, which lead to the formation of folding and faulting. The open folds generally have hinges that plunge to the E-NE. Moreover, according to poles of M-planes, I identified at least two

different deformation phases, which can be summarized to be oblique and strike slip dominated.

I also studied the tectonic geomorphology by using geomorphic indices (such as hypsometric curve and integral, longitudinal channel profiles, channel steepness and concavity and mountain front sinuosity) to characterize the deformation along the OF and the surrounding region where the regional morphology was shaped with a joint-effect of palaeo- and neo-tectonics and other morphological factors such as palaeoglacial processes. The highest hypsometric integral (HI), steepness and concavity values, which indicates the 'young age' topography related with the uplift, generally occur along the Munzur Mountains in the east and around the Kemaliye Region in the west. The high HI and steepness at the Kemaliye Region, where there is negligible evidence for palaeoglacial and karstic activity, is interpreted to be the result of tectonic uplift. This sudden tectonic uplift of the Kemaliye Region is based on the change of the fault's strike, which generates a transpressional setting.

This compressional deformation is not only expressed within the geomorphic signals in the steepness and concavity analyses, but it is also well defined with kinematic features along fault surfaces and the exposure of a single palaeoseismological trench at Yukarı Yuvacık Site. This trench site is morphologically characterized by a linear valley with at least two terrace treads, which are delimited from the bedrock at each side of the valley. This first palaeoseismological study along the OF reveals three palaeoevents in the last 7000 years within the fluvial sediments. Radiocarbon dating of stratigraphic layers yields an average recurrence of eathquakes 2400±765 years, which suggests a higher seismic potential for the OF than the previous suggestions.

Furthermore, the main motivation is to understand the role of the OF in the deformation of Anatolia together with other intra-plate structures. Although there are still many gaps, one of the most possible mechanism can be the existence of a higher convergence strain zone as a result of convergence between Eurasia and Arabia, which does not only rotate the strike of the OF, making it to gain a compressional component of motion, but also affect other parallel/sub-parallel fault zones in the same sense (Şengör et al., 1985; Zabcı et al. submitted).

In summary, the results of my study simply suggest that the OF is an active seismogenic sinistral strike-slip fault with an average recurrence of earthquakes 2400±765 years within the Anatolian Block. Along the strike of the OF, it shows all type of tectonic structures from strike slip to extensional and compressional due to the geometric changes in the fault's strike. Although the deformation character varies, the cumulative deformation, which slip rate is calculated as approximately 2.5 mm/yr from the age and offset of the Karasu River, is constant along all length of the fault.

The OF and other intra-plate faults of the Anatolian Block carry the whole deformation, which penetrates from boundary condition, heteregeously and creates big scale cataclastic flow as deformation mechanism of Anatolia.

OVACIK FAYI'NIN UZUN SÜRELİ DEFORMASYONU VE DEPREM TARİHÇESİ: ANADOLUNUN LEVHA-İÇİ DEFORMASYONUNA ETKİSİ VE KATKISI

ÖZET

Avrasya ve Arabistan levhalarının çarpışma sonrası birbirlerine yakınlaşmaya devam etmeleri ve Hellenik yay boyunca Afrika'nın Avrasya levhasının altına dalması Anadolu'nun deformasyonunu etkileyen iki ana tektonik unsurdur. Anadolu Bloğu'nun Avrasya'ya göre batıya doğru saat yönünün tersinde rotasyonal hareketi, Kuzey ve Doğu Anadolu Makaslama Zonları (KAMZ ve DAMZ) tarafından karşılanmaktadır. Anadolu ve çevresi, doğrultu atımlı tektoniğin (Orta Anadolu 'ova' Neotektonik Bölgesi), gerilmeli tektoniğin (Batı Anadolu Gerilme Bölgesi) ve sıkışmalı tektonik rejimin (Doğu Anadolu Kısalma Bölgesi) baskın olduğu hemen hemen her türlü yapısal unsuru bünyesinde barındırmaktadır. Levha sınır elemanları olan KAMZ ve DAMZ'na ek olarak, Anadolu'nun içinde birçok KD-doğrultulu sol yanal ve KB-doğrultulu sağ yanal doğrultu atımlı fay bulunur. Neredeyse tüm tektonik yapıların toplam deformasyonu paylaşması, Anadolu ve içinde bulunan her bir yapısal unsuru levha içi deformasyonu çalışmak için yerbilimleri açısından oldukça ilgi çekici hale gelmektedir. Mikrosismisite de, Anadolu Bloğu'nun iç kısmının önemli ölçüde deformasyona sahip olduğuna işaret eder. Aletsel deprem kayıtları, mekansal olarak ayrıntılı bilgi verir, ancak fayların uzun süreli deformasyonunu göz önüne aldığımızda, yalnızca yeryüzü dinamiğinin anlık görüntüsünü temsil eder. Bu nedenle, palaeosismisite, levha içi bölgelerin uzun süreli deformasyonunu anlamak adına zamansal kontrol sağlayan önemli veri kaynaklarından biridir.

Anadolu Bloğunun doğu sınırına yakın yerde bulunan KD doğrultulu birbirine parallel iki sol yanal doğrultu atımlı fay (Malatya-Ovacık Fay Zonu ve Orta Anadolu Fay Zonu) diKkat çekmektedir. Bunlardan özellikle Malatya- Ovacık Fay Zonu'nun, Doğu Anadolu Fayından daha önce Anadolu bloğunun doğu sınırını oluşturduğu önceki çalışmalarda iddia edilmiştir. Bu durum Malatya-Ovacık Fay Zonunu Anadolu'nun deformasyon mekanizmasını anlamak için çok değerli kılmaktadır. Malatya-Ovacık Fay Zonu'nun kuzeydoğu üyesi olan Ovacık Fayı (OF), Anadolu Bloğu'nun doğu sınırına yakındır. Topoğrafya üzerinde OF'nin oldukça belirgin bir izi olmasına rağmen, sadece tek bir noktada belirlenmiş jeolojik kayma hızı bulgusu dışında aktif tektonik özellikleri haKkında çok az bilgi bulunmaktadır. Bu tez, fay deformasyon dağılımını ve karakterini anlamak için doğrultusu boyunca jeoloji, tektonik jeomorfoloji ve paleosismolojik çalışmaları kapsar. Bölgenin jeolojisi, stratigrafinin en altında bulunan Keban metamorfikleri (PzMzk) ile başlar. Keban metamorfikleri çalışma bölgesinde yoğun dağılım gösteren ve genelde kalın mermerden oluşan bir birimdir. Daha önceki çalışmalar bu birim içerisinde Perian- Triyas aralığında fosil bulmuş olsalarda bu çalışmada Keban metamorfikleri içerisinde hiç fosil bulunamamıştır. Bu metamorfikler olistostromal fasiyesteki Kemaliye Formasyonu (Kk) tarafından uyumsuz olarak örtülür. Kemaliye Formasyonu bölgenin en karmaşık birimidir. Özellikle Kemaliye bölgesinde vadilerin tabanında yeşilşist fasiyesinde metamorfizma geçişmiş kalsi-türbiditler görülürken bazı yerlerde olistostrom blokları

gözükmektedir. Birimin çok fazlı deformasyano uğraması birimi daha karşık yapmaktadır. Munzur kireçtaşı (Mzm) bu iki birim üzerine bindirme fayı ile gelmiş, Kretase ofiyolitlerinin (COp) güney yönlü bindirmesi ile de üzerlenmiştir. Bölgenin en karakteristik birimi olan Munzur kireçtaşı resifal kireçtaşından pelajik kireçtaşına giden transgressif bir seridir. Birim genelde masif olarak gözükmekte ve kesintisizbir istif sunmaktadır. Kratese yaşlı ofiyolitik istif ise Munzur ve daha yaşlı birimler üzerine güney verjanslı bindirmektedir. Esas olarak kireçtaşı ve ince kırıntılı kayaçlar içeren Tersiyer örtü çökelleri (Tc) tüm eski birimler üzerinde uyumsuz olarak yer alır. Bütün bu birimler, Çöpler granitoyidlerinin (g) sokulumu ile kesilir. Çalışma bölgesinin güneybatı kısmında yaygın olarak bulunan Yamadağ Volkanik Kompleksi (Ty), bazaltlar, andezitler ve doleritlerden oluşmaktadır. Ovacık Havzası, bölgenin en genç birimleri olan Kuvaterner yaşlı çökellerden (yamaç molozları (Qd), alüvyal yelpaze çökelleri (Qaf), morenler (Qm) ve akarsu çökelleri (Qal)) oluşur. Çalışma bölgesi, çok fazlı deformasyon etkisi ile kıvrımlanmış ve faylanmıştır. Genelde baskın olan açık kıvrımlanma eksen çizgisi D-KD yönüne doğru dalımlıdır. Bölgede bulunan faylar genelde yoğun deformasyondan ötürü tekrar aktive olmuştur. Bunların izleri birbirini kesen fay çizikleri ile belirlenmiş ve kesen kesilen ilişkisişne göre de aralarındaki ilişki anlaşılmaya çalışılmıştır. Bunlara ek olarak, her bir birim için ayrı ayrı bulunan M-düzlemlerinin kutupları hem oblik hem de doğrultu atımlı tektonizmanı varlığını gösterdiği söylenebilir.

Ovacık Fayı ve çevresindeki alan boyunca deformasyonu karakterize etmek için hipersometrik eğri ve integral (HI), boyuna kanal profilleri, kanal dikliği ve konkavitesi (ksn, θ), Vadi tabanı genişlik – yükseklik oranı (Vf) ve dağ ön eğriliği (Smf) gibi jeomorfik indeksler kullanarak tektonik jeomorfolojisi çalışılmıştır. Kullanılan bu jeomorfik indisler genelde düşey atımlı faylar için kullanılsa da doğrultu atımlı faylarda oluşan ve deformasyon karakterini belirten düşey hareketler için önemli bir araçtır. Bu indisler sonucunda çıkan rakamlar daha önceki çalışmalara göre yorumlanmış ve fay segmentlerine göre sınıflandırılmıştır. Bu indisler bir bölgenin topoğrafyası üzerinde hakim olan süreçleri belirtir. "Genç yaş" topografyasının tektonik yükselme hakimiyetini işaret eden yüksek hipersometrik integral (HI), diklik ve konkavlık değerleri (ksn, θ), genellikle doğuda (Munzur Dağları boyunca) ve batıda, Kemaliye Bölgesi'ne işaret eder. Fakat Munzur Dağları'nın morfolojisi, paleo- ve neo-tektonik yapıların ve paleoglacial ve karstik süreçler gibi diğer morfolojik faktörlerin etkisi altında şekillenmiştir. Bu yüzden Kemaliye Bölgesi'ndeki buzul ve karstik yapıların Munzur Dağları'na oranla daha az olması, bu bölgenin daha çok tektonik kuvvetlerin etkisi ile şekillendiği yorumuna varılabilir. Kemaliye bölgesindeki bu tektonik yükselim fayın geometrisindeki değişime (sıkışmalı büklüm) ve Malatya Fayı ile etkileşiminden meydana gelir. Ayrıca Ovacık Havzası ve Munzur dağları arasında kalan drenaj alanı için dağ önü eğriliği ve vadi taban yükseklik-genişlik indisleri kullanıldı. Bu indisler Ovacık Havzasının hem kuzey hem güney kolunda ikitoplamda dört farklı segment üzerinde hesaplandı. Bazı çalışmalar bu iki indisi kullanarak özellikle dağ önü havzalarında düşey yükselimi hesaplamakta kullanıldığını göstermektedir. Bu yaklaşımdan yola çıkarak hesaplanan Vf ve Smf değerleri ile Ovacık Havzasının kuzey sınırının yıllık 0.5 mm 'lik bir yükselime sahip olduğu hesaplanmıştır.

Bölgenin sıkışmaya bağlı tektonik yükselimi sadece jeomorfik indislerle değil, aynı zamanda Yukarı Yuvacık hendek yerinde yapılan paleosismolojik çalışmada yüzeylenen yapılar da dikkati çeker. Bu hendek alanı, anakaya ile sınırlandırılan iki adet taraça ve bir adet alüvyal fan içeren çizgisel bir vadi içerisindedir. Ovacık Fayı üzerinde kaydelilmiş 6 üstü bir deprem bulunmamaktadır. Fakat tüm büyüklüklere baktığımızda OF boyunca aktivite olduğu görülmektedir. Deprem kayıtlarının tarihi

yaklaşık 100 yıldan öteye gidemeyeceği için paleosismoloji çalışması çok önem kazanmaktadır. Bu kapsamda 18 metre boyunda 2.5 metre derinliğinde ve 1.5 metre genişliğinde Yukarı Yuvacık hendeği açılmıştır. Hendeğin doğu duvarının 8 metresi haritalanmıştır. Diğer kısımlar fay zonundan çıkan su yüzünden çökmüştür. OF boyunca yapılan bu ilk paleosismolojik çalışma, fluvial çökeller içinde üç farklı eski deprem kayıtlarını ortaya çıkartmıştır. Stratigrafik tabakaların radyokarbon tarihlendirilmesi ile belirlenen eski deprem tarihleri sırası ile hasaplanmıştır. Toplanan 16 yaştan stratigrafiye uygun olan 6 yaş kullanılmıştır.Bu yaşlar Oxcal yaş modelinde kullanılarak eski deprem seviyelieri için aralık bulundu. En genç olay M.Ö. 56 yılından sonra meydana gelmiştir. Bu olay sınırı için üstten sınırlayan bir yaş olmadığından sadece alt sınırına bağlı bir yorum yapılır. İkinci eski deprem olayı ise M.Ö. 2950 – 1600 yılları arasında meydana gelmiştir. Bu hendek çalışmasında belirlenen en yaşlı eski deprem olayı ise M.Ö. 4700- 3022 yılları arasında meydana gelmiştir. Bu yaşlar ile birlikte hesaplanan ortalama deprem tekrarlanma aralığı 2400 ± 765 yıl olarak bulunmuştur. Bu bulgu, OF'nin daha önceki düşüncelere göre daha yüksek bir sismik potansiyeli olduğunu gösterir.

Bölgede morfolojik olarak en belirgin yapılardan biri olan Karasu Nehri doğrultusu boyunca birçok sol yanal büklümler göstermektedir. Bu büklümler hem ana fay kolları hem de özellikle Kemaliye bölgesinde bulunan tektonik çizgisellikler ile karşılanmaktadır. Bu büklümler kuzeyden güneye sırası ile 2.4 ± 0.4 km, 2.45 ± 0.65, 1.1 ± 0.1 km and 8.75 ± 2.05 km olarak hesaplanmıştır. Bu ölçümlerden yola çıkarak Karasu Nehrinin toplam atımı yaklaşık olarak 14.5 km olarak hesaplanmıştır. Bu toplam atımın, Pliyosen yaşlı Karasu Nehrine oranı yaklaşık 2.5 mm/yıl olarak hesaplanmıştır. Hesaplanan kayma oranı fayın tek kol olduğu doğu kısmında da benzer olarak bulunmuştur. Bu oranlar bize Ovacık Fayı boyunca toplam deformasyonun sabit kaldığını, doğuda tek bir kol üzerinde batı tarafında ise birbirine parallel kollar tarafından paylaşıldığını göstermektedir.

Bunlara ek olarak, OF'nin Anadolu'nun deformasyonu içindeki rolü ve diğer levha içi yapılarla olan ilişkisi bu bloğun iç eformasyon özelliklerinin anlaşılması için büyük önem taşır. OF ve buna paralel diğer levha-içi faylar, belirli bir noktada doğrultusunu değiştirip sıkışmalı bir bileşen kazanır. Bu rotasyonel kuvvet Avrasya ve Arap levhalarının çarpışması sonucu oluşan yüksek konverjan yamulma zonlarının etkisi ile olabilir (Şengör et al., 1985). Bunun yanısıra Anadolu Bloğu içerisinde bulunan diğer doğrultu atımlı faylar (Orta Anadolu Fay Zonu, Tuz Gölü Fay Zonu) hem kayma miktarı hem de deprem tekrarlanma aralığı bakımından Ovacık Fayından daha yavaş olarak çalışmaktadır. Bu durum Orta Anadolu 'ova' neotektonik bölgesinin kendi içerisinde doğuda daha yoğun deformasyona sahip olduğunu, batı sınırına yaklaştıkça hem deformasyon yoğunluğunun düştüğünü hem de deformasyon karakterinin sıkışmalıdan gerilmeliye geçtiğini göstermektedir.

Bu çalışmada elde edilen sonuçlar, OF'nin Anadolu Bloğu içinde aktif sismojenik sol yanal doğrultu atımlı bir fay olduğunu gösterir. OF'nin doğrultusu boyunca, her türlü yerel gerilmeler ve sıkışma alanları, fayın geometrisi ve diğer fay kolları ile etkileşimi olduğu yerlerde görülür. Deformasyon karakteri çeşitli olsa da, toplam deformasyon, kuzeydoğu kısmında tek fay kolu ile taşınırken, batı kısmında birbirine paralel/yarıparalel kollar tarafından paylaşılmaktadır.Bu fay üzerinde yapılan ilk paleosismolojik çalışmada son 7 bin yılda 3 farklı deprem seviyesi belirlenmiş ve deprem tekrarlanma aralığı olarak 2400 ± 765 yıl olarak bulunmuştur. Ovacık Fayı ve Anadolunun diğer levha içi fayları sınır koşullarından gelen deformasyonu heterojen olarak taşımakta ve Anadolu içerisindeki deformastyonu kataklastik akma olarak taşımaktadır.

1. INTRODUCTION

The dynamics of the earth is explained with the movement of the crust, which is carried by mobile belts (Wilson, 1965). The idea of Wilson's mobile belts makes the base of the today's plate tectonics theory. This theory implies that the earth's lithosphere is composed of finite number of plates, which have regular motion with respect to each other along three kinds of boundaries (Şengör, 1990). These three types of plate boundaires are: (1) Divergent, where an oceanic lithosphere is created by sea floor spreading along Mid-Ocean Ridges (Dietz, 1961), (2) Convergent, where a plate is destroyed by subduction processes along trenches, and (3) Horizontal motions where there is no destruction or creation of the lithosphere along the strike slip boundaries. (Wilson, 1965).

Plates are rigid blocks and have narrow boundaries where almost all deformation localized along it (Fig. 1.1). The rigidity of plates means that the distance between two points within the same plate does not change with time. In other words, there is no significant deformation in plates' interior, except at their edges (Le Pichon, 1968; McKenzie andParker, 1967; Morgan, 1968; Wilson, 1965). However, recent studies shown that although major deformations are located at plate boundaries, some plates' interiors also deform, which is referred to as intra-plate deformation (Storti et al., 2003; Wiens et al., 1986). In order to clarify the rigidity problem, (Gordon, 1998) suggests that the narrow and diffuse plate boundaries have different slip rates. The diffuse plate boundaries are wide deforming zones, which are surrounded by two or more rigid plates (Gordon, 1998). Rate of motion of the diffuse plate boundaries is between 2 to 15 mm/yr., whereas it is less than 2 mm/yr. in intra-plate regions (Gordon, 1998). According to this classification, plates are grouped as component and composite plates based on the type of boundaries (Gordon, 1998), where a component plate is delimited by diffuse plate boundaries such as Nubia and Somalia plates and a composite plate is bounded by narrow plate boundaries such as the African Plate that includes Nubia and Somalia component plates (Gordon, 1998) (Fig. 1.2). However, even after such kinds of revised ideas, the intra-plate deformation is still a controversial concept (Scholz et al., 1986)

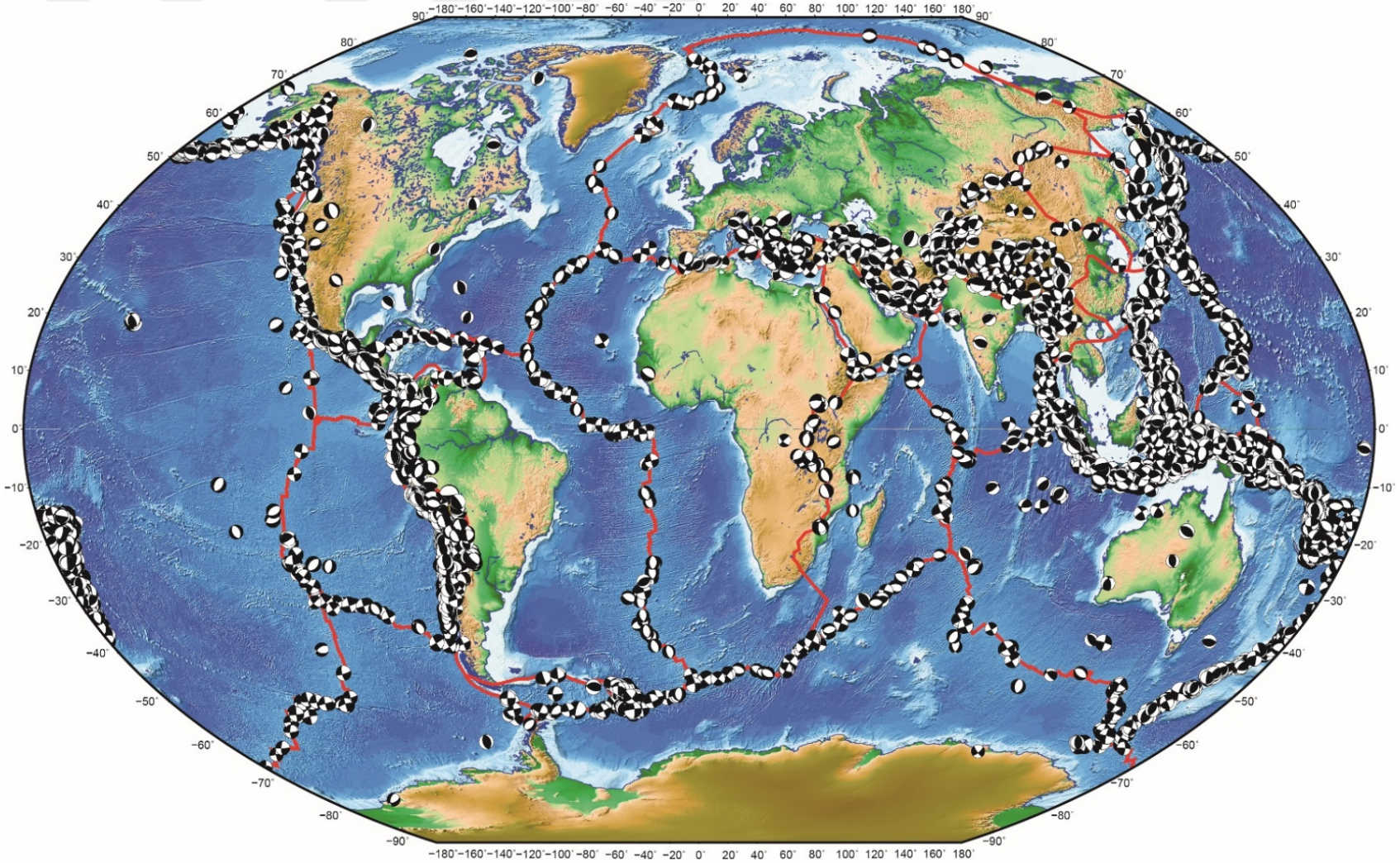

Figure 1.1 : Map showing the plates and their boundaries (Bird, 2003) and earthquakes (M>5.5) with their focal mechanism solutions (Ekström et al., 2012a). Red lines are plate boundaries. Although most of the earthquakes are located at plate boundaries, some intra-plate regions also show significant deformation such as North America, Tibet, Altaids, Anatolia and Australia.

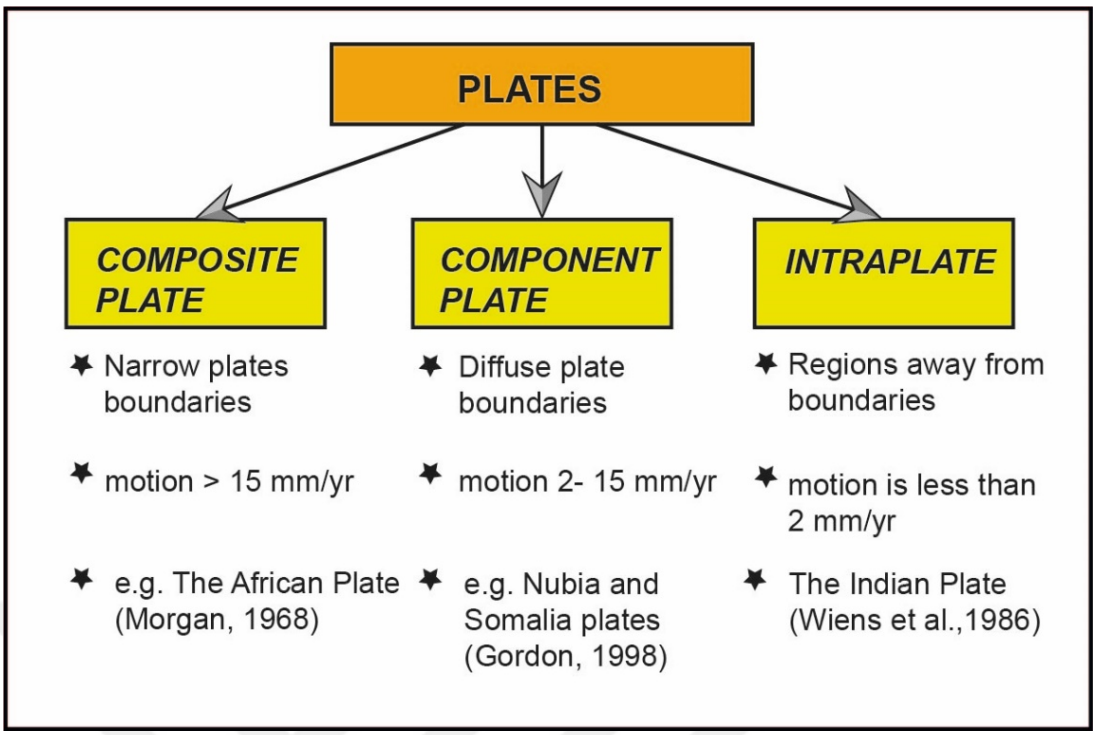

Figure 1.2 : Types of plate boundaries according to their boundary types and rate of motion (slip rate). Compiled from (Gordon, 1998; Morgan, 1968; Wiens et al., 1986). Intra-plate regions are away from both type of boundaries and they are characterized by low deformation rates.

The worldwide seismicity indicates that most of the seismic activity is located along the plate boundaries where interaction of at least two plates has taken place (Fig. 1.1) (Bird, 2003; Isacks et al., 1968). High magnitude earthquakes represent these boundaries, which are deformed with a continuous rate by relative motion of plates. Therefore, timing of big earthquakes can be estimated by faults' slip rate and recurrence interval of big events (Liu et al., 2011). However, earthquakes of intra-plate regions are less frequent than those within the plate boundaries (Liu et al., 2011). Establishing of the recurrence interval for intra-plate earthquakes is quite difficult, because of not only their irregularity but also lack of seismic records and long-time duration between events. The enigmatic structure of intra-plate earthquakes and their direct effects on human society always attract attention of various disciplines in earth sciences. Best examples of intra-plate earthquakes are from the New Madrid Seismic Zone (United States) (Braile et al., 1982; Tuttle et al., 2002; Zoback et al., 1980), Australia (Clark et al., 2012; Demets et al., 1994), and North China (Liu et al., 2011). These studies try to figure out how intra-plate earthquakes work, what their relations with former weak zones and their recurrence intervals are. Anatolia, which is one of the significant components of a puzzle in the complex tectonic setting of the Eastern Mediterranean region, is an ideal place to study the changing deformation character

within a crustal block. Seismicity of the Anatolian Block is defined by both inter - and intra-plate faults (Fig. 1.3).

Figure 1.3 : Neotectonic structures of the Eastern Mediterranean region. The North Anatolian (NASZ) and East Anatolian (EASZ) shear zones make the northern and eastern boundaries of the Anatolian Block and meet at the Karlıova Triple Junctions (KTJ), whereas structures such as the Malatya-Ovacık Fault Zone (MOFZ), Central Anatolian Fault Zone (CAFZ) and Tuz Gölü Fault (TZF) are strike-slip intra-plate faults of the Anatolian Block. The map compiled and simplified from ((Akyuz et al., 2006; Akyuz et al., 2013; Avagyan et al., 2010; Duman andEmre, 2013; Hall et al., 2014; Koçyiğit andBeyhan, 1998; Le Pichon et al., 1995; Nyst andThatcher, 2004; Philip et al., 1989; Saroglu et al., 1992; Searle et al., 2010; Shaw andJackson, 2010; Şengör et al., 1985b; Şengör et al., 2014; Şengör et al., 2008a; Şengör et al., 2005). Basemap is from GEBCO (http://www.gebco.net/data_and_products/gridded_bathymetry_data/).

During the middle-late Miocene, collision between the Arabian and Eurasian plates and the subduction between African and Eurasian plates start the neotectonic period of Turkey and the adjacent regions (Şengör, 1980; Şengör et al., 1985b). The Anatolian Block is being extruded westward with respect to Eurasia along its boundary faults, North Anatolian (NASZ) and East Anatolian (EASZ) shear zones (Fig. 1.3). Although the main deformation is localized along the boundary faults, intra-plate faults also participate to the deformation of Anatolia such as the Central Anatolian Fault Zone (CAFZ), the Malatya-Ovacık Fault Zone (MOFZ), and the Tuz Gölü Fault (TZF) (Fig. 1.3). The neotectonic period causes formation in four different provinces of Turkey,

from which the Central Anatolian ‘ova’ Province is one of the seismically quietest one (Şengör et al., 1985b). The Ovacık Fault (OF), which is the north-eastern member of the MOFZ, is located close to the eastern boundary of the ‘ova’ province (Fig. 1.3). Even though the OF has very attractive tectonic geomorphology, the seismic activity and many active tectonic properties of this fault is poorly known. Any study on the OF, especially its structural, morphotectonic and palaeoseismologic aspects contribute to the spatial and temporal behaviour of this particular fault system and in a broader sense shed a light on the mechanism of internal deformation of Anatolia.

1.1 Study Region: The Ovacık Fault and its surroundings

The study region stretches along the length of the Ovacık Fault (OF), which extends between the Erzincan Basin (EB) in the northeast and the Arapgir Region in the southwest (Fig. 1.4). The study region embraces three different cities of Turkey, Tunceli, Erzincan and Malatya, particularly within the districts of Ovacık, Kemaliye and Arapgir. Due to the logistical problems in the northeastern part of the OF (the Ovacık Town and the surrounding region), I focused on the western / southwestern parts of the study region. Thus, my own observations are mainly from the western parts of the OF, neverthless the geology of the eastern parts is mainly compiled from the previous studies and remote sensing data.

Continental climate dominates in the study region. Rate of snowfall is generally higher than precipitation rate especially for mountainous areas. Annual precipitation rate for three main disticts, Arapgir, Kemaliye and Ovacık, stays within a spectrum of about 525 - 650 mm (www.mgm.gov.tr) (Table 1.1).

The study region is one of the most morphologically attractive regions of Turkey. The Munzur Mountains (geologically the northeastern extention of the Taurus Mountains.), the Ovacık Basin (OB) and the Karasu River (main branch of Euprathes) are the main morphological elements of the study region (Fig. 1.4). The study region is one of the morphologically attractive region of Turkey. The Munzur Mountains are geologically the northeastern extention of the Taurus mountain belt. Their highest pick rises above 3400 m that is also the highest elevation of the study region, whereas the lowest elevation of the region (the Karasu River) is around 850 m. The Munzur Mountains stretch along the NE-SW strike and incised by drainage networks. Effect of glaciation makes indented topography with glacial valleys, cirques, roche mountonnes, dolines.

Table 1.1 : Total Precipitation rate for Arapgir, Kemaliye and Ovacık districts, which are settlements along the strike of the OF (www.mgm.gov.tr). From the meteorological data there is no much differences between the climatic condition along the region.

Total Precipitaiton (mm)	Arapgir	Kemaliye	Ovacik
January	84.5089	58.2345	62.241
February	78.9958	54.4321	60.5895
March	81.9175	64.4335	69.1543
April	87.2411	74.7987	81.9552
May	60.2298	62.8366	68.5537
June	20.2479	25.1703	27.7862
July	3.67052	5.34158	6.11226
August	1.54565	3.08122	4.04467
September	7.39194	9.27815	11.4941
October	49.9891	46.0975	55.1164
November	75.7673	58.1344	67.7405
December	95.8963	66.9076	72.7013
Annual	647.40181	528.74615	587.48913
Winter	259.401	179.5742	195.5318
Spring	229.3884	202.0688	219.6632
Summer	25.46407	33.5931	37.94313
Fall	133.14834	113.51005	134.351

The Ovacık Basin, which is bounded by the Munzur Mountains in the north, is about 25 km long depression composed of morain and alluvial fan deposits, which are cut by the OF. The Munzur River pass through the Ovacık Basin in the east-west direction and connected to Euprathes. The most prominent drainage of the region is the Karasu

River that flows roughly in a N-S direction in the west of the study area and forms a narrow canion along its stretch (Fig. 1.4).

1.2 Motivation and Scope of the Study

An earthquake is one of the dangerous events of the nature, which may lead to the death of many people and can cause great damage to the infrastructures. From the scientific view, the study of earthquakes' structures contributes to a better understanding on the deformation mechanism.

Turkey is one of the best places for studying earthquakes and deformation due to its complex tectonic setting. It is important not only for its plate boundary faults, which have high potential seismic risk to produce big and frequent earthquakes, but also for its intra-plate faults, which are crucial for understanding the deformation mechanism within the Anatolian Block. Especially, the spatiotemporal seismic behaviour of intra-plate faults is critical parameters for understanding the structures of intra-plate earthquakes and their seismic hazard potentials.

The Ovacık Fault (northeastern member of the Malatya – Ovacık Fault Zone) with its attractive morphology is one of the sinistral strike slip faults of the Central Anatolian 'ova' Neotectonic Province. (Figs. 1.3 and 1.4). Limited number of records of historical earthquakes and the absence of palaeoseimic studies make the OF attractive for these type studies because of its impressive tectonic morphology. From these points of views, my aim is to investigate the distribution and character of the deformation, to evaluate the seismic risk potential and the spatio-temporal behaviour of the OF, and to understand its role in the deformation of the Anatolian Block and any other similar regions all over the world in this thesis.

1.3 Materials and Methods

This study is mainly composed of three parts and use three different approaches: First, I started with investigating the geology of the region. Using my own field observations, I compiled the geological map of the region. For this work, I used topographic maps of 1:25.000 scale, a geological hammer, a loop and a handheld GPS. I supported my field observations with analysis of multi-spectral Landsat 8 OLI Satellite Images. The utility of remote sensing helps in understanding the geology and the interpretation of geological structures in the study region Thereby, processing of reflection bands of

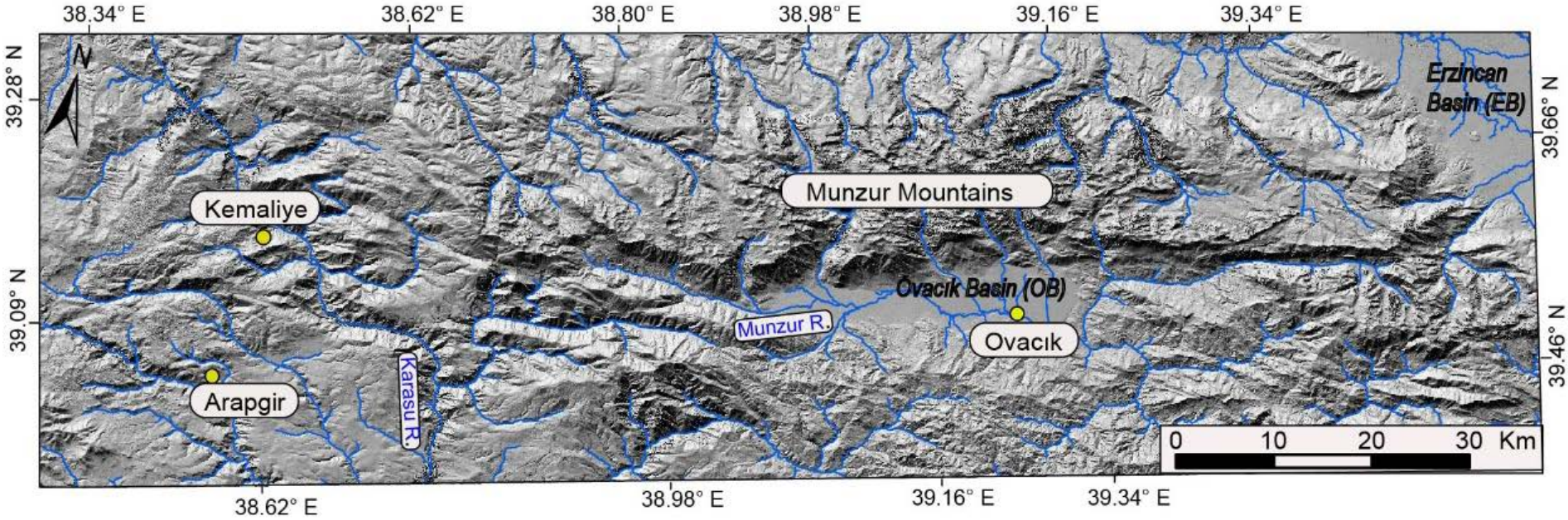

Figure 1.4 : Morphologic elements of the study region. Blue lines are drainage networks, the Karasu and Munzur Rivers are the main trunck rivers of the region. The Ovacık (OB) and Erzincan (EB) basins are lower-lying mountain front basins.

visible, near infrared and short infrared waves of images aid to establish the best contrast between different lithological units and compare the resulting images (for detail information please see Chapter 3.3). The Landsat analyses is made by Envi Lidar 5.3 and ArcGIS 10.3.1 software packages.

Secondly, I investigated the morphology with several computer-based programs, by using digital elevation models (DEMs) of aerial photos (down sampled to 1 m ground pixel resolution), SRTM 1-ARC (30 m pixel resolution) and TANDEM-X (12 m pixel resolution). I quantified the active morphology by using geomorphic indices such as longitudinal channel profiles, hypsometric curves and integrals, channel steepness and concavity indices and mountain front sinuosity (Keller andPinter, 1996). The drainage basins along the OF were extracted from TANDEM-X data by using River tools and ArcGIS 10.3.1 computer programs. I used these two programs for calculation of indices, including longitudinal channel profiles, hypsometric curves and integrals and mountain front sinuosity, whereas the channel steepness and concavity are calculated by Topo Toolbox module (Schwanghart andKuhn, 2010; Schwanghart andScherler, 2014) coded for the MATLAB software.

The last step is the palaeoseismological study. To investigate palaeo-events, I opened a trench on one of the southwestern segments of the OF. The trench wall was logged and sampled to construct and determine the timing of individual event horizons. Collected radiocarbon samples were dated by using accelerator mass spectrometry (AMS) in the BETA Analytics Inc., USA. The calibration of samples and age modelling of the trench was done by OXCAL (Ramsey andLee, 2013), using the calibration curves of (Reimer et al., 2013) We used Agisoft Photoscan Professional Software to produce the photomosaic of the trench wall. During the processing, I manually eliminated the blurred and oblique angle photos to increase the quality of the mosaic. I entered the GPS coordinates as a ground control point for each edge of the grid which is recorded during the logging. The key point and tie point limit are used as 70.000 and 1.000. Then dense cloud, texture and photomosaic were processed gradually.

Detailed methodology of all my studies are presented in related chapters.

2. BACKGROUND: TECTONIC SETTING OF THE STUDY REGION

Interaction between the Arabian, Eurasian and African plates shape the complex tectonic setting of the Eastern Mediterranean Region (Dewey andŞengör, 1979; McKenzie, 1972b; Şengör et al., 1985b). Within this tectonic setting, Anatolia is affected by successive convergence – collision related events through its history. Today's tectonic style of the Anatolian Block is mainly related with the history of the Tethyan oceans. After the closure of the Tethyan Ocean, continuous intracontinental collision during the Palaeocene – early Eocene times along the İzmir-Ankara and Inner-Tauride sutures formed much of the present land area of Anatolia (Şengör andYılmaz, 1981). The last strong deformation occurred during the middle to early-late Miocene with the collision between Eurasia and Arabia along the Bitlis-Zagros Suture, which has essential impact on the high mean topography of the eastern Turkey (Eastern Turkey High Plateau; (Şengör et al., 2008b) and it corresponds to the beginning of the neotectonic period in this particular region (Şengör and Yılmaz, 1981; Şengör et al., 1985). Since the middle to late Miocene (~13 Ma), timing of collision and post-collisional convergence between the Arabian and Eurasian plate in the east, and on-going existence of subduction of the African plate beneath the Hellenic – Cyprus Trench in the west lead to the formation of today's tectonics regime of the Anatolian Block (Le Pichon andKreemer, 2010; McKenzie, 1972a; Şengör et al., 1985b) (Fig. 2.1). In this sophisticated tectonic setting, the Anatolian Block has westward motion relative to the Eurasian Plate along its boundary faults, the North Anatolian Shear Zone (NASZ) in the north and the East Anatolian Shear Zone (EASZ) in the east (Fig. 2.1). This westward motion is accommodated by conterclockwise rotation with the increasing magnitude of movement from about 20 mm/yr in the northeast to about 30 mm/yr in the southwest (Fig. 2.1) (Reilinger et al., 2006). This motion takes place from a zone of convergence toward a free boundary, which is called escape tectonics, and has been identified in various regions including Tibet (Tapponnier et al., 1982) and Anatolia (Burke andSengör, 1986; McKenzie, 1972a; Şengör et al., 1985b). However, there are still many different hypotheses on the mechanism of the westward extrusion of Anatolia.

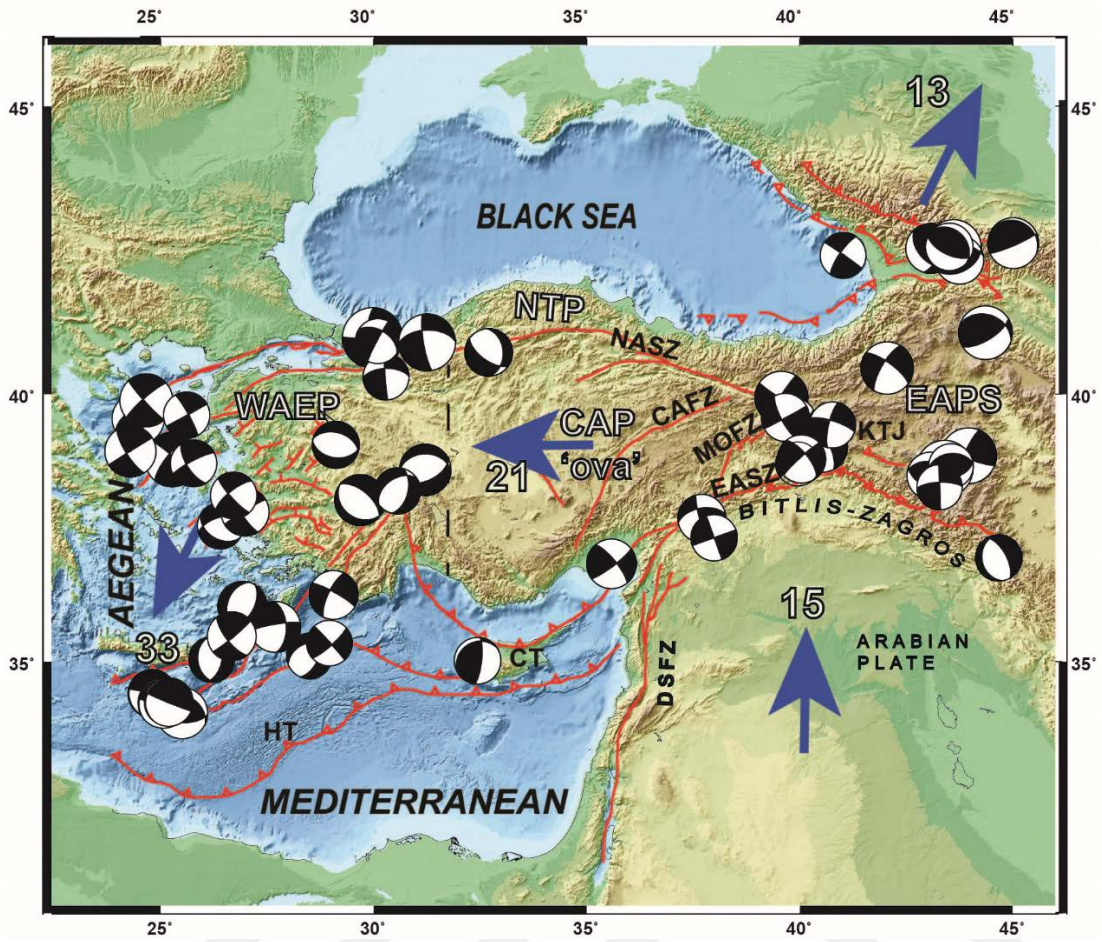

Figure 2.1 : Major tectonic elements of the Turkey. Anatolian block is bounded by North Anatolian (NASZ) and East Anatolian (EASZ) Shear zones and sliced into pieces by intra-plate faults such as the Malatya- Ovacık Fault Zone (MOFZ), the Central Anatolian Fault Zone (CAFZ) and many faults in the Agean Region. All (red) lines with saw teeth are thrusts; lines with hachures represent normal faults; and all solid lines are strike-slip faults. Focal mechanism solutions show character of deformation (Ekström et al., 2012b) Blue arrows and corresponding numbers are plate velocities with respect to Eurasia (Reilinger et al., 2006). Key to lettering: KTJ: Karlıova Triple Junction, CT: Cyprus Trench, HT: Hellenic Trench, EAPS: East Anatolian Province of Shortening, CAP: Central Anatolian 'ova' Province, WAEP: Western Anatolian Extensional Province, NTP: North Turkish Province. Black dash line is transition zone between extensional to ova province. Base map is from GEBCO (http://www.gebco.net/data_and_products/gridded_bathymetry_data/).

Some of them claim that the escape tectonics is caused by the syn-collisional convergence along the Bitlis-Zagros suture, which leads to extra forces to gravitational potential energy at its boundaries by the late Serrovanian (McKenzie, 1972; Özeren and Holt, 2010; Şengör et al., 1985). Le Pichon and Kreemer (2010) take into consideration the results of the radial spreading of the asthenosphere due to the East African Plume. The existence of the Plume triggers the northward motion of Arabia,

which results the difference in gravitational potential energy between the east Anatolian high plateau and the west Anatolian low land, has contribution to the lateral extrusion of the Anatolia. Reilenger et al. (2006), claim that there is no more convergence between the Arabian and Eurasian plates and the main westward motion of the Anatolian Block is enhanced by slab rollback along the Hellenic and Cyprus trenches. The effect of the slab pull forces in the southwest, along the Hellenic - Cyprus subduction, is claimed to be sufficient to accommodate all westward motion of Anatolia (Chorowicz et al., 1999; Reilinger et al., 2006). Additionally, (Dhont et al., 2006) claims that the westward motion of Anatolia and thickening of the Anatolian Plateau in the east are associated with the extension and strike slip tectonics in the west. Lastly, (Faccenna et al., 2006) suggest that the thermal flow of the Afar plume and the effect of slab break of in the Bitlis area are responsible of the lateral motion of Anatolia.

The most significant products of Anatolia's neotectonic period are the North Anatolian (NASZ) and the East Anatolian (EASZ) shear zones, which forms the northern and eastern margins of this block, respectively. The 1500 km-long dextral NASZ, with it is ~25 mm/yr. of slip rate, begins around Karlıova in the east and terminates at the Aegean Sea in the west (Fig. 2.1). Along its entire length, it represents pure strike slip, transtentional and transpressional regimes (Barka, 1992; Şengör, 1979). The sinistral 550 km-long EASZ, which has about 10 mm/yr. of slip rate, forms the eastern boundary of the Anatolian Block (Reilinger et al., 2006; Şengör et al., 2008b). Both of these shear zones meet each other at the Karlıova Triple junction (KTJ in Figs 1.3 and 2.1). In the neotectonic frame of Anatolia, the whole deformation is accomplished in four major provinces; (1) the East Anatolian Province of Shortening (EAPS), (2) the North Anatolian Province (NTP), (3) the West Anatolian Extensional Province (WAEP), and (4) the Central "ova" Province (CAP), which all have their own identical deformation styles (Şengör et al., 1985) (Fig. 2.1). The East Anatolian Province of Shorthening is mainly affected by the collision and the continental convergence between the Arabian and the Eurasian plates. The Bitlis-Zagros Suture in the south, the EASZ in the west and the Caucasus in the north bound the region. As the result of the convergence, the region is exposed to thickening, shortening and uplift of the

lithosphere. The rate of shortening is calculated to be 10 ± 2mm/yr (Reilinger et al., 2006). This province is characterized with the E-W oriented compressional basins such

as Muş-Lake Van and Pasinler and the N-S trending volcanic fissures (Şengör et al., 1985b; Şengör et al., 2008b).

The North Anatolian Province is the least seismically active region of Turkey and is bounded by the NASZ in the south and Black Sea in the north (Bozkurt, 2001).

In the Western Anatolia Extensional Province, the N-S extension, which is formed by "tectonic escape model" relatively westward motion of Anatolia (Dewey andŞengör, 1979; Görür et al., 1995; Şengör, 1987; Şengör et al., 1985a), "back arc spreading" soutwestern migration of the Hellenic Trench leads to back arc extension in Aegean (Le Pichon andAngelier, 1979; McKenzie, 1978), "Orogenic collapse" thinning of overthicked crust after the collision (Seyitoğlu andScott, 1991; Seyitoğlu andScott, 1992) and "episodic" includes both orogenic collapse and tectonic escape models (Koçyiğit et al., 1999) generates E-W trending grabens such as Büyük Menderes, Küçük Menderes and Gediz (Bozkurt, 2001). The rate of extension is about 30-40 mm/yr. to the southwest, which is higher than the rate of lateral motion of Anatolia (20 mm/yr.) (Bozkurt, 2001; Reilinger et al., 2006; Şengör et al., 1985b).

The Central Anatolia 'ova' Province (after this point, I will shortly name this as CAP) is bounded by the NASZ in the north, the EASZ in the east and the Western Extensional Province in the west (Şengör et al., 1985). My study region is placed on the eastern boundary of this specific province; thus, I explain the CAP in more details below.

2.1 Central Anatolian 'ova' Province and the Ovacık Fault

Microseismicity on the Anatolian Block shows that the whole deformation is not only localised along the NASZ and the EASZ, but Anatolia is internally deformed as well (Fig. 2.2a). The 'ova' province consists of many strike slip faults such as the CAFZ and the MOFZ that lie parallel to each other and have same sinistral sense of motion (Bozkurt, 2001; Koçyiğit andBeyhan, 1998)

The MOFZ, which is one of the prominent member of many active structures of the CAP, sharing the total internal strain with other intra-plate faults of the Anatolian Block (Figs. 2.1 and 2.2b). The OF, the northeastern member of the MOFZ, located close to the eastern boundary of the CAP and extends about 110 km between the EB in the northeast and Arapgir (Malatya) in the southwest, where it makes a junction with the Malatya Fault (MF) (Fig. 1.4). The geometry of the OF is described by various

researches (Aksoy, 1996; Arpat andŞaroğlu, 1975; Kaymakci et al., 2006; Westaway andArger, 2001b) in details especially for the Ovacık Basin and the fault's southwestern sections. Particularly, (Arpat andŞaroğlu, 1975) shows deformed Quaternary alluvial fans and moraines, which clearly mark the tectonic activity along the northern margin of the Ovacık Basin. The OF has mainly a NE-striking geometry from the Erzincan Basin to the Karasu River, in which the deformation is mainly localised along a single fault strand. However, close tothe Karasu River, it bifurcates into three parallel/sub-parallel branches (Fig. 2.2).

2.2 The Origin, the Age and the Offset of the Malatya-Ovacık Fault Zone and the Ovacık Fault

Ideas on the origin and activity of the OF are still controversial. Previous studies do not imply ages older than 13 Ma for the time interval when the westward escape of the Anatolian Block started because of the Arabian- Eurasian Collision (Chorowicz et al., 1995; Dewey and Şengör, 1979; Şengör, 1979; Şengör et al., 1985). Koçyiğit and Beyhan (1998) suggest that intra-plate faults must post-date the northern and eastern boundary structures of the Anatolian Block, (the NASZ and the EASZ). They also suggest that the MOFZ and the CAFZ are splays of the NASZ. Contrary to this interpretation, other researchers claim that the OF was active between 5-3 Ma as the eastern boundary of the Anatolian Block and then the deformation was transferred to the EASZ by abandoning its former location (Westaway andArger, 2001; Westaway et al., 2008; Westaway et al., 2006). In spite of ideas supporting that the OF became active in about 3 Ma (Westaway andArger, 2001; Westaway et al., 2008; Westaway et al., 2006), recent GPS measurements and stress analysis suggest the opposite (Aktuğ et al., 2013c; Kaymakçı et al., 2006; Özener et al., 2010). Moreover, microseismic activity (AFAD, 2013), and a morphometric study Yazici et al. (2016) clearly show that the OF is one of the active structures of the central Anatolia 'ova' province and has a key role on the internal deformation of Anatolia (Fig. 2.2). According to multiple studies, deformation rate on the OF is significantly slower than the main boundary faults. Taking into consideration the time of collision as the origin of the OF (~13 Ma) and the offset measurements of 12.5 and 20 km (Chorowicz et al., 1995), the very-long term slip rate is about 1 mm/yr.

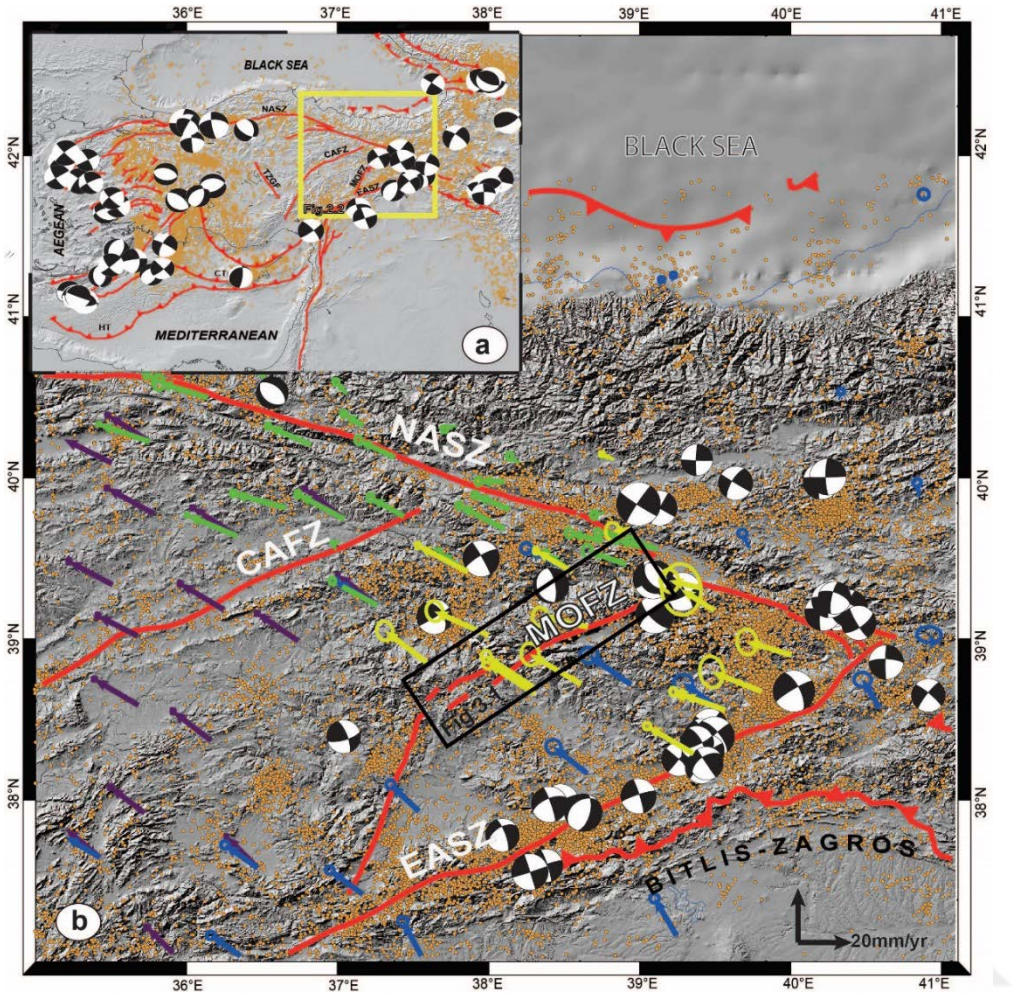

Figure 2.2 : (a) The main active tectonic structures and focal mechanism solutions of Turkey and the adjacent region. (b) The zoomed area of the central-to-eastern Turkey (Yellow rectangle in a), including the sinistral Ovacık Fault. Orange small dots indicate the instrumental seismicity since 1900 (downloaded from Kandilli Observatory, (Kalafat et al., 2009), GPS velocities are represented by arrows in colours (blue arrows show Reilinger et al. (2006), yellow ones are from (Özener et al., 2010), green ones are from (Tatar et al., 2012) and purple arrows are from (Aktuğ et al., 2013b, 2013c)) and focal mechanism solutions shows the main earthquakes of the region (Ekström et al., 2012a)

The total cumulative slip along the OF is also suggested to be as high as 27 km (Westaway ve Arger, 2001), while Westaway et al. (2008) purpose a maximum slip of about 8 km by using the sinistral deflection of the Karasu River. According to the 3 Ma of suggested activity of the fault and this slip measurement yield a more higher slip-rate of about 2 to 3 mm/yr. Contrary to 'abondoned activity' hypotheses, Kaymakçı et al. (2006) claims that the OF is still active and the total offset along the OF does not exceed 20 km. The modelled elastic block-based horizontal slip rate is 1.2±0.3 mm/yr along the OF (Aktuğ et al., 2013a; Aktuğ et al., 2013c). However, the first morphochronological slip rate study by using 36Cl dating of offset

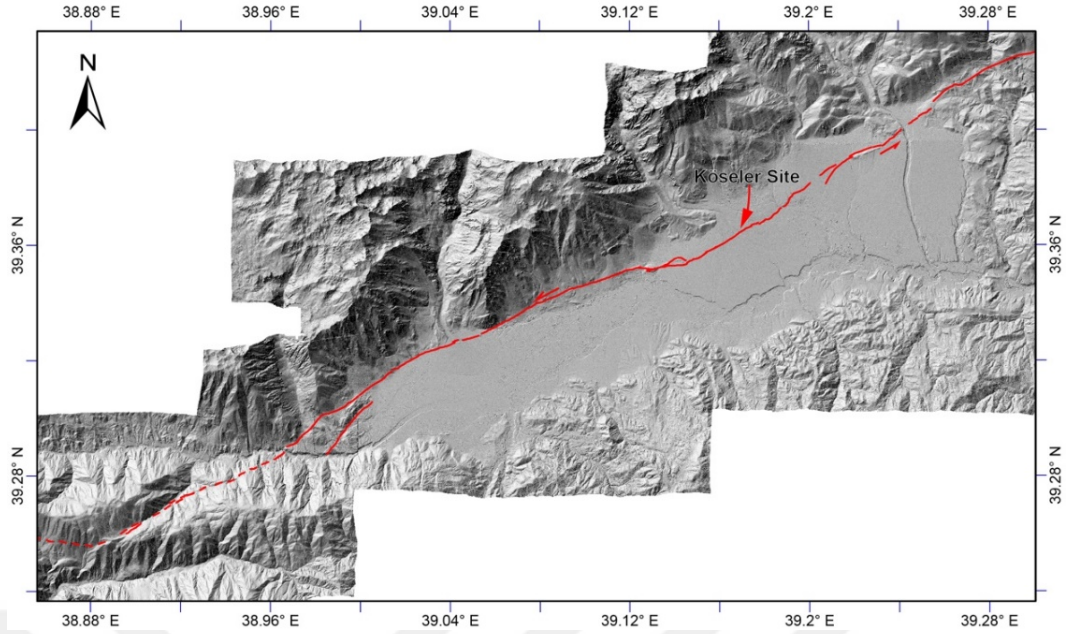

Figure 2.3 : The hillshade map showing the Ovacık Basin, which is bounded by the Munzur Mountains in the north. The first morphochronology-based slip rate site of Zabcı et al. (2017) is shown with a red arrow.

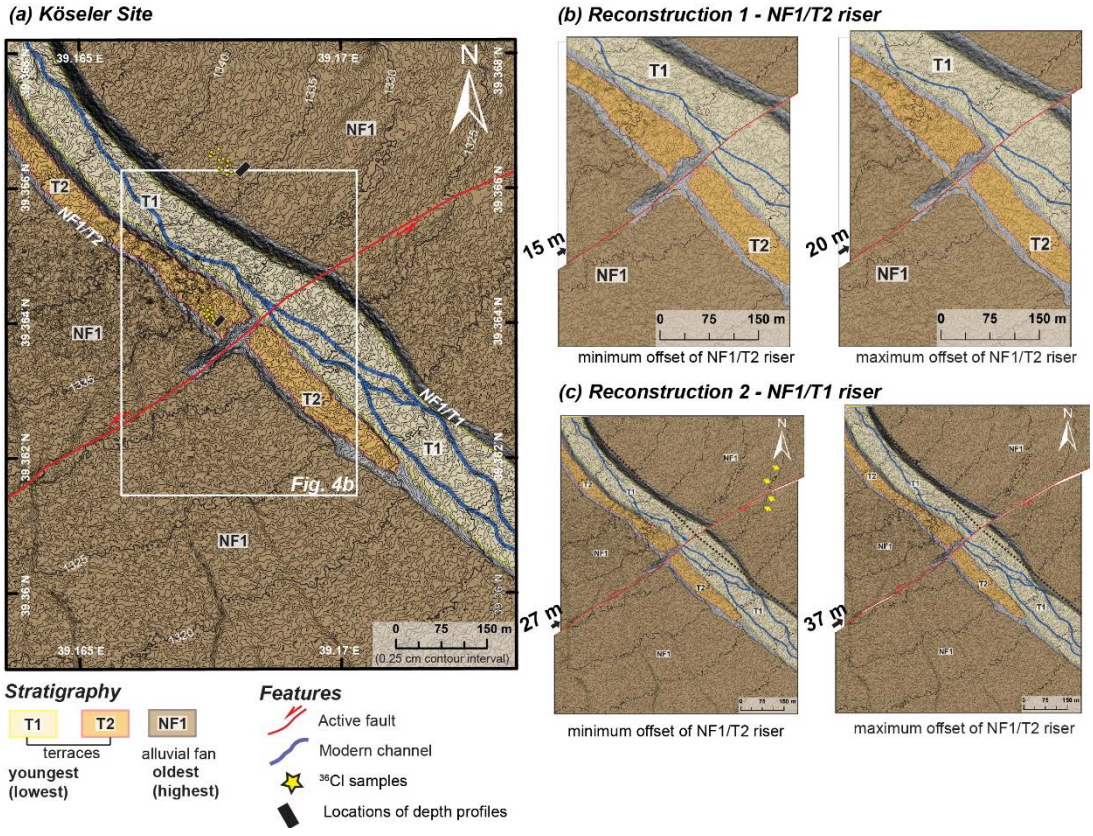

Figure 2.4 : (a) The surficial geological map of the slip rate study of the Zabcı et al. (2017). (b) and (c) are the reconstructions of the total slip for the NF1/T2 and NF1/T1 risers, respectively.

alluvial fan and terrace deposits at the OB yields a higher deformation rate than the geodetic constrains. The alluvial fan surface (NF1), the strath terrace (T2) and the

modern channel (T1) are sinistrally displaced by the OF at the Köseler Site (Fig. 2.3). Offsets of the NF1/T2 and NF1/T1 risers are measured as 15-20 m and 27-37 m, respectively. The surface exposure ages and modelled depth profile ages suggest two different slip rate estimates 1.4±0.3 mm and 2.5+0.7/-0.6 mm, respectively, for the same section of the fault. Considering the high amount of inheritance within the alluvial fan and terrace levels, authors suggest the higher slip rate for the last 6-8 ka history of the OF (Zabcı et al., 2017)

3. GEOLOGY AND NEOTECTONIC DEFORMATION OF THE REGION

The Anatolian Block and the surrounding region are mainly formed under the effect of multiple convergent-collisional events, which are mainly related with the history of the Tethyan oceans. The closure of Palaeo-Tethys led to the deformation on the northern mountain range (the Pontides) during the middle Jurassic in Turkey (Şengör and Yılmaz, 1981). It is then followed by the collision of Anatolide – Tauride Platform with Pontides, which were initiated after the Palaeocene – early Eocene closure of the northern branch of Neo-Tethys (Şengör and Yılmaz, 1981). The last strong deformation occurred during the middle Miocene with the main collision between the Eurasian and the Arabian plate, which has essential impact on the high mean topography of the eastern Turkey (Şengör et al., 2008) and it corresponds to the beginning of the neotectonic period in this particular region (Şengör, 1980; Şengör et al., 1985). This post-collisional rearrangement of tectonic units formed four different neotectonic provinces; the East Anatolian Province of Shortening, the North Turkish Province, the Central Anatolia 'ova' Province and the Western Anatolian Extentional Province (Şengör 1980; Şengör et al., 1985). All these provinces have their own deformation characters such as the compression dominated Eastern Anatolia and the extention dominated Western Anatolia. The 'ova' province, which is delimited with the North Anatolian Shear Zone (NASZ) in the north, the East Anatolian Shear Zone (EASZ) in the east and the Western Extensional neotectonic province in the west, is seismically quitest one after the North Turkish Province (Şengör et al., 1985).

The study region covers the Ovacık Fault and the surrounding region, from the Erzincan Basin in the northeast to Arapgir (Malatya) in the southwest (Fig. 3.1). The geological units of the region are the Keban metamorphics, the Munzur Limestone, the Kemaliye Formation, the Ophiolitic mélange all of which are bounded by faults of various kinematic type (Fig. 3.1). Lack of previous studies especially for precise isotropic age determinations for different units and detailed geologic maps make it difficult to understand the geology of the region. In this chapter, geological

descriptions are mainly based on results of the previous studies and personal field observations for the western part of the Karasu River. For the eastern part, I mainly used multispectral satellite images in addition to previous studies.

3.1 Stratigraphy and Petrography

Along the strike of the Ovacık Fault, 9 different geological units are exposed (Fig. 3.1 and Appendix A). From older to younger, they are: the Keban Metamorphicsmetamorphics, the Munzur Limestone, the Kemaliye Formation, the Ophiolitic mélange, the Tertiary cover deposits, the Çöpler granitoid, the Yamadağ volcanic complex and the Quaternary deposits. Contact relation of the Keban metamorphics, the Munzur Limestones and the ophiolitic mélange are thrusts, whereas younger deposits generally overlie older units with unconformities s (Fig. 3.2 and Appendix A and B).

The low-grade Keban metamorphics (PzMzk) contain marbles and schists, which are unconfomably overlaid by the Kemaliye Formation (Kk) (Fig. 3.2). The Kemaliye Formation, which includes olistostromal facies with blocks of marbles, cherts, magmatics and metamorphics, has exposures mostly at the bottom of valleys. The characteristic unit of the study region, the Munzur Limestones (Mzm), forms the Munzur Mountains to the north of the Ovacık Basin (Fig. 3.1 and Appendix A). The Munzur Limestone is a transgressive sequence of limestone that starts with shallow marine fossiferous limestone passing up to deep marine pelagic limestone (Özgül et al., 1981). The allocthonous Munzur Limestones is thrusted over the Kemaliye Formation and Keban metamorphics (Fig. 3.2). The Cretaceous ophiolitic complex (Cop) are thrusted over the Munzur Limestone from north to south (Topuz et al., 2013) Figs. 3.1 and 3.2). Later, the Tertiary cover deposits (Tc), which include mainly limestone and fine grain clastic rocks, are unconformably overlies all older units (Fig. 3.2). Then, the region cuts by intrusion of the Çöpler granitoids (g), which most probably happened during the Eocene (Bilgiç, 2008). The Yamadağ Volcanic Complex (Tya), which widely spreads at the southwestern part of the study reigon, is composed of basalts, andesites and dolerites (Ekici et al., 2007; Kürüm et al., 2008) (Fig. 3.2). The Quaternary sediments such as debris flow deposits (Qd), alluvial fan deposits (Qaf), morains (Qm) and alluvium (Qal) are the youngest units of the region where they have best exposures in the Ovacık Basin (Figs. 3.1 and 3.2). The Ovacık

Fault cuts all of these units. The OF generally follows contact zones of old units and leads to offset units and Quaternary terraces in the Ovacık Basin.

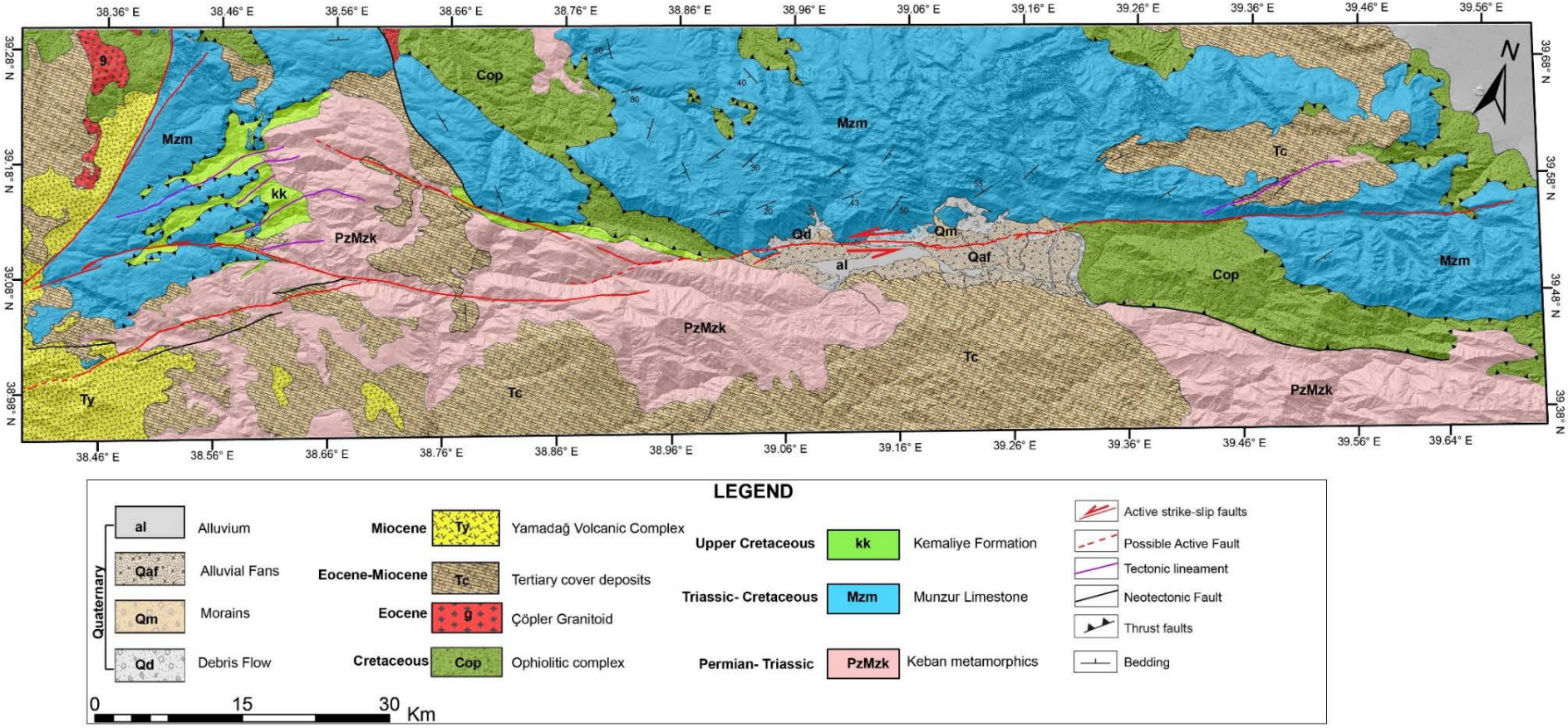

Figure 3.1 : Geological map of the study region. The Keban metamorphics (PzMzk), the Munzur Limestone (Mzm), the Ophiolitic mélange (COp) the Tertiary covers (Tc), are located mainly eastern part of the region whereas the Çöpler granitoid (g) and the Yamadağ volcanic complex (Ty) cover the western part of the region (Bilgiç, 2008; Emre et al., 2012a,2012b,2012c; Özgül et al., 1981, Tarhan, 2008).

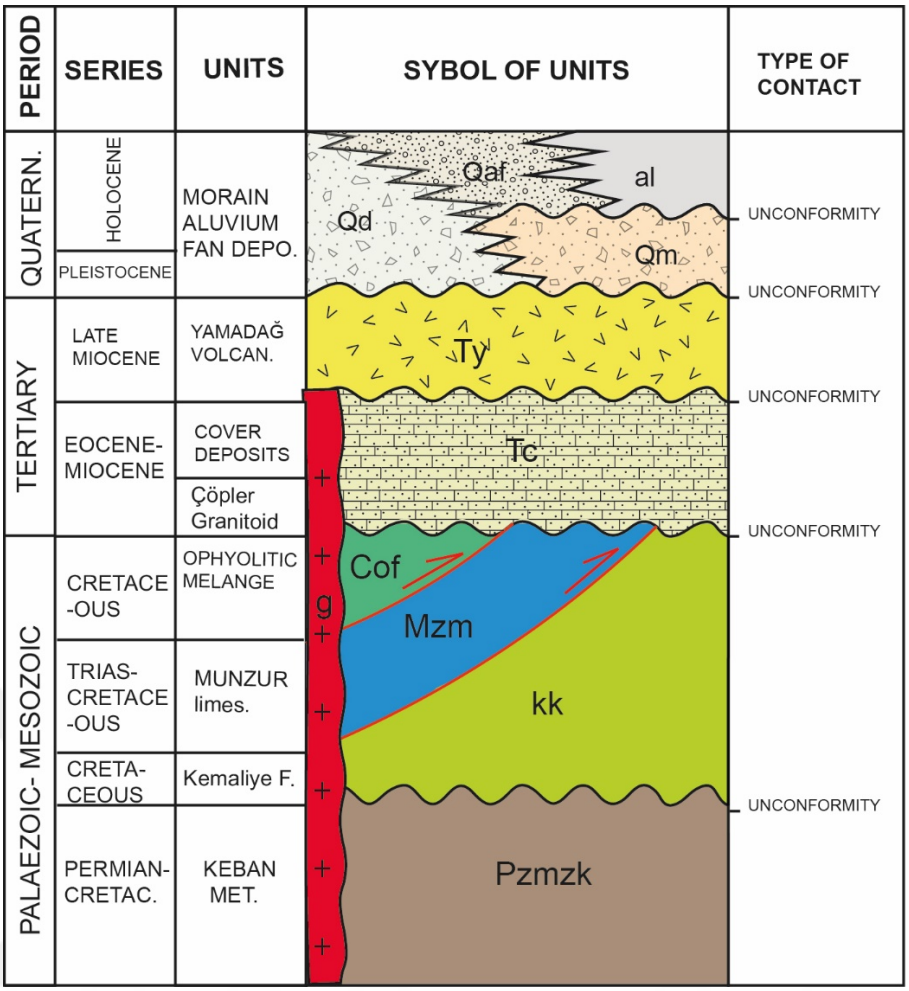

Figure 3.2 : The simplified stratigraphic coloumn of the study region.

3.1.1 Keban metamorphics (PzMzk)

The oldest unit of the study region is green schist facies Keban metamorphics (Özgül et al., 1981). The unit covers huge areas in the study region especially at the southern part of the Munzur Mountains (Fig. 3.1). Along the stretch from Kemaliye to Arapgir, mountainous area is composed of mainly marbles of the Keban Metamorphics.

The Keban metamorphics is generally composed of large volumes of marbles and intercalation of metapelitic schists. Schists are generally fine grain rocks, brownish in colour and have sedimentary origin. Mineral composition of these schists is quartz, feldspar, muscovite and chlorite within calcareous fine grain silicic-clastic matrix, which indicate that the unit is metamorphosed under green schist facies metamorphism. Schists are very thin in the study region, contrary to marbles of the unit that is situated within a very thick package. Marbles of the unit show medium to thick foliation planes, which are even surfaces and parallel to each other. Deformation

within the unit is high as domination of thrusts that divide it into slices (Fig. 3.3 a). Secondary calcite veins (Fig. 3.3d) cut the unit. Dark grey colour marbles of the unit are generally similar to Munzur Limestone in places; thus, it is difficult to distinguish these units (Fig. 3.3). However, the main difference of marbles within the Keban metamorphics form the Munzur Limestone is recrystallization degree of calcite minerals.

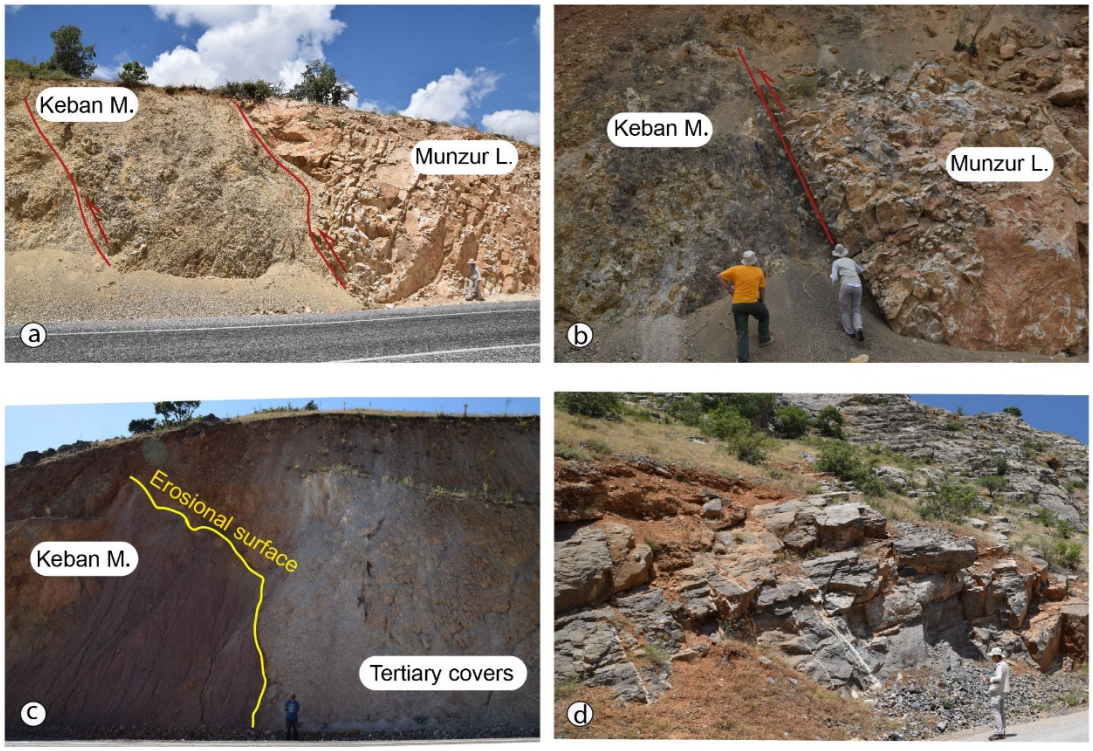

Figure 3.1 : Outcrops of the Keban metamorphics. (a and b) Thrusts between the Keban Metamorphics and the Munzur Limestone, (c) Unconformable stratigraphic contact between Keban and Tertiary deposits, (d) Outcrop of the Keban's marble, which has E-W trending calcite veins.

The Cretaceous Kemaliye Formation and Tertiary cover deposits unconformably overlay the Keban Metamorphics (Bilgiç, 2008; Özgül et al., 1981) (Fig. 3.3c). However, the Munzur Limestone is thrusted over the Keban metamorphics (Fig. 3.3b). The lower contact of the Keban Metamorphics does not expose in the study region.

According to previous studies, fossils including Neohemigordius sp., Agathammia sp., Orbitolina sp., Textulariella sp. give a time interval from Permian to Cretaceous for the Keban Metamorphics (Bilgiç, 2008). A Mizzia velebitana fossil that gives Upper Permian age found in the mid-section of the unit (Özgül et al., 1981). Some corals, rudists and fossil traces represent the late Triassic - Jurassic age for the

stratigraphically upper parts of the unit. Moreover, Cuneolina sp., Orbitolina sp. and Textulariella sp. indicate that the formation was continous during the Cenomanian stage (Bilgiç, 2008). However, during our fieldwork we could not find any fossil within the Keban Metamorphics. From the fossil findings reported in the previous studies and lithological composition of rocks, it inferred that the Keban Metamorphics correspond to shelf type neritic environment (Bilgiç., 2008; Özgül et al., 1981).

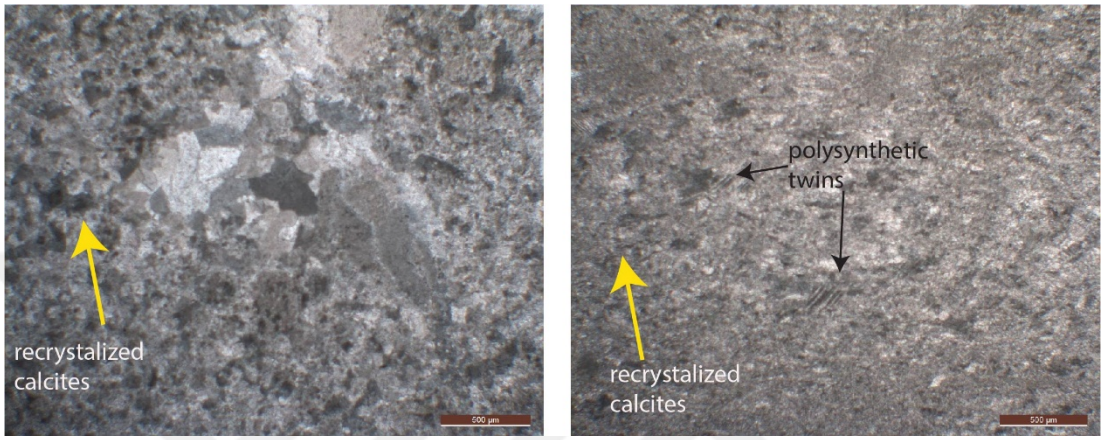

Figure 3.2 : Thin sections of the Keban marbles under cross-polarized light. Recrystallization of grains with reducing of grain size clearly show metamorphic feature of the unit.

Two different samples from marbles of the Keban Metamorphics are investigated under optical microscope (Fig. 3.4). Samples are almost composed of calcite minerals. Size of calcite grains are very fine because of recrystallization by deformation and metamorphism, which leads to grain boundary migration as well. Interestingly, foliations are very weak in the thin sections, although the unit shows foliation in outcrop scale. Calcites also shows polysynthetic twins that form as a result of deformation.

3.1.2 Munzur limestone (Mzm)

A light grey to white coloured allochthonous body of limestones are mapped as the Munzur Limestone that spreads over the northern part of the study region. The Munzur Moutains, eastern continuity of the Tauride belt, are mostly composed of the Munzur Limestone, which are unconformably covered by the Quaternary deposits of the Ovacık Basin at the eastern part of the study region. Özgül et al. (1981) name this continuous sequence of limestones as the Munzur Limestone.

The Munzur Limestone starts with algeous reefal limestone and continues to laminated limestone, oolite limestone and ends up with pelagic limestone as a transgressive

sequence (Özgül et al., 1981). It shows an uninterrupted deposition from the late Triassic to Cretaceous without any significant lateral and vertical changes (Bilgiç, 2008; Ozer et al., 2004; Özgül et al., 1981). During the fieldwork of this study, I observered the Munzur Limestone along the Karasu River. Along this stretch, limestones show thick to medium bedding planes and in some places, it has massive texture. Bedding planes of this light grey colour limestones are various from wavy to parallel. Best exposures of the Munzur Limestone are along the Taş Road at the northern part of the Kemaliye Region (Fig. 3.5).

Figure 3.3 : General structure of the Munzur Limestone. Grey coloured massive Munzur Limestone forms walls of the canion along the Karasu River. The view is from north to south.

The Munzur Limestone is an allocthonous body, which has thrust boundary with all units below, the Keban Metamorphics and the Kemaliye Formation, and it is tectonically overlain by the Ophiolitic mélange. The Tertiary cover deposits unconformably overlies the Munzur Limestone in the mountainous areas, whereas Quaternary deposits cover the Munzur Limestone at the OB in the eastern part of the region.

Limestones, which have approximate stratigraphic thickness around 1200 m, are deposited from shelf to deep marine environment (Özgül et al., 1981). Fossils succession from Algaes, Rudists, Gastropods to Globotruncana that infers a transgressive sequence, are found during previous studies (Bilgiç, 2008; Özgül et al.,

1981). The uppermost part of the Munzur Limestone consists of planktonic foraminiferas, Globotruncana helvetica, Globotruncana tricarinata, Globotruncana linneiana, Globotruncana renzi, Globotruncana arca, Pithonella ovalis, indicate a Turonian to Campanian age (Ozer et al., 2004). The oldest fossil finding yields the Norian (Upper Permian) (Özgül et al., 1981). However, personally I could not observe any fossils or trace of the fossils in the western part of the Karasu River.

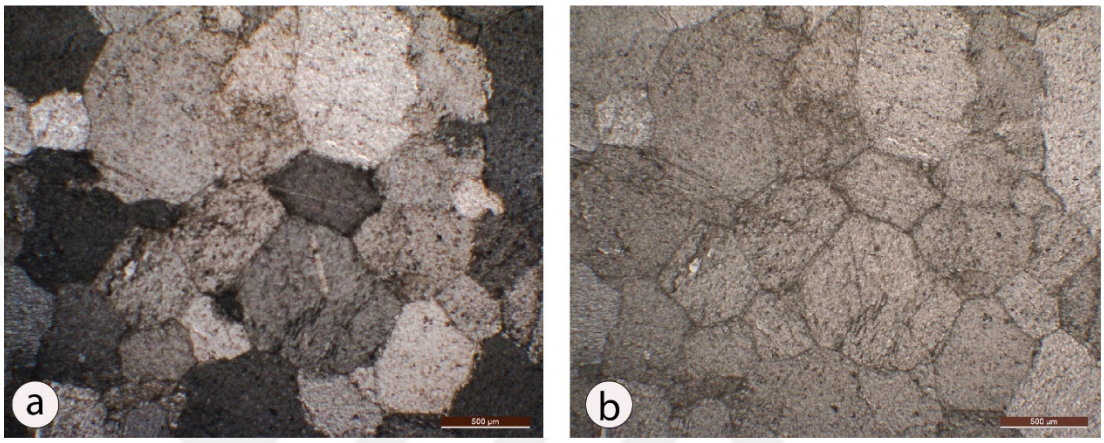

Figure 3.4 : The Munzur Limestone under polarized and plane light. Sparitic limestone with regular shape of the calcite grains indicate that lack of metamorphism contrary to the Keban marbles.

A thin section sample of the Munzur Limestone shows undeformed calcite minerals, which show very few traces of twinning, with sizes around 100 – 500 microns. According to Folk carbonate rock classification, it is a sparitic limestone, which belongs to lower sections of this tectonostratigraphic unit.

3.1.3 Kemaliye formation (Kk)

Wide spread clastic sediments around the Kemaliye Town, which includes coherently foliated silici-clastic rocks with intercalation of limestones and variable type of blocks with various ages and sizes as an olistosromal facies, are mapped as the Kemaliye Formation (Özgül et al1981).

The unit is mainly composed of yellowish brown coloured fine grain silici-clastic rocks (shales and sandstones) with horizons of thinly to medium foliated recrystallized limestone as calc-turbidites. Quartzes, feldspars and chlorites dominate the minerological composition of the clastic rocks that are very similar to schists of the Keban Metamorphics. The unit was metamorphosed under the greenschist facies. Alternation between the clastics and recrystallized limestone is not homogeneous.

Recrystallized limestones constitute thick volumes where the clastics thinly intercalate to it, in places. However, the main structure of the unit is composed of thick volume of clastic rocks, which are intercalated with recrystallized limestones. These limestones sometimes show pinch and swell structures and pinching out to the clastic rocks. Both clastics and recrystallized limestones show coherent foliations, which are generally represented by wavy surfaces. The unit shows asymmetric folding, which has the vergence to the south. Moreover, additional structural observations of folds, faults and S- C structures show the domination of top to south sense of motion.

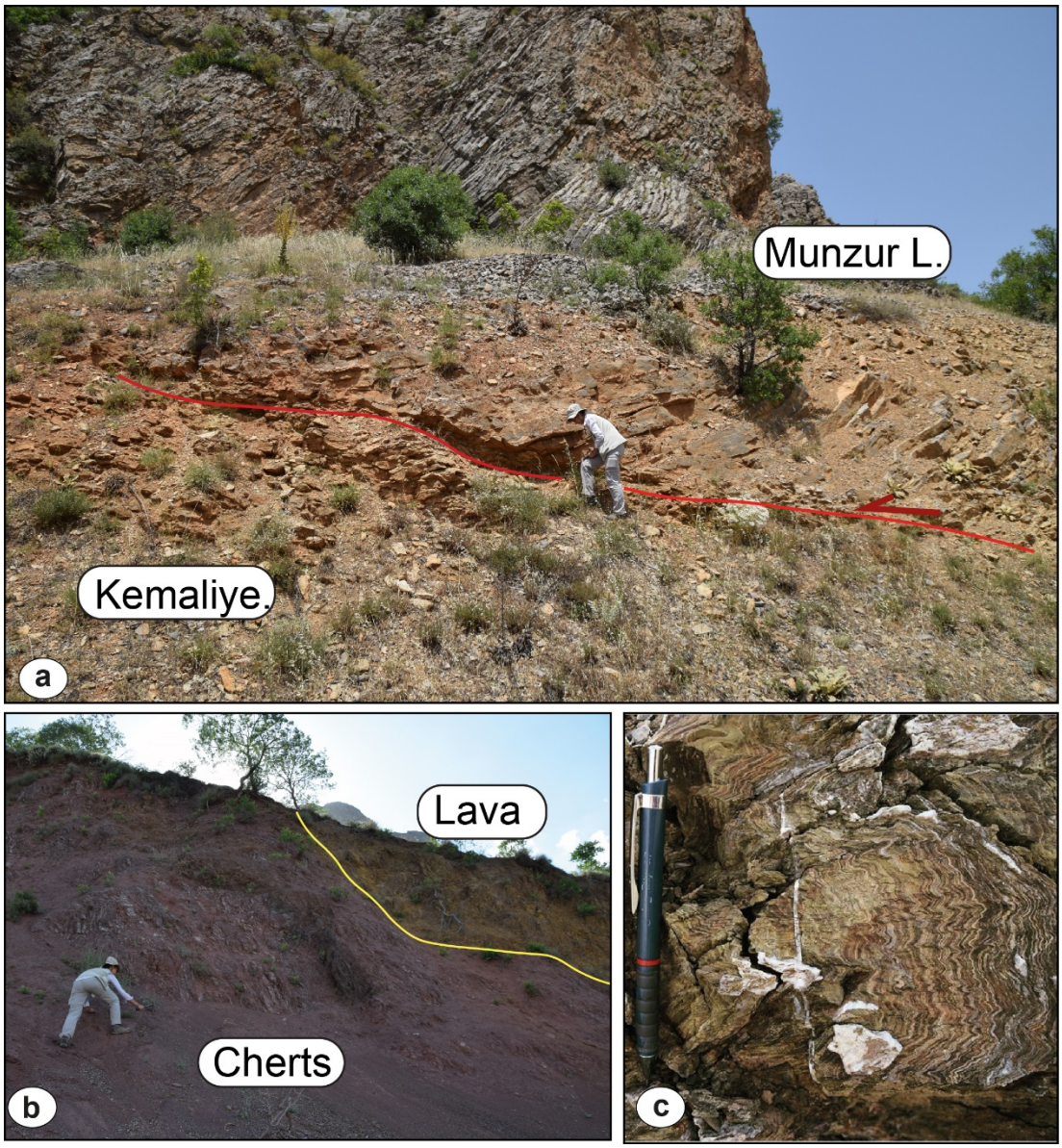

Figure 3.5 : Outcrop views of the Kemaliye Formation. (a) The thrust contact between silisi-clastic rocks of the Kemaliye Formation and the Munzur Limestone, (b) the contact between the chert block and the basaltic lava in the olistostrom, (c) microfolding between crenulation cleavages (C-stuructures) in the silici-clastic rocks of the Kk

The Kemaliye Formation place to place shows olistostromal facies, which are made of of clastic, lava, chert and ophiolitic blocks. The blocks have various sizes, which are embeded in a fine grain clastic matrix of shale composition. Cherts are the largest blocks in the olistostrom, which show thinly coherent bedding (Fig. 3.7b). Black coloured lavas are mainly basaltic in composition, which appear as elliptic blocks in the olistostrom (Fig. 3.7b). All blocks within the olistostrom are very alterated and bounded by faults, which generate tectonites. Faults generally dip to the south and represented by limonites at fault zones. Previous studies suggest that blocks in the Kemaliye Formation are derived from the Keban metamorphics, the Munzur Limestone and the Ophiolitic complex (Bilgiç, 2008; Özgül, 1981). Some fossil findings from the limestone blocks give ages from the Permian to Cretaceous (Bilgiç, 2008; Özgül, 1981). However, the lack of detailed stratigraphic, petrographic studies and absence of age determinations, it is difficult to make a complete stratigraphic and sedimentological evaluation.

The Kemaliye Formation uconformly overlies the Keban metamorphics and is tectonically overlain by the Munzur Limestone. In the western –southwestern parts of the study region this formation is exposed at the bottom of linear valleys where the Munzur Limestone comprises the top of the hills. (Fig. 3.8). The tertiary cover unconformably overlies the Kemaliye Formation.

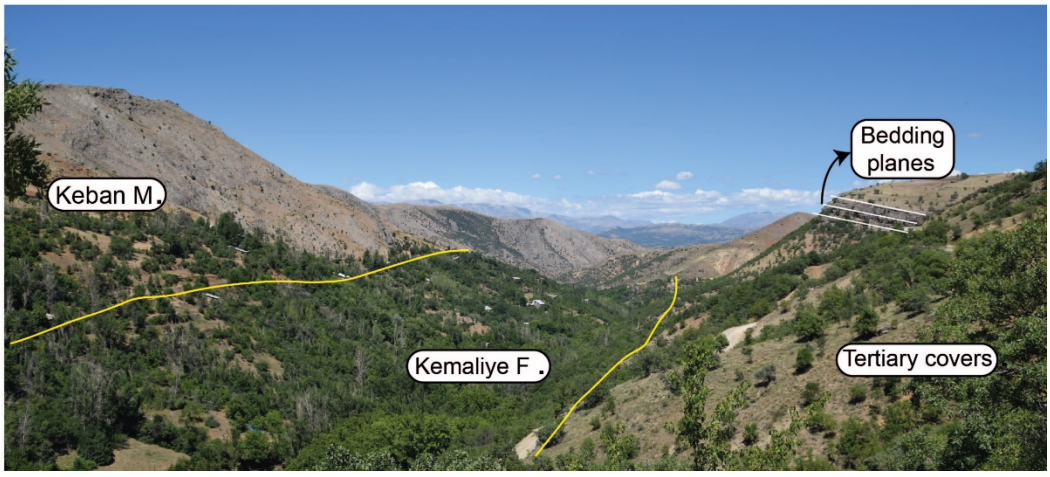

Figure 3.6 : The clastic rocks of the Kemaliye formation covers bottom of valley, whereas the hilltops are made of the Munzur Limestone. Moreover, Tertiary deposits unconformably cover both of these units.

The age of the formation is not well known but it is evaluated to be as late Campanian-early Maastrihtien, which is mostly based on its stratigraphic position (Bilgiç, 2008).

Thin sections of tectonites are very complex and do not give detailed information. However, one of the thin sections includes some pyroxenes, zeolites and an isotropic granate mineral within a cement composed of opaq minerals, which all indicate the granulite facies metamorphism (Fig. 3.10a and b).

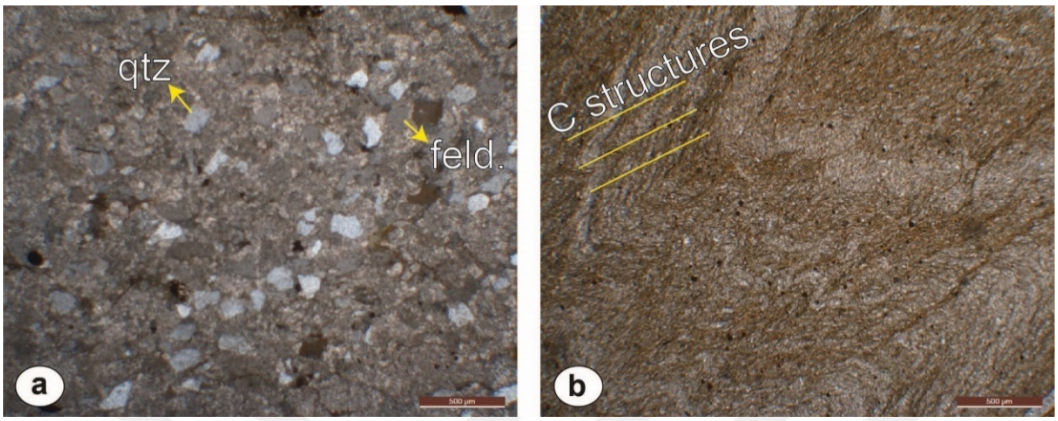

Figure 3.7 : Thin sections of the silici-clastic rocks under cross polarization. (a) a sandstone of the Kk, which includes mainly quartz and few feldspars in a fine clastic cement (b) a fine grain rock which shows microfolding between C structures.

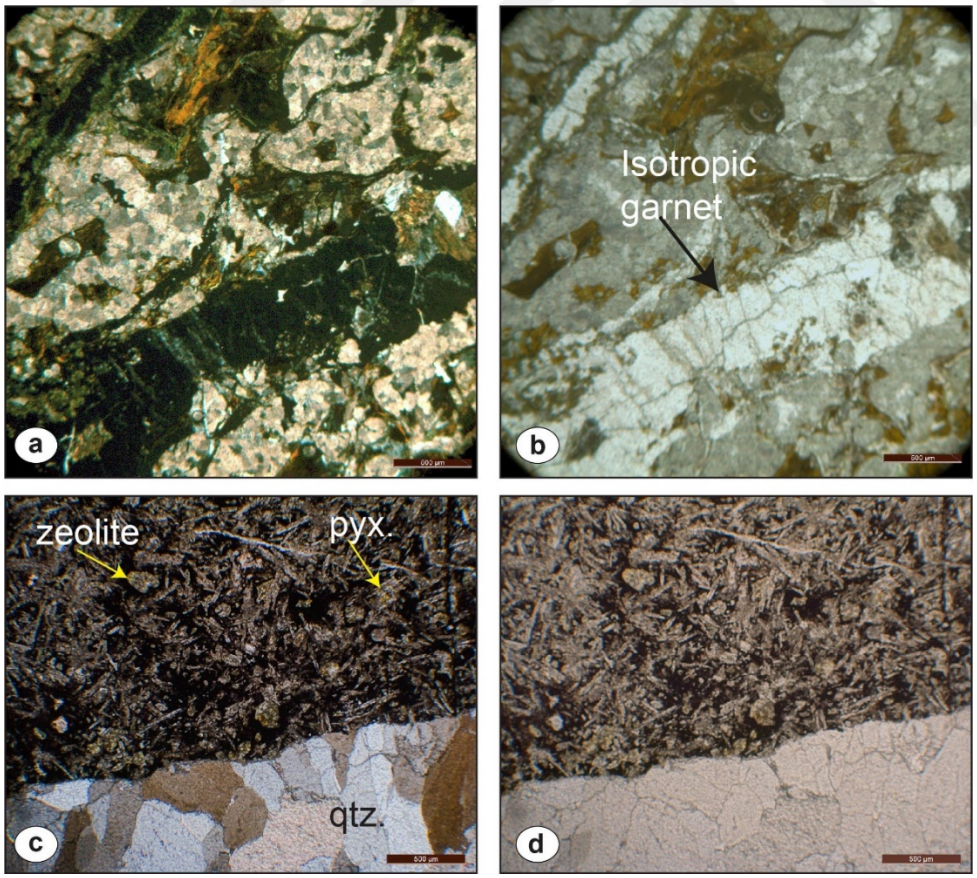

Figure 3.8 : Thin sections from blocks in olistostroms. a and b are from a magmatic body which includes isotropic garnet under cross and parallel polarization respectively. c and d are very alterated basaltic lava that is later cut by quartz vein.

The other thin section of a basaltic tectonite includes brownish coloured pyroxenes and plagioclases in a matrix that is fully composed of opaque minerals (Fig. 3.10c and d). In the thin section, zeolites also look in circular shapes. The rock has a basaltic composition that is later cut by a weakly metamorphosed quartz vein.

From this point of view, I interpret that the Kemaliye Formation was formed olistostramal facies rock includes blocks of ophiolite, chert and basaltic lavas emboded in fine grain silici-clastic matrix. According to previos studies, depositional environment of the Kemaliye Formation is interpreted as an unstable marine environment.

The Kemaliye Formation shows all kind of deformation in various directions which are related with multiple deformation.

3.1.4 Ophiolitic melange (COp)

The Ophiolitic mélange that exposed in the study region is named as the Refahiye ophiolitic mélange (Yılmaz et al.,1985; Aktimur et al., 1986), Eriç ophiolitic mélange (Özgül et al 1981), and Divriği ophiolitic mélange (Tunç et al., 1991). It is mainly exposed at the edges of the Ovacık Basin and to the west of the Malatya Fault (MF) (Fig. 3.1).

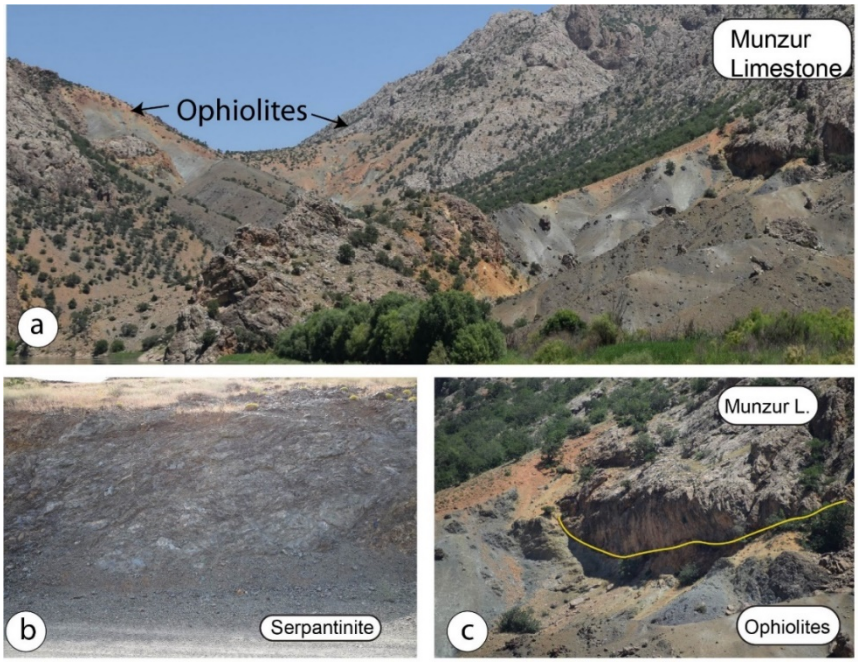

Figure 3.9 : Outcrops of the ophiolitic mélange. (a) and (c) are thrust contact between the ophiolitic mélange and the Munzur Limestone. These outcrops are located at the northern part of the Karasu River. (b) is an outcrop of a serpantinate at the western part of the Malatya Fault (Appendix 1 and 2)

The COp includes large volume of greenish serpentinate, dunite, peridotite, gabbro and limestone blocks. Fossil findings in the limestone blocks suggest the late Permian age for the unit (Özgül et al., 1981). However, the emplacement of the ophiolitic mélange is assumed as late Campanian – early Maastrichtian based on the stratigraphic relation, where Upper Cretaceous-Eocene flysch and clastic sediments unconformably cover the ophiolitic mélange (Sarifakioğlu et al., 2009; Topuz et al., 2013). In addition, the crystallization age of the isotropic gabbro collected from the mélange in the region, which is located to the north of the study area, is early Jurassic (U-Pb zircon age) (Uysal et al., 2015).

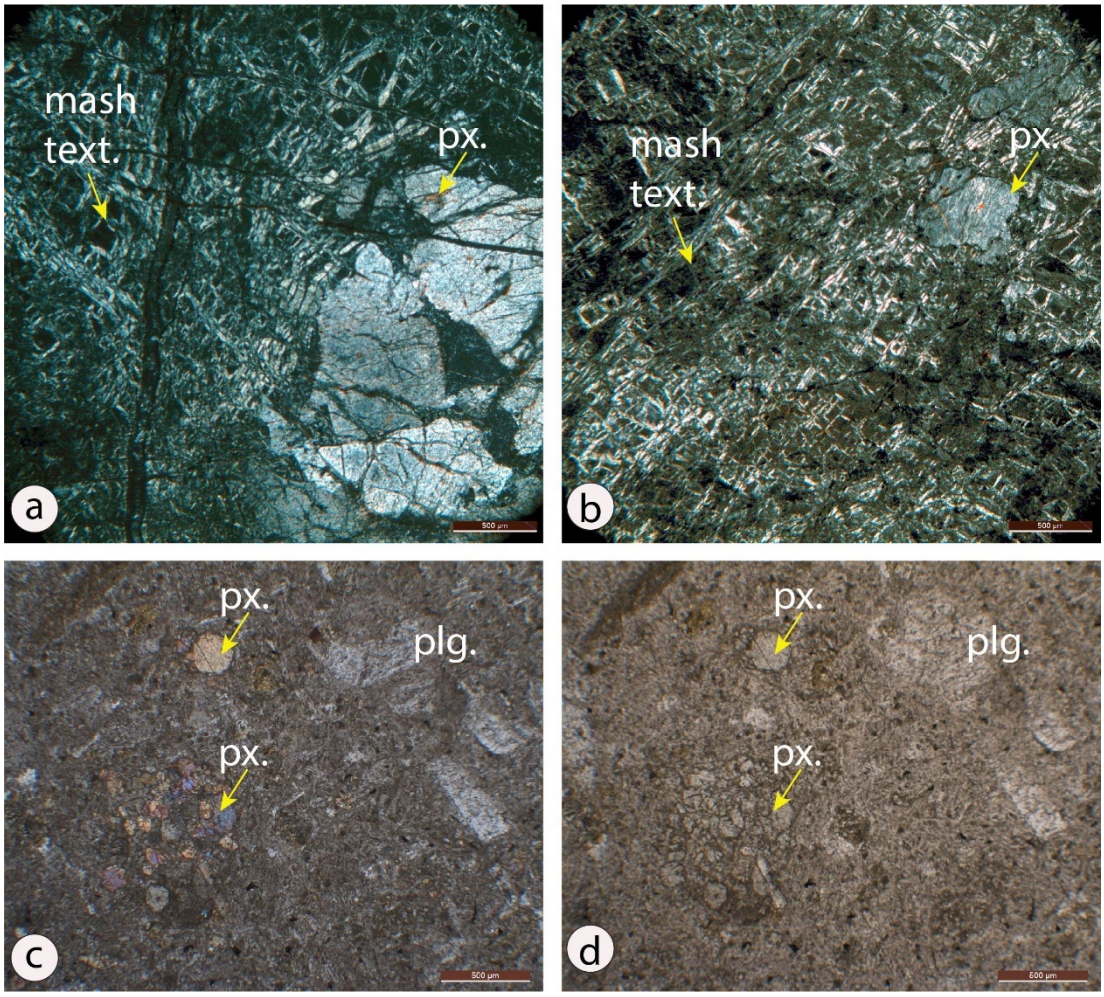

Figure 3.10 : Thin sections of the ophiolitic mélange. Lefthand side are views under cross polarization, whereas righthand side are with parallel polarization. (a) and (b) show a clear sample of a serpentinate with its typicall mash texture. (c) and (b) belong to a magmatic body in the mélange, which is diabasic in composition and texture

These ophiolitic rocks thrust over the Munzur Limestone with the vergence from north to south – southeast and a steep fault surface. The formation of this ophiolitic mélange started with the rifting processes during the Triassic – Cretaceous, then after the

convergence it was uplifted and emplaced during the late Creteceous (Ozer et al., 2004). This unit is generally located at the northern part of the region, where the region is affected both by the OF and the MF. The Malatya Fault at the northern end of the MF reactivates the old thrust contact between Cretaceous Ophiolitic melange and the Munzur Limestone. This reactivation leads to rotation of the fault plane in places (Fig.3.11c).

The Cretaceous ophiolites spread on the valleys of the Munzur Mountains where the relief is low.

The thin section of serpantinite shows clear mash texture with pyroxene phenocrstal. All primary texture are missing in the thin section because of serpantinization (Fig. 3.12 a; b). The other sample is from a diabase dyke within the mélange. This light grey coloured intrusive rock includes mainly plagioclase and pyroxene. Plagioclases, which are phenocrytals within the matrix, form the porphyritic texture (Fig. 3.12 c; d).

3.1.5 Tertiary cover deposits (Tc)

In the study region, I mapped all young clastics and carbonate rocks as Tertiary cover deposits. This unit includes the Eocene Subasi Formation (Özgül et al., 1981), the Bozbel Formation (Kurtman, 1973), the Dedek Formation (Özgül et al., 1981), the Miocene Başpınar formation (Özgül et al., 1981) and the Eocene – Miocene Kırgeçit Formation (Aksoy, 1996b, a). Since different ages are suggested to the same unit with the absence of absolute dating, I combined all these units and map them as a single one in order to avoid this age complexity.

This cover deposits are exposed along the Ovacık Fault. However, main volume of this rocks is located to the southwestern part of the region. This unit unconformably overlies all older units, the Keban Metamorphics, the Kemaliye Formation, the Munzur Limestone and the Ophiolitic mélange, whereas the Çöpler granitoid and the Yamadağ Volcanic Complex intrude through it.

These cover deposits are composed of conglomerates, sandstones, shales, marls and limestones from younger to older stratigraphic order. The conglomeratic and clastic rocks, which are generally located around the Yaylacık Village, are cemented with calcite. This cement comprises Nummulit sp., Alveolin sp. and Ostrea shells that reflect the shallow marine environment. Majority of conglomerates composed of grains of the Munzur Limestone and the Keban Metamorphics. It is generally para-conglomerate with various grain size and various grain sorting.

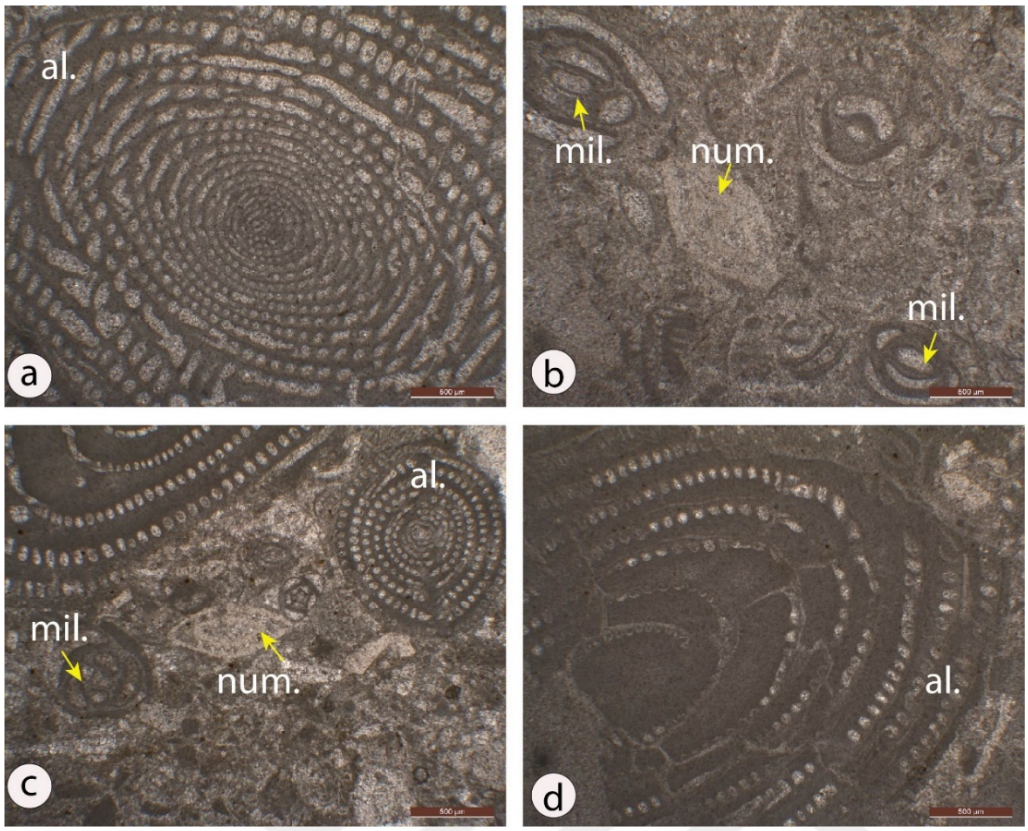

Figure 3.11 : Thin sections of the Tertiary cover deposits. The biomicritic limestones includes *Alveolina sp*. (a, c, d), *Nummulites sp.* (b, c) and *Miliolidae* (b, c) fossils.

Figure 3. 14: Outcrop views of the Tertiary cover deposits. (a) is a continuous section of a fossilferous limestone that is cut by a normal fault (red dashed line) close to the Arapgir Town. (b) and the cross-cutting relationship (yellow line) between the Yamadağ Volcanic Complex and the Tertiary cover deposits

Figure 3.12 : (Continue): Outcrop views of the Tertiary cover deposits. (a) is a continuous section of a fossilferous limestone that is cut by a normal fault (red dashed line) close to the Arapgir Town. (b) and the cross-cutting relationship (yellow line) between the Yamadağ Volcanic Complex and the Tertiary cover deposits.

3.1.6 Çöpler granitoide (g)

The light grey coloured plutonic rocks cut all older units, especially in the northwestern parts of the study region. This rock is mapped as the Çöpler graniotid (Bilgiç, 2008; Tunc, 1991) and vary in composition from quartz monzonite and monzodiorite (Bilgiç, 2008).

Figure 3.13 : The outcrop of the intrusive body of the granitoid. In some part of the outcrop the columnar fractures of the rock is preserved (yellow arrow)

Deformation and alteration is high in the unit as it is exposed very close to the Malatya Fault (MF). The unit is exposed within a shear zone that is the MF and comes to same position with the ophiolitic mélange. The unit composed of intrusive and epiclastic volcanic rocks. The intrusive body shows systematic cooling structures (Fig. 3.15).

The thin section includes plagioclase, amphibole, K-feldspar and few quartzes. It has a granular texture with phenocryst of plagioclase and amphiboles. According to mineralogical composition, the rock should be monzonitic composition.

This unit is intruded through the Tertiary cover deposits and all older units in the northwestern part of the study region. However, it is probably related with the Eocene tectonism of the Anatolian Block This unit has wide spread by its magmatic, volcanic and volcano-clastic rocks.

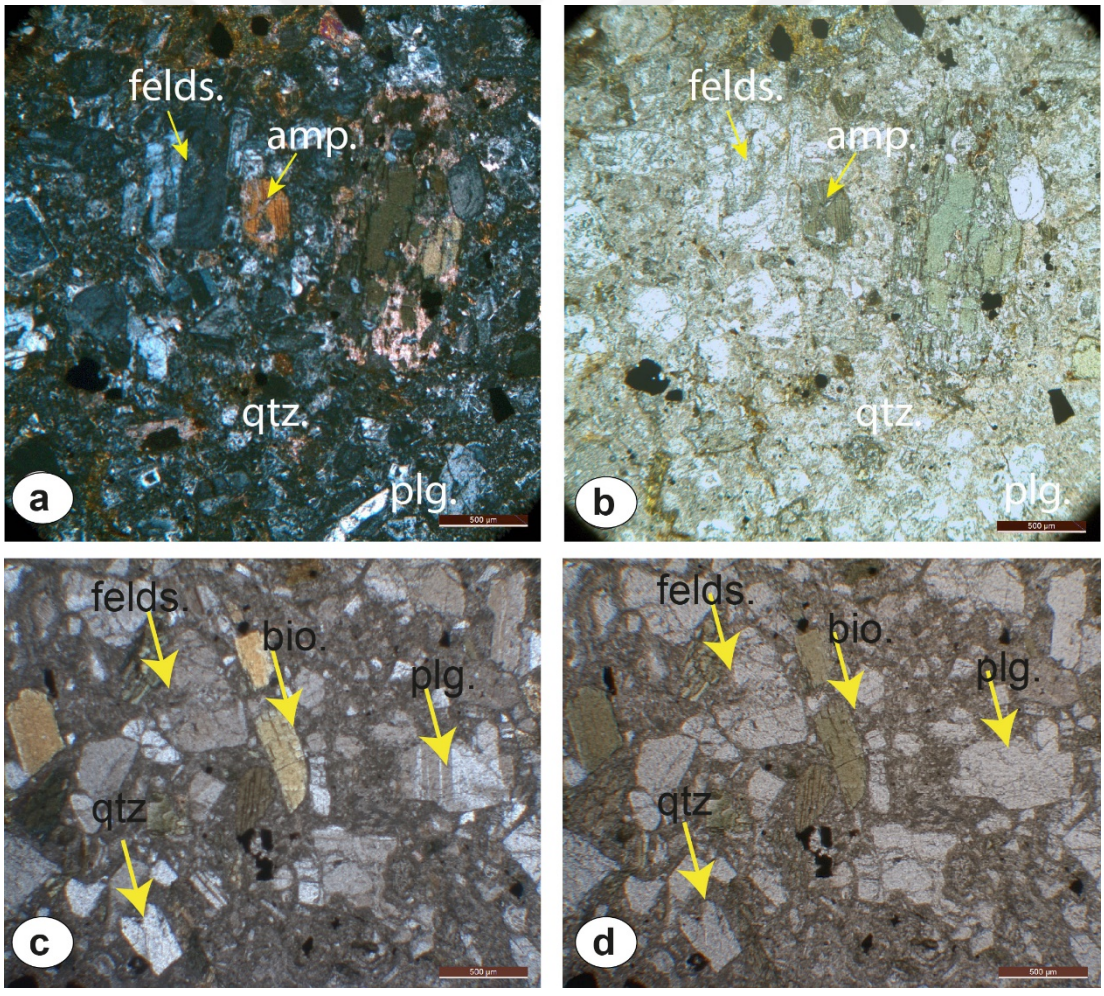

Figure 3.14 : Thin sections of the Çöpler granitoid. (a) the mineralogical composition is plagioclase, amphibole, feldspar and few quartzes in the intrusive body. Porphyritic texture with phenocrytals of plagioclase and feldspar infer a monzonitic composition. (b) The epiclastic rock of the unit, which is composed of feldspar, quartz, biotite and plagioclase.

The age of emplacement of the granitoid body was later than late Campanian (Özgül et al., 1981). However, Tunç (1991) claims that this unit also cuts the Eocene units, which means that the age of the intrusion should be later than Eocene. Furthermore, two isotophic age determinations give intrusion age of 37.2 ± 2.5 and 44.5 ± 2.5 My (Middle-late Eocene) (Yazgan, 1983).

3.1.7 Yamadağ volcanic complex

A large volume of volcanic rocks at the southern part of the study region is mapped as Yamadağ Volcanic complex (Cengiz ve diğ., 1993). The complex includes plutonic, volcanic and pyroclastics rocks along the southwestern parts of the study region.

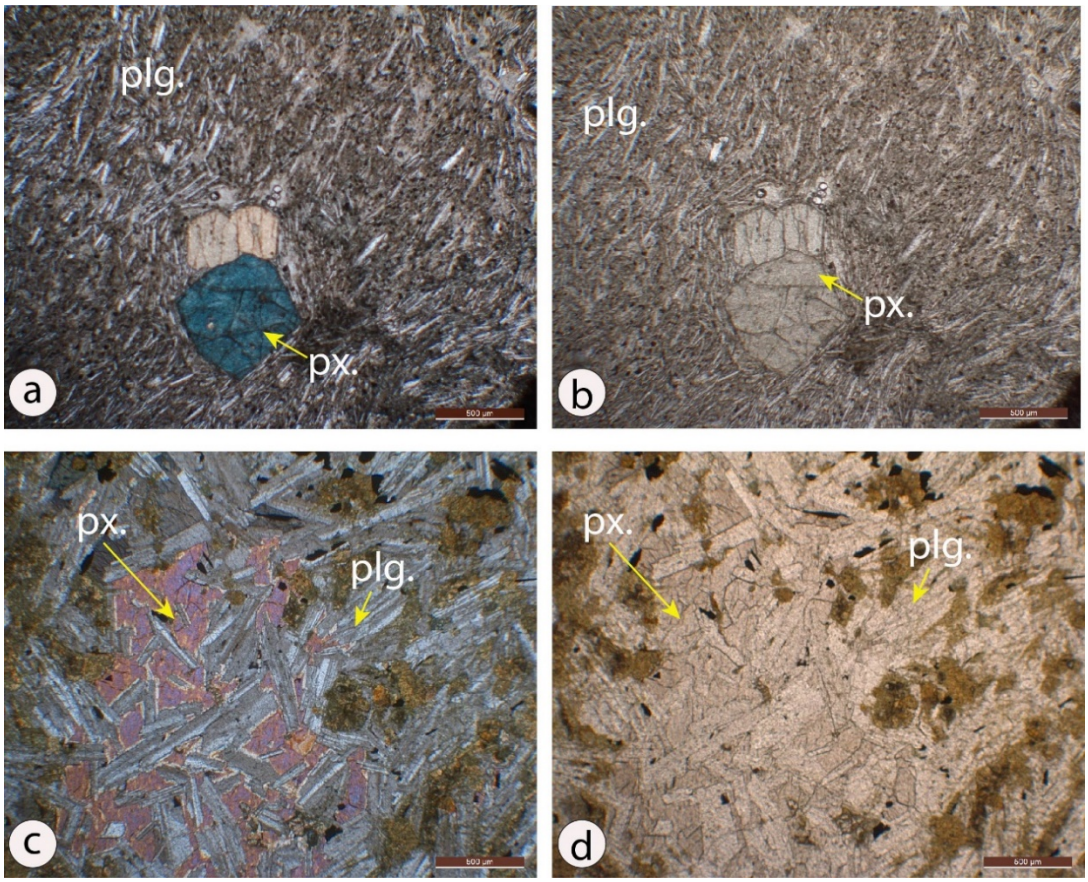

Figure 3.15 : The Yamadağ Volcanic Complex under optical microscope. (a) and (b) show a basaltic composition with the existence of plagioclases and pyroxenes under cross and parallel polarization, respectively. Plagioclases show preffered orientation of flow foliation. (c) and (d) a sample of dolerite that show granular texture with phenocrysts of pyroxenes and plagioclases.

This complex is composed of basaltic and andesitic lavas, tuffs, and dolerites. The most complete sections are exposed around Arapgir. The colour of the exposed rocks is generally greenish grey to black. The complex also includes vesicular bubbles and

coloumnar basalts. Previos studies divide the complex into 3 petrochemical subgroups: subalkaline basalts, trachyandesites, and dacites. Trace and REE geochemical data for the subalkaline basalts and the trachyandesite reflects an E-MORB type mantle source, whereas the dacite magma suggest an OIB type a lithospheric mantle source (Kürüm et al., 2008). 40Ar/ 39Ar age determination yields 15.8 ± 0.2 Ma for basaltic lava flows and 17.6 to 14.7 ± 0.1 – 12.2 ± 0,2 Ma for dacitic lavas (Kürüm ve diğ., 2008). According to age and magma sources, the Yamadağ Volcanic Complex was generated within a post-collisional extentional setting (Kürüm et al., 2008)

However, (Ekici ve diğ., 2007) suggest that the begining of the collision between the Eurasian and Arabian plates happened around 12 Ma and they interpret this date as the time of emplacement for the Yamadağ Complex. The chemistry of volcanic rocks indicates the melting of metasomatized mantle, crystal fractiation, magma mixing and assimilation of crustal material. An 40K/ 40Ar age dating using the whole rock shows that the complex formed during 15 ± 0,5 – 12 ± 0,5 Ma.

Thin section of basalt includes mainly plagioclase and pyroxene with microlitic texture. Plagioglaces preserve its flow texture. Other lithology in the complex includes plagioclases and large pyroxenes with clear ophitic texture, suggesting a doleritic composition and texture. The existence of orthopyroxenes in the dolerite suggests that it is tholeiitic in composition.

3.1.8 Quaternary cover

Quaternary deposits are mainly located in the Ovacık Basin. The valleys of the Munzur Mountains show morains, which are formed mostly during the last glacial maximum. Moraines, which consist mainly of limestone gravels eroded from the Munzur Limestones and carried by glaciers, cover the basement rocks unconformably in the northern part of the Ovacik Basin. The ridge, which is located to the south of the Gözeler Village and is composed of morain sediments and is bounded by the Ovacık Fault from the north (Fig. 3.18b). Alluvial fan deposits and fluvial river deposits cover moraines in the study area. In addition, the northern margin of the Ovacık Basin is covered with debris flow. Morphologically the most dominant structures are alluvial fans of the Ovacık Basin, which are located at both northern and southern sides of the basin. Nevertheless, the most wide-spread fans are found at the northern part of the OB. The northern alluvial fans are composed of pebble-to-boulder size gravels, which derived from Munzur Limestones, whereas the fan deposits on the southern side are

derived from the Tertiary cover deposits and the Keban metamorphics. These alluvial fans are cut by the OF. The all riverbeds including Munzur and Karasu have alluvium deposits at their modern channels

Figure 3.16 : (a) a photo of the Ovacık Basin where an alluvial fan, a tributuary channel and a morain are indicated by yellow arrows. (b) The Quaternary geological map of the Ovacık Basin (Zabcı et al., submitted).

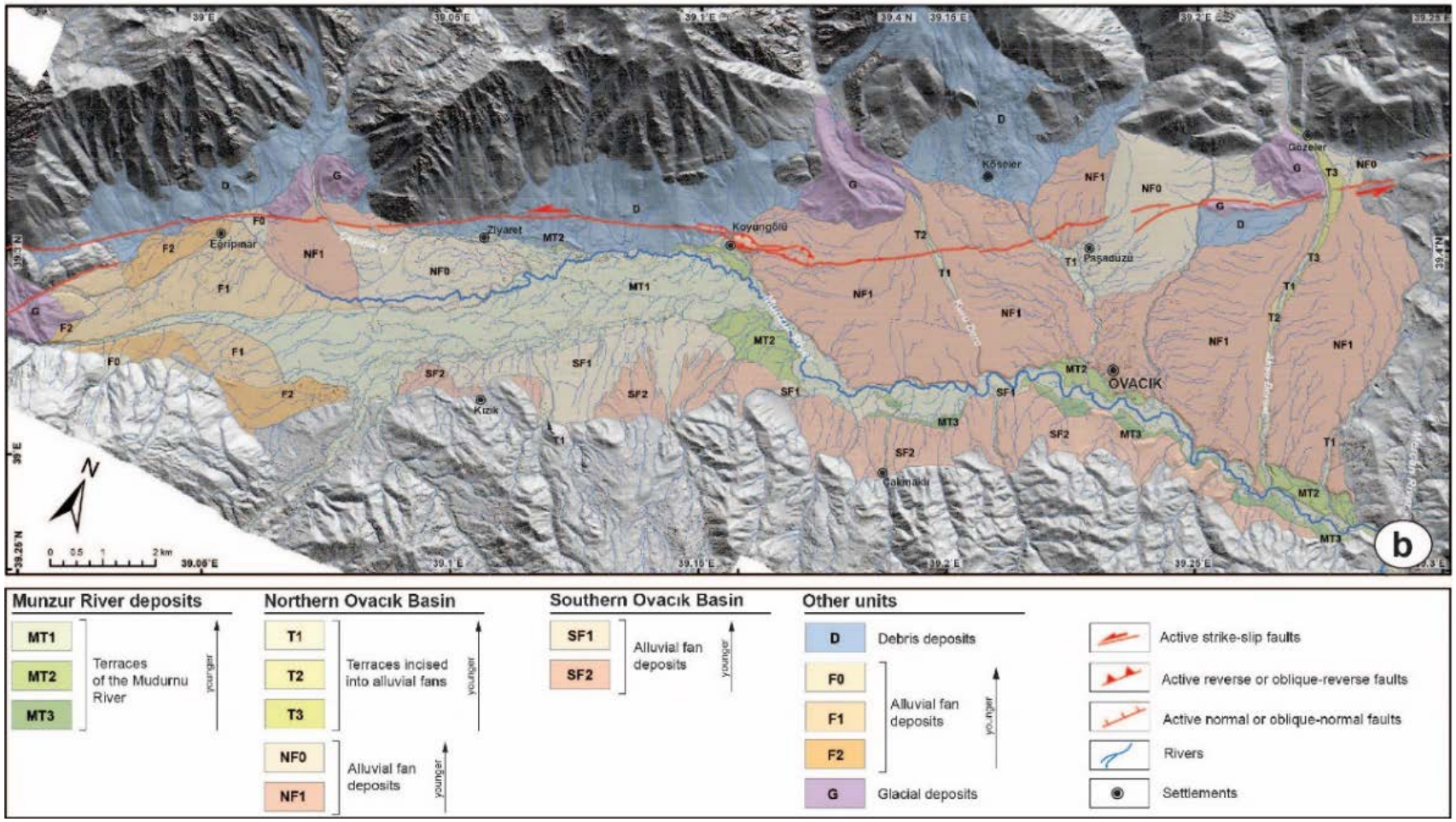

Figure 3.18 (Continue): (a) a photo of the Ovacık Basin where an alluvial fan, a tributuary channel and a morain are indicated by yellow arrows. (b) The Quaternary geological map of the Ovacık Basin (Zabcı et al., submitted).

3.2 Structural Geology

The complex geological setting of the region makes difficult for the analysis of the geological structures and the determination of the different deformation phases. During the fieldwork, the main focus of the data collection was related to the understanding of the recent deformation of the Ovacık Fault and the surrounding region. Unfortunately, I could not pay equal attention to older phases of deformations recorded in the rock. Because of that in this section, only most general structures related to paleo-tectonic period were described, whereas the structures of the neotectonic period are better investigated.

The study region is deformed by multi-character processes from the thrust dominated compression to strike-slip tectonics and even extention during palaeo and neo- tectonic periods. The study of the paleo-tectonic structures is mostly based on the orientation of bedding planes in the Munzur Limestone and Tertiary cover deposits and foliation planes of the Keban Metamorphics and the Kemaliye Formation. Nevertheless, my field data point out that units, especially the Keban metamorphics and the Kemaliye Formation, have various orientations. Measurements from faults in different lithologies also suggest a change in the stress direction in time. On the other hand, the neotectonic deformation is mainly dominated by the strike slip tectonics in the study region. The relatively young units, the Tertiary cover deposits, the Yamadağ Volcanic Complex and the Quaternary deposits, and active fault segments of the OF provide data on the character of the neotectonic deformation in the study region.

3.2.1 Folds

Foliations in the Keban Metamorphics and the Kemaliye Formation have various dip directions, which are dominantly to the NE. A tight fold, which is clearly represented in the density diagram with the increasing density (black dashed line represents the best fitting girdle of poles of foliations in the Fig. 3.19). The red star in the same density diagram indicates the fold hinge with plunge direction and plunge of 58°/23° (Fig. 3.19a, b).

The Munzur Limestones dip to the north and southeast, which form an open fold with and obtuse angle (90˚-120˚) between limps. A girdle (black dash line) and its pole (red star) indicate that the hinge of the fold has plunge direction and plunge of 61˚/13˚ (Fig.

3.19c, d). The Tertiary cover deposits gently dip to the east. The density diagram of this unit shows an open fold, which has a fold hinge with 72˚/20˚ plunge direction and plunge (Fig. 3.19e, f). From these stereonet analyses of limited measurements, it can be assumed that all study region gently dips to the east in the western part of the OF.

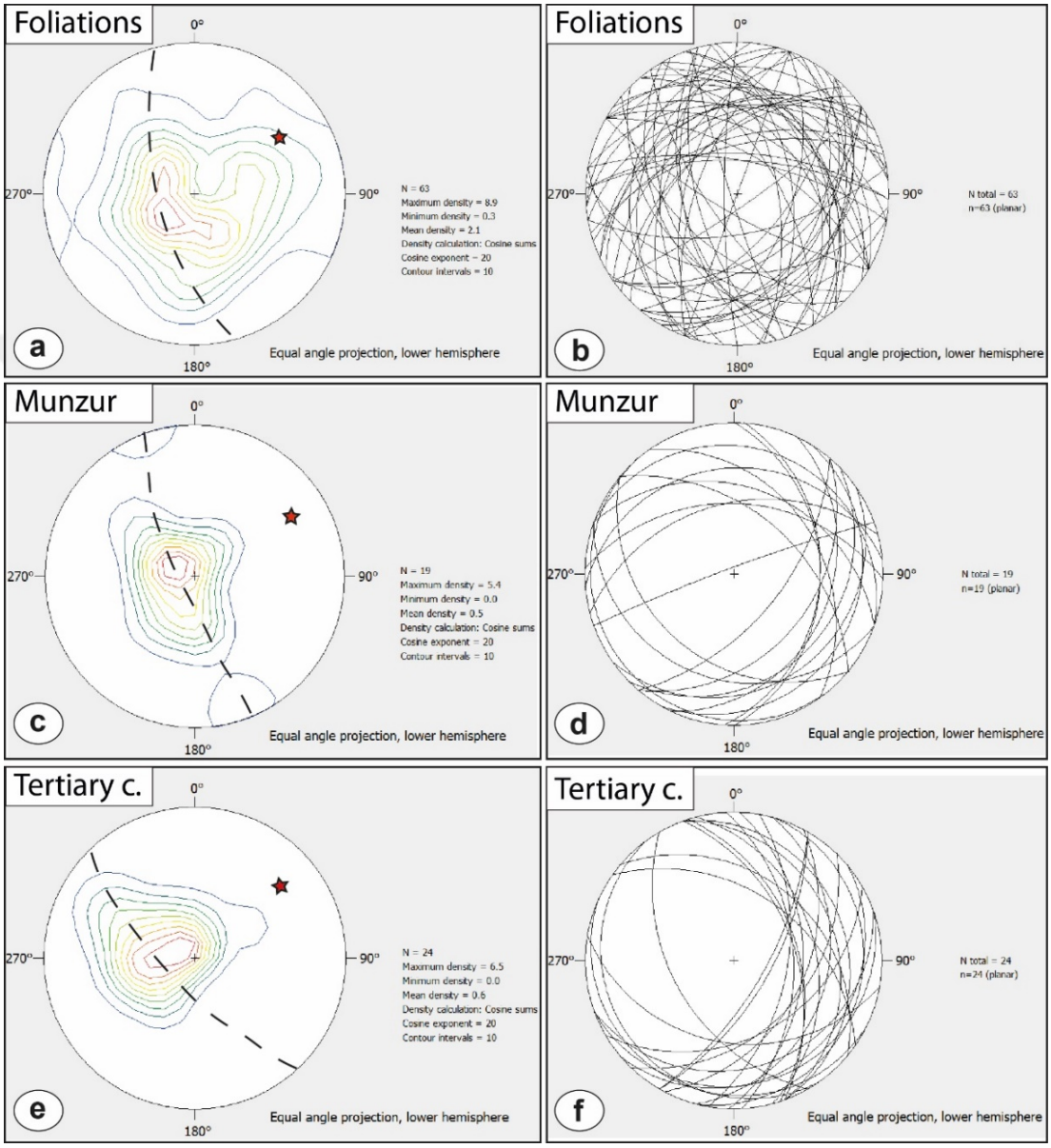

Figure 3.1 : Orientation of the planar structures in the main units of the region. (a) Density diagram of foliation planes in the Keban Metamorphics and the Kemaliye Formation, (b) great circles, which show folded structure with main dips to E-NE. (c) density diagram and (d) great circles of bedding planes in the Munzur Limestone, which show NE- E orientation of dip directions. (e) density diagram and (f) great circles of bedding planes in cover deposits, which also show mainly E- NE dipping direction. Black dashed lines in density diagrams are best fitting line of poles, whereas its pole (red stars) refers to the fold hinges.

3.2.2 Faults

The study region has tremendous number of faults in various orientation and they show different kinematic properties. However, it is difficult to obtain a regular pattern because of high deformation in the region (Fig. 3.20). Many fault planes show different orientation of striations, because of regeneration of existing fault planes through different deformation phases.

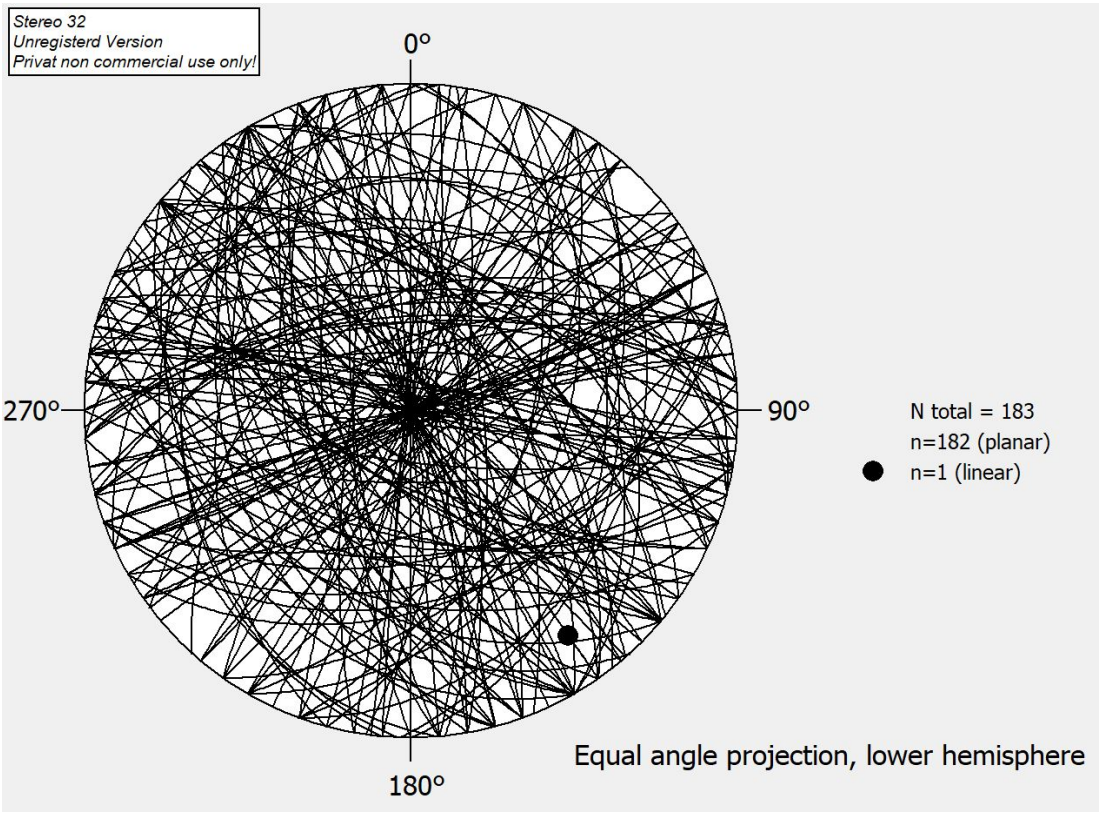

Figure 3.2 : All measured faults in the study region. Complexity of the region can be understood from the figure.

To analyse this complex pattern; first, I classified my measurements according to geological units in order to include a temporal control. Then, I plotted fault planes, measured striations and movement planes (M-planes) in order to understand the principle stress directions by following the methodological steps of (Aleksandrowski, 1985). That's why I plotted fault planes, striations, and determined M–planes for the Kemaliye Formation, the Munzur Limestone and the Tertiary cover deposits separately. However, I observed that fault striations are not well developed in the Yamadağ Volcanic Complex, which shows shallow level deformation rather than deeply buried faults with a higher confined pressure. Therefore, there is no M- plane solutions for the Yamadağ Complex.

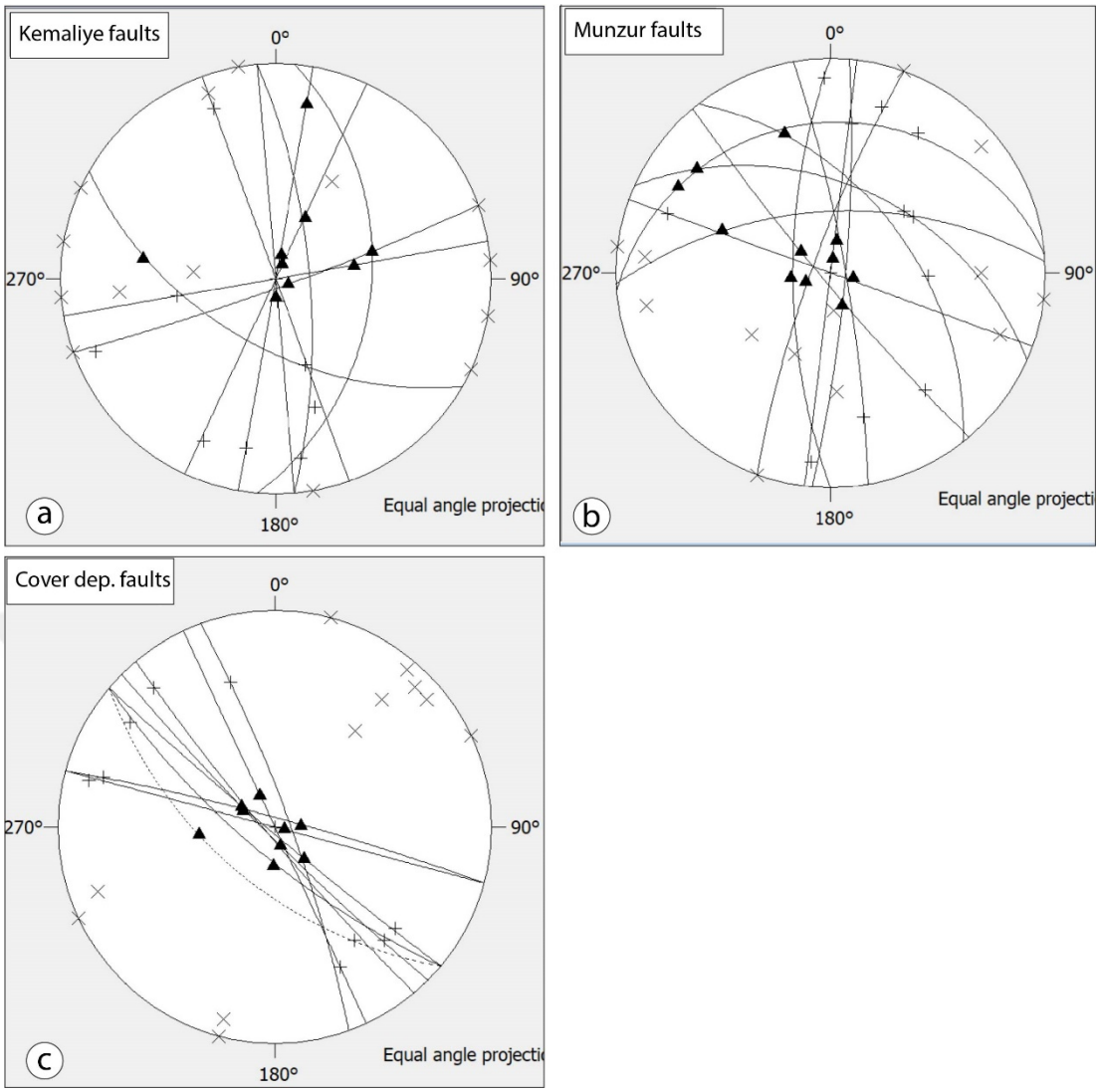

Figure 3.3 : Stereonets showing fault planes (great circles) and their poles, where (x) are for striations, (+) are for fault planes' poles and black triangles show poles of movement planes. (a) Individual analysis for structures of the Kemaliye Formation, (b) Munzur Limestone, and (c) Tertiary cover deposits.

In these diagrams (Fig. 3.21), fault planes and its poles represented by great circles and x symbols, where black triangles are poles of the movement planes (M-planes). The distribution of sigma 2 (σ_2, or, σ_{int}) is represented by the pole of the M-planes on the stereonet. However, a common concentration of the poles of M-planes are located around the centre of the stereonet for almost all units, which indicates a strike-slip dominated tectonic setting. The Kemaliye Formation and the Munzur Limestone have different orientations of σ2, which points an oblique strike slip faulting with a compressional component (Figs. 3.21a, b, c; Fig. 3.22). It is clear that these data are not sufficient in order to understand the long-term deformation of the region. However, interpretation of all available data is an incremental step and contribution on

understanding the structural history of this poorly known region. From this point of view, I can say that the northern part of the study region, especially the western part of the Karasu River, where the Ovacık Fault and Malatya Fault meet each other, has a transpressional tectonic setting. However, to the south, around Arapgir, strike-slip deformation becomes dominant.

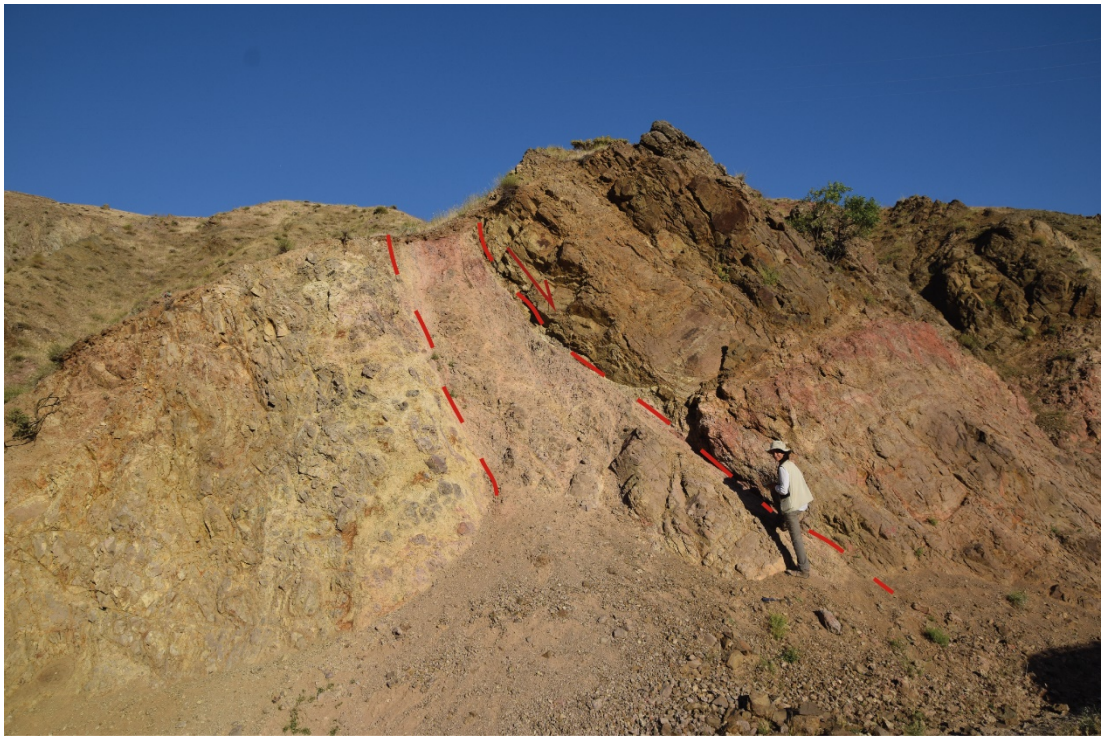

Figure 3.4 : A normal fault zone within the Yamadağ Volcanic Complex. Although the unit is deformed by many faults, the absence of striations indicate of shallow level deformation and prevent the construction of M-planes and palaeostress analysis.

3.3 Remote Sensing

The remote sensing is a developing technic that allows us to analyise any object by using ‘remotely’ obtained data. Electromagnetic (EM) and Ultraviole (UV) waves are emmited by objects on the surface of the earth and some of them are reflected back. Sensors of data collecting devices (e.g. satellites) receive the reflected or radiated waves, which change according to the type of the object.The LandSat images are mainly used to analyse geological structures and surface monitoring especially for volcanic areas, mineral resources, mass movements (Blackett, 2014; Mwaniki et al., 2015).

The Landsat-8 is the new product of the Landsat series from the NASA, which can be accessed freely. The Landsat 8 carries two push-broom instruments: The spectral

bands of the OLI sensor, which provides additional spectral bands especially for analysing water resources and cirrus clouds, and the Thermal Infrared Sensor (TIRS). The Landsat 8 OLI images have nine band push-broom (8 of them at 30 m ground pixel resolution and one panchromatic band at 15 m resolution) that stretch between the visible, near infra-red, and the thermal infrared bands with four mirror telescope (Gawad et al., 2016). This satellite provides images with different band ratios, which are widely use to understand and monitor the geology, geohazards and structures by using the different reflection paths of different mineralogical composition (Blackett, 2014; Gupta, 2017; Mwaniki et al., 2015).

Band ratios serve to emphasize the subtle differences of various surface covers utilizing their spectral response, while correcting the shadowing effect. To complete the geological map of the study region by utilizing the remote sensing analyses is especially for the places where it is forbidden or diffucult to enter such as the east-northeastern parts of the Ovacık Fault.

The Landsat 8 OLI images, representing the minimum vegetation, snow and cloud coverage were selected from the archive (November of 2014) of the USGS free database. I processed images by using ENVI 5.3 software to visualize the best contrast of different lithological units.

The Landsat 8 OLI data are composed of images and their metadata. The Pre-processing of these images includes the Radiometric Calibration by using the FLAASH method to reduce the scattering effect of atmosphere dark object substruction of calibrated images, which converts atmospheric reflectance to surface reflectance. According to the general flow chart of the landsat images resampling data range of bands by using Band Math tool was applied to calibrated image. Then, the noise reduction tool was applied to eliminate the irrelavent data from the image (Blackett, 2014; Mwaniki et al., 2015).

After these pre-prossing methods, I applied radiometric enhancement by using data stretching and saturation stretch tools to increase colour saturation of different lithologies for the region. Lastly, I applied HSV (Hue Saturation Value) transformation to have suitable image based on spectral characteristics (reflectance data) of the lithologies and PCA (Principle Component Analysis), which displays the maximum contrast from several bands with three primary display colour (Gawad et al., 2016). By using these processed images and the application of different band ratios , I tried

to choose images with best contrasts to understand the spatial distribution of different lithological units and their boundaries along the Ovacık Fault and the surrounding region.

Natural colour composite image of bands 4, 3, 2 in RGB with HSV transformation covers the study area (Fig. 3.23).

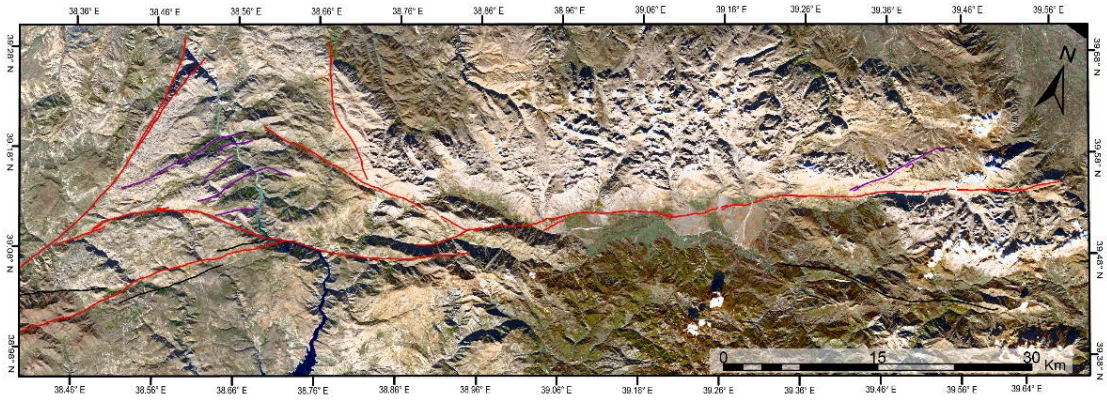

Figure 3.5 : The HSV transformation with band ratio of 4, 3, 2 of the study region.

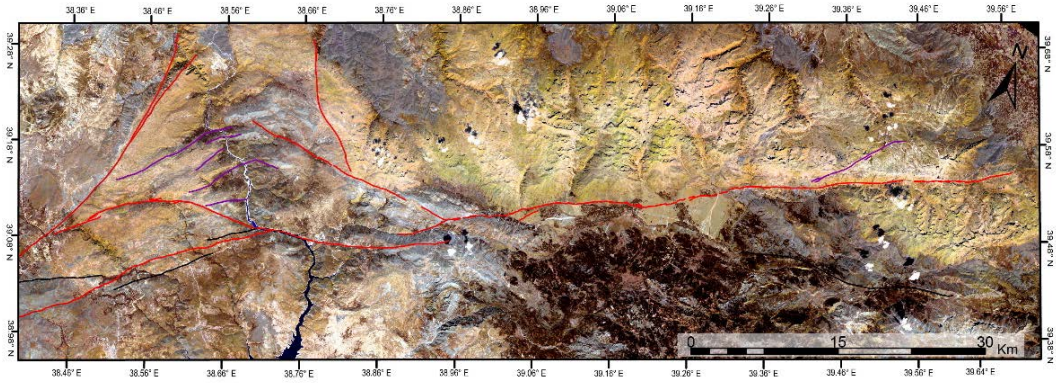

Figure 3.6 : The HSV transformation with its saturated stretch of the region.

The HSV image of the region with its saturated stretch represents different colours for different lithologies (Fig. 3.24). The best colour contast is from the Munzur Limestone and the Ophiolitic mélange. The Munzur Limestone has yellowish colour, wheras the Keban metamorphics is poorly defined with yellowish brown colour. The distinguishment between the Keban matamorphics and the Munzur Limestone was also difficult during the field excursions related with the similar appearance of these units.

The last image is composed of band ratios of 4-3-6 and 2-7-3 (Fig. 3.25). This colourfull image represent light purple colour for the Munzur Limestone, while reddish

brown colour is for the Miocene volcanics (the Yamadağ Volcanic Complex) at the western part of the region. Moreover, lineaments especially around the Kemaliye region, at western flank of the Karasu River, are clearly visible within the processed image (Figs. 3.23, 3.24 and 3.25). These lineaments are product of the diffuse deformation zone at the west-southwestern part of the Ovacık Fault.

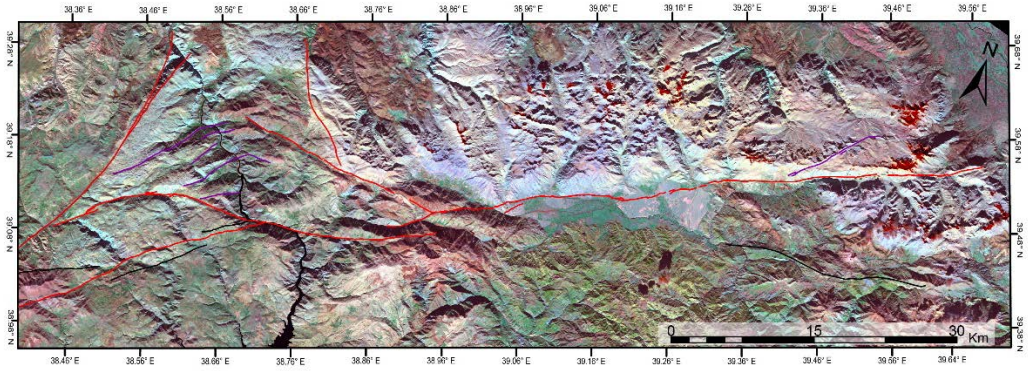

Figure 3.7 : Band ratio of 4-3-6 and 2-7-3 bands.

These obtained basic maps were compared with the existing geological maps, and it was observed that the resultant lithological units and the contacts between them were overlapped in some parts. It is seen that multi-band images such as Landat 8 have been processed to be a powerful tool in the extraction of lithological units in areas where the settlement sites are sparsely.

3.4 Active Fault Segmentation and Tectonic Lineaments

The term segment was used for the rupture distribution of the historical earthquakes at the beginning but later on, it corresponds static, geological and structural features of a finite region (McCalpin, 2009). The well-supported studies for segmentation are earthquake ruptures. However, in the absence of historic surface rupture, segmentation can be done by using the variety of features. Geometrical segments for a particular fault is the second most common used type of segmentation, after historical surface rupture. Any change in strike (bigger than 5 degrees) of the fault and /or type of endpoints, which are related with the releasing- restraining bends, step overs, and changing the slip rate are criterias for construction of geometric segments in strike slip faults (McCalpin, 2009).

The geometric discontinuities in the fault segment can the boundary of earthquake segmentation as well (Bilham andKing, 1989; Kadinsky-Cade andBarka, 1989;

McCalpin, 2009; Sanders). Many studies show that there is a correlation between restraining bend and earthquake rupture based on the length and angle of the bend

(Kadinsky-Cade andBarka, 1989) However, studies on NASZ show that an earthquake can effect more than one geometrical segments of a fault as well (Barka andKadinsky-Cade, 1988). Therefore, geometric segments play significant part of earthquake behaviour of a particular fault.

The OF are classified into nine different geometric segments. Table 1 shows the feature of the segments. Segmentation is made by change in strike of the fault (between fs6, fs7, fs8), releasing and restraining bends (between fs2-fs3) of the endpoints. This segmentation is helpful to understand and make a judgement about the behaviour of the future earthquakes.

The fs1 segment, which is 36.3 km length with 64˚ strike, starts from the northeastern end of the OF and continuous to the eastern edge of the Ovacık Basin (OB). Along the strike it follows the northern wall of a fault- related linear valley. The fs2 segment, which has releasing bend / stepover with the fs1, cuts alluvial fans of the eastern part of the OB. The OF has the best exposure on this particular segment (Fig. 3.27). The fs 2 segments, which is 12.5 km length with about 56˚ strike, has restraining bend at the western end. The fs3 segment starts from the restraining bend with 14 km length and 62˚ strike bounds the northern mountain front of the western OB. Although, the fs4 has similar strike (just 3 ˚ difference), it is better to separate it from the fs3 where its trace is very weak on the topography. The 25 km long fs5 segment, which has almost E-W strike has restraining bend based on the sinistral kinematic of the OF. The surface trace of the fs6 segment is not well documented on the topography of the region, however, deflections of rivers indicated existence of the fs6. Eastern end of the fs6 is not connected to previous fault segments, whereas it connects with the fs7 segment, which is responsible the main sinistral deflection of the Karasu River. The fs7 together with the fs8 segments reflect an arc shape surface trace, which creates compressional setting at the north of these segments, where they meet with the sinistral Malatya Fault.

The 25 km long last segment, fs9, starts from the middle of the fs7 as a sub-branch and ends to southwest where it meets with the Malatya Fault. This fault segmentation does not reflect the earthquake segmentation. This segmentation will help to understand

change in deformation along the OF detail. However, if an earthquake occurs at fs1 segment, most probably the fs1, fs2, fs3 and fs4 show earthquake rupture for the earthquake.

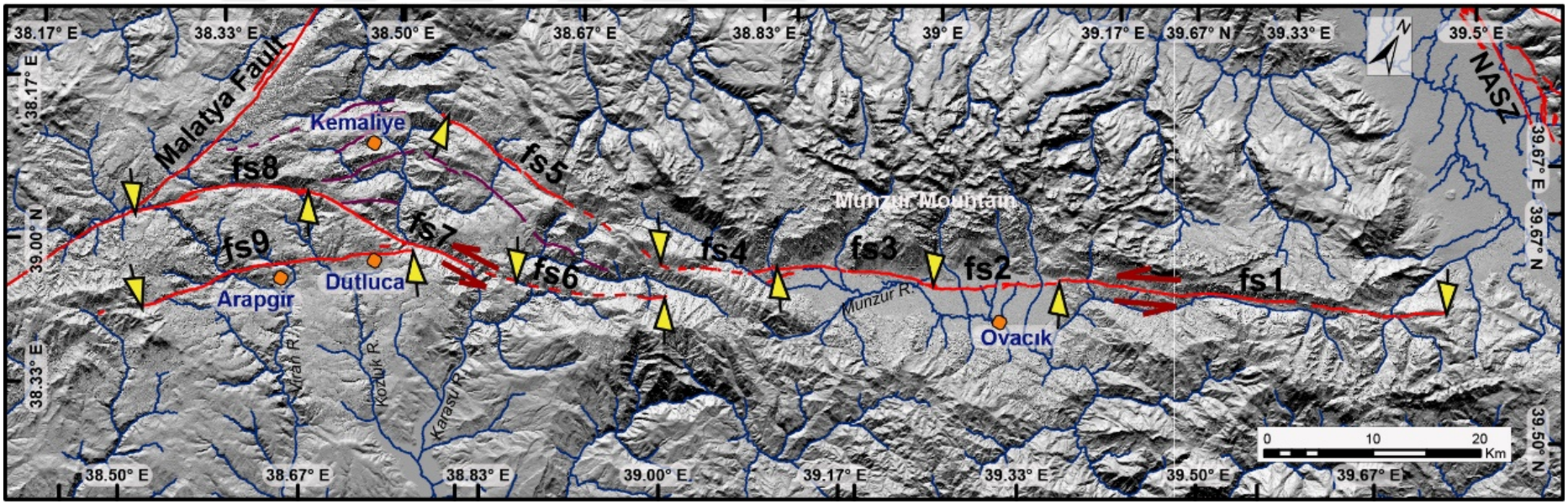

Figure 3.8 : Fault segmentation along the OF. Yellow arrows indicate start and end points of each geometric segments. All segments are named from northeastern to southwestern as fs1 to fs9

One of the significant criteria for behaviour of the OF is the amount of offsets along the individual segments. Moreover, if we focus the morphology of the region, a left lateral (sinistral) offsets along main Karasu river indicates sinistral deflection as well (Fig. 3.28).

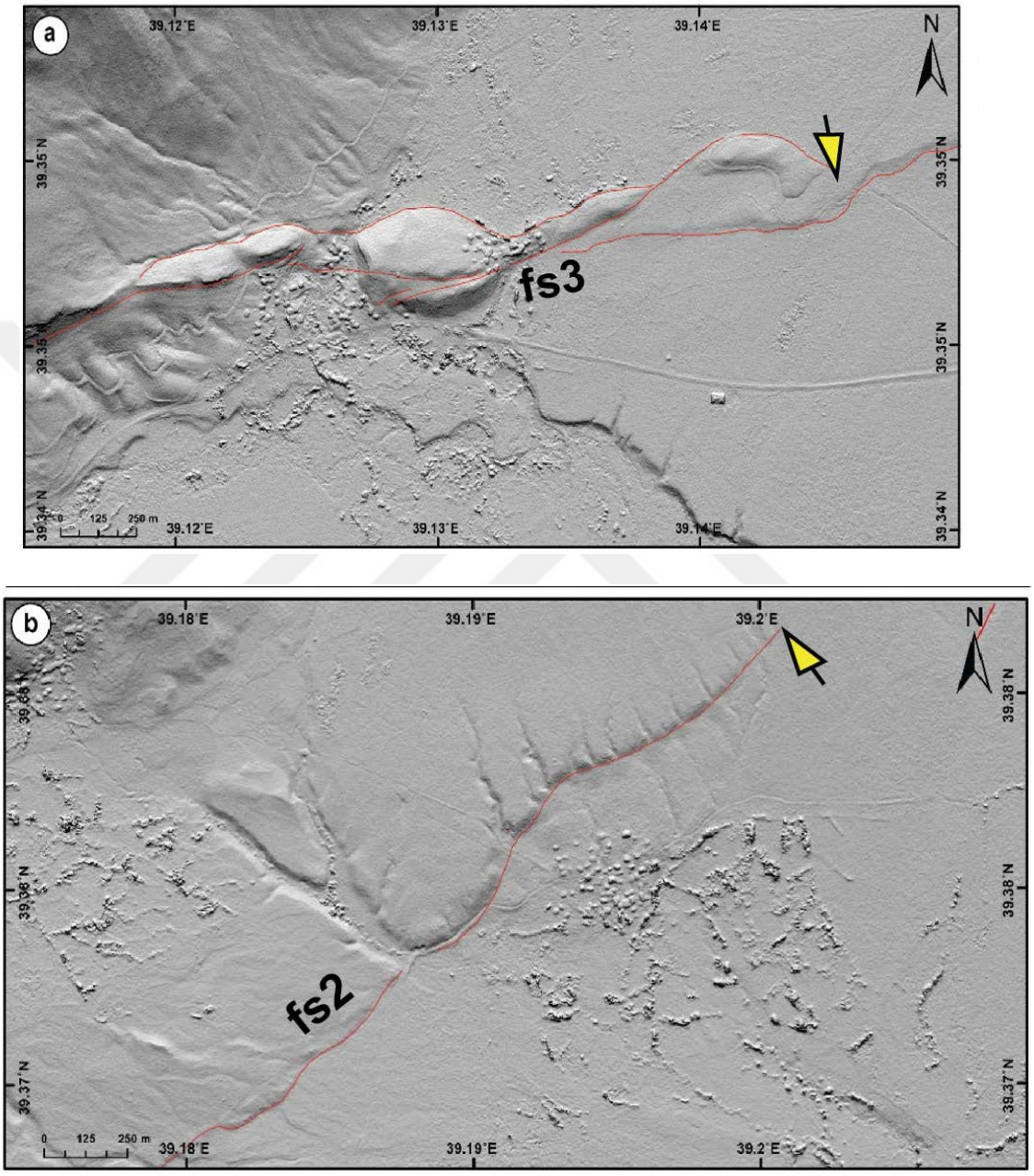

Figure 3.9 : Endpoints of the fs2 and the fs3 segments

The sinistral deflections of the drainages are measured and named from a to d. The most important sinistral offset is the deflection on the Karasu river on the fs7 segment (from d- d’ and d’’-d’’’ in Fig.3.28). Main noticeable example is from d which has mean value of 8.75 km ± 2. 05 km sinistral deflection with 10.8 km maximum (d-d’) and 6.7 km minimum value (d’’- d’’’).

Table 3.1. Feature of all different fault segments of the OF.

Segment Name	Length (km)	Strike(˚)
fs1	36.3	64
fs2	12.5	56
fs3	14	64
fs4	10	62
fs5	25	94
fs6	19	68
fs7	16	85
fs8	17	58
fs9	25.5	53

However, the Karasu has also other small deflections further to the north where these offsets can be carried by the tectonic lineaments (purple lines in Fig. 3.28). The amount of offsets on these lineaments are various, from north to south a-a' is 2.4 km ± 0.4 km, b-b' is 2.45 km ± 0.65 km and c-c' is 1.1 km ± 0.1 km. Therefore, total amount of sinistral deflection on the Karasu is approximately 14.7 km, which is conformable with the possible lithological offset.

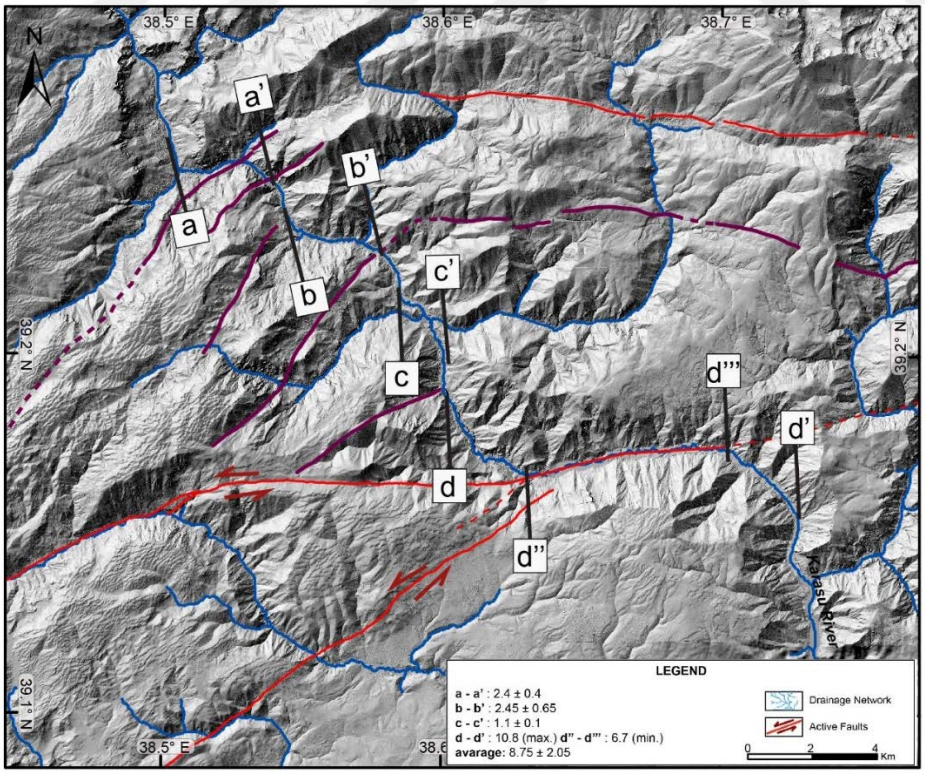

Figure 3.10 : The measured offsets along the Karasu River. Each individual deflection is related with the tectonic lineaments and the active strands of the OF. The sum of these deflections yield approximately 14.7 km as a cumulative offset of the Karasu River

4. TECTONIC GEOMORPHOLOGY

Morphology of a landscape is formed by competition between external and internal processes. External processes are related with the atmospheric conditions of the earth including, erosion (river, wind), and climate (glacials, deserts), whereas internal processes based on forces from beneath the earth such as tectonics. Understanding the stage of a landform, whether it is under the dominance of internal or external processes, drainage systems are the most prominent proxies (e.g. Keller and Pinter, 1996; Molin et al., 2004; Pérez-Peña et al., 2009). Their response to the climate, geology and tectonics make it powerful tool to quantify the landscapes' stage especially in tectonically active regions (e.g. Burbank and Anderson, 2011; Clark et al., 2004; Keller and Pinter, 1996; Kirby et al., 2007; Kirby et al., 2003; Kirby and Whipple, 2001; Miller et al., 2012; Schoenbohm et al., 2004; Snyder et al., 2000). There are some geomorphic indices quantifies mathematically the feature of drainages. These indices are most sensitive to vertical topographic anomalies, which are formed under the influence of not only tectonic forces but also with the climate. Although geomorphic indices have limited applications at regions with horizontal deformation, these methods provide valuable information on the vertical component of motion along the strike-slip faults (e.g. {Silva, 2003 #2594}; Tarı and Tüysüz, 2016; Yıldırım, 2014). However, it is important to recognize triggering factors (internal or external) of landscapes while evaluating its stage. High elevated areas with deep incisions of a drainage system used to infer recent uplift as an evidence of interior factors such as tectonics whereas similar signals are documented for glacial regions (external processes) as well (Brocklehurst and Whipple., 2004; Molnar and England 1990, Kirkbride and Mathew 1996; Egholm et al., 2009; Prasicek et al., 2015; Sternai et al., 2011).

The study region comprises of many attractive morphological structures, which can carry traces of active tectonics. In this chapter of the thesis, I will discuss the stage of landscape and its character along the OF based on geomorphic indices.

NE- SW trending the Munzur Mountains with 3500 m summit, comprises northeastern part of the region. The Munzur Mountains, which are the eastern continuation of the

Taurus Mountain, show attractive glacial morphology by its remarkable glacial valleys, cirques. The Karasu River, the main branch of the Euphrates that cuts region through north to south is the main drainage system of the region. The Munzur Mountain is situated in the eastern part of the Karasu River, delimits the northern boundary of the Ovacık Basin (OB). The 25 km length OB is a lower lying mountain front basin, which contains alluvial fans, terraces, and E-W draining Munzur River. To the west of the Karasu River, drainage network has dendritic structure and has bigger basins rather than the eastern part where sizes of drainage basins are very small. This under recognize region is good to study of tectonic geomorphology with the help of geomorphic indices. To understand the morphology of glaciated and non-glaciated lands and their interaction with active tectonics by using basic geomorphic indices.

4.1 Palaeoglacial and Karstic Morphology of the Region

The Munzur Mountains are documented to include significant ice fields larger than 500 km^2, which consists of 800 cirques and 40 main glacial valleys mainly to the north of the Ovacık Basin (Yeşilyurt et al., 2015). With this extent, the size and magnitude of palaeoglaciation is the second largest after the Eastern Black Sea Mountains (Akçar et al., 2007; Akçar et al., 2017; Yeşilyurt et al., 2015). Although today's Equilibrium-Line Altitude (ELA) is about at 3600-3700 m, it was at ~2750 m during the Last Glacial Maximum (LGM) (Bilgin, 1972). However, the glaciers descended down to 1600 m, or even 1350 m at the Ovacık Basin (Bilgin, 1972; Çılğın, 2013; Yeşilyurt et al., 2015), which is clearly marked with glacial valleys and moraines. The Munzur Mountains are mainly characterised by valley type glaciation; however, some parts show plateau-type glaciers. Cirques, roche mountonness, glacier troughs, pulverized surfaces and morains reflects the glacial morphology at the eastern part of the Karasu River. Besides glaciation, karstification also has intensive effect on the geomorphology through the Munzur Mountains as it's mainly composed of the Munzur Limestone. First karstic depressions are reported to be formed above the altitude of 2500 m. These karstic depressions deepened as the result of tectonic uplifting since middle Miocene (Çılğın et al., 2014 and references therein).

Many karstic landforms, such as dolines, uvalas and fluvio-karstic depressions, are reported in various places in the eastern part of the Munzur Mountains (Çılğın et al., 2014). The palaeoglaciation and karstification are mostly limited to the eastern Munzur Mountains (to the north of the Ovacık Basin) and they are not so much continuous to

the west of the Karasu River (Akçar et al., 2017; Bayrakdar et al., 2015), except some horizontal karstic features on the high plateau of the western Munzur Mountains. Base level changing in vertical karsts and glacial features can affect the value of geomorphological indices. Taking into consideration of all interacting factors, it is better to differentiate landscape in terms of glaciated and karstic regions to non-glaciated- non karstic regions.

4.2 Materials and Methods

Hypsometric curve and integral (HI) to discuss the landscape's stage along the OF, longitudinal channel profiles, normalized channel steepness and concavity (ksn, θ) indices to infer topographic anomalies formed by tectonic processes along the OF and mountain front sinuosity (Smf) to quantify the balance between erosion and active tectonics along the mountain-front of the Ovacık Basin (OB) are geomorphic indices that are used in this study. All of these indices extract information about the tectonic, climate and lithological factors on the regional morphology.

TanDEM-X digital elevation model (DEM) data, which provide 12 m spatial resolution, is used for all analyses. First, drainages, which have a Strahler order higher than three, were extracted after sink filling of the DEM of study region by using the D-8 algorithm of Rivertools 4 and ArcGIS Hydrology tools (Fig. 4.1). Secondly, I choosed 36 drainage basins (DBs) for which individual DEM files were prepared according to their drainage divides, by using the extract tool of the ArcGIS Desktop 10.3.1. Extracted drainage basins are named starting from northeastern to southwestern (1- 36) (Fig. 4.1). In later stages, computer programs, Rivertools (for Hypsometric curve and integral, channel profile and concavity), ArcGIS Desktop (Mountain Front Sinuosity), and Matlab (Channel steepness and concavity) are used to calculate geomorphic indices from DEMs of DBs or all coverage of the study region.

4.2.1 Hypsometric curve and integral (HI)

The hypsometric curve represents the ratio between the area and altitude of a drainage basin, and is plotted by the relative area (values between 0 to 1) to the relative height (values between 0 to 1) (Strahler, 1952) and is calculated by;

$$\mathrm{HI} = \frac{\mathrm{H}_{mean} - \mathrm{H}_{min}}{\mathrm{H}_{max} - \mathrm{H}_{min}} \qquad (4.1)$$

where H_{mean}, H_{min}, H_{max} represent the mean, minimum and maximum height, respectively.

The shape of the curve and HI represent the maturity level of the morphology basically in three classes: (a) Convex hypsometric curves and high HI show relatively 'young age' stage, which is characterized by a deeply incised and a rugged topography, (b) *S* shaped curves and an intermediate value of HI imply a 'mature age' stage, which is characterized by equilibrium in geomorphic processes, and (c) Concave curves and low values of HI reflect a relatively 'old age' stage, where the erosion is the main shaping process on topography (Keller and Pinter, 1996; Strahler, 1952; Walcott and Summerfield, 2008). The high HI shows 'younger morphology', thus they may point tectonic uplift in regions where we have similar lithology and erosion rates.

In addition to tectonics, lithology, glaciation and karstification have also strong effect on the hypsometry value. Different strength of lithology, increase in erosion by glacial and change in base level in karstic region have effect on the hypsometry (Brocklehurst and Whipple, 2004; Egholm et al., 2009; Prasicek et al., 2015; Sternai et al., 2011). Especially for the region that was under the effect of glaciation shows change in hypsometry in response to glacial erosion and have hypsometric maxima just below

The hypsometry of each basin is calculated by processing DEM files with Rivertools 4, in which each basin is extracted according to its drainage divides. Additionally, basin sizes, which can affect the hypsometry, are calculated (Table 1). Finally, these curves and HI values are classified to geometric segments of the OF and then these classes are correlated among themselves in order to understand the effect of the fault geometry on the distribution of active deformation along the whole fault zone and the surrounding region (Fig. 4.3).

4.2.2 Longitudinal channel profiles

In tectonically active regions, the curvature of the longitudinal profiles of bedrock rivers provide sensitive data for assessing the local uplift, change in lithology and erosion rate (Stock and Montgomery, 1999; Burbank and Anderson, 2001). The incisions of bedrock rivers are dependent on the climatic oscillations, the strength of the rock, base level and/or the properties of the sediment load that they have (Duvall et al., 2004). Rate of change in channel gradient as a function of drainage area, which is shown by longititudanl profiles, defines concavity.

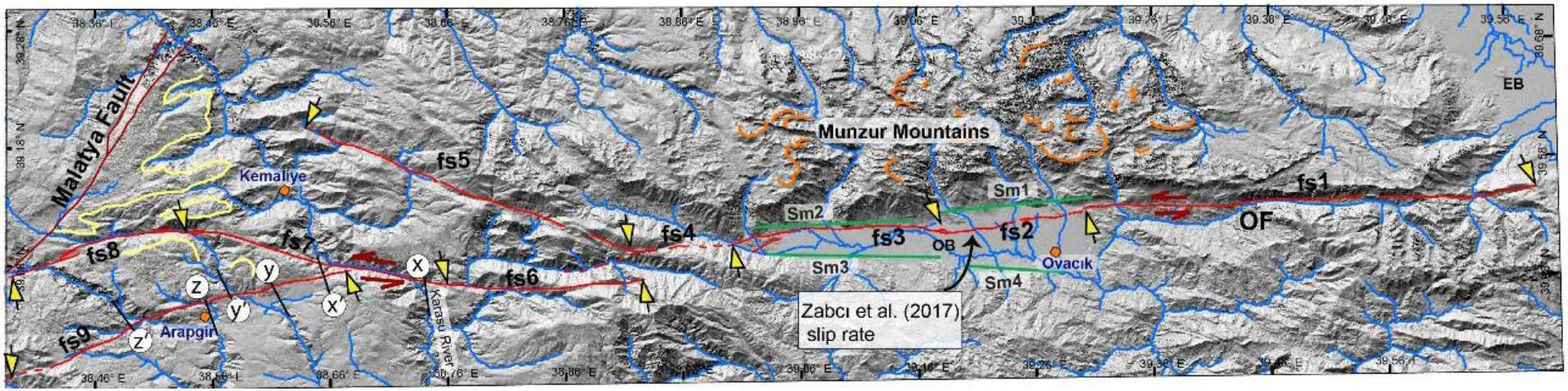

Figure 4.1 : The digital elevation model of the study region, which shows the different segments of the OF. The orange lines along the Munzur Mountains reflects the cirques, which are related with glacial processes, and uvalas, whereas to the west of the Kemaliye Region yellow lines indicates the horizontal karst. X-X', Y- Y' and Z-Z' are sinistral deflection of rivers and green lines in the OB (Sm1, Sm2, Sm3 and Sm4) are the mountain fronts. Faults are compiled and modified from Emre et al., (2012a), Emre et al., (2012b), Emre et al., (2012c) except f9 segment. EB is the Erzincan Basin, OB is the Ovacık Basin.

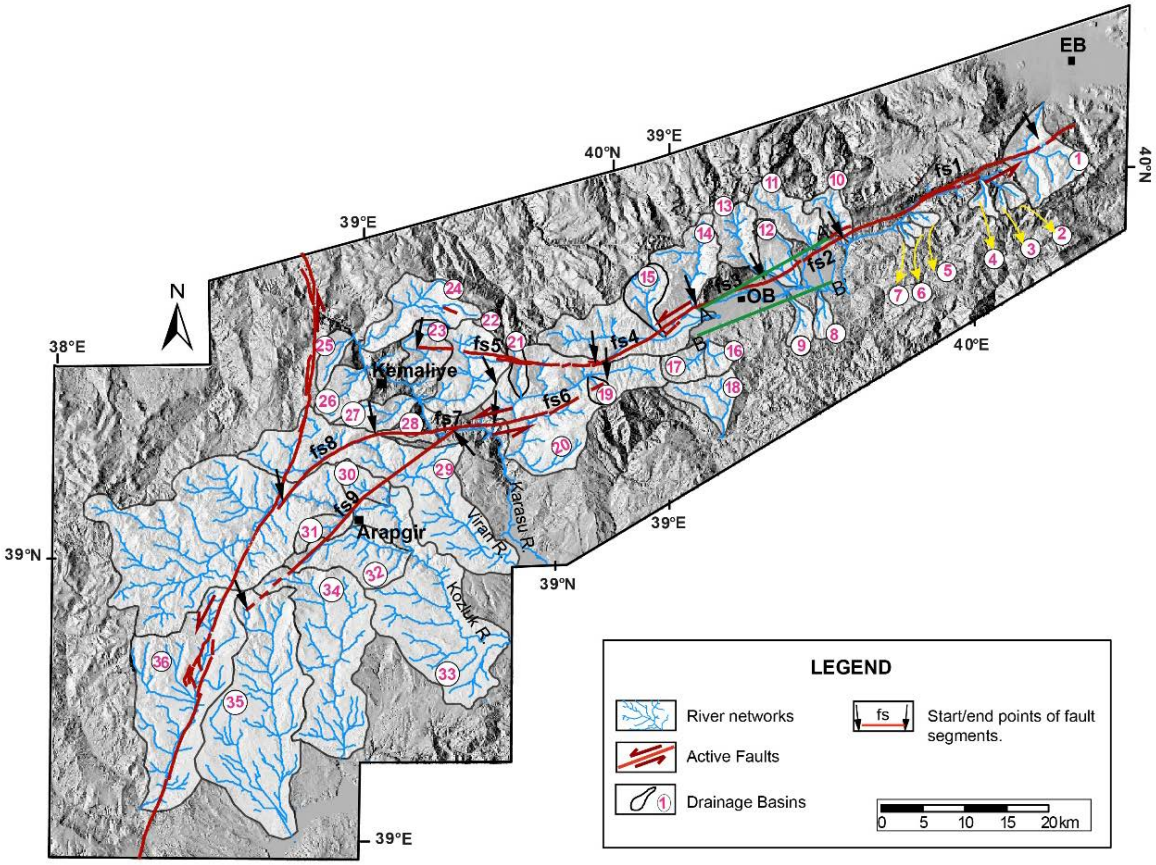

Figure 4.2 : The drainage network and basins along the OF. Drainage basins (DBs) are named from 1-36 various in sizes. Green lines along the both north and south margin of the OB are location of the Smf index.

Concavity of a river profile defines the stage of the landscape, where high concave profiles reflect equilibrium between uplift and erosion rate and convex profiles indicate domination of uplift (Perez-Pena et al., 2010). Therefore, the longitudinal channel profile is a strong tool to analyse the stage of landscape evolution, base level change, knickpoint migration, lithology and climatic changes (Kirby et al., 2003). All rivers in steady state topography indicate balance between rock uplift and erosional processes or sediment flux, whereas transient river profiles reflect abrupt change in elevation or in gradient. These anomalies with sharp changes in channel profiles, knickpoints, are indicators of a sudden change of base level response to different lithology or external / internal processes (Whipple, 2004).

Channel profiles were extracted along the main trunks of basins using the Rivertools 4 from TanDEM-X data (Fig. 5 and Appendix). Our aim is not only to find knickpoints related to the tectonic and erosional processes, but it is also to discuss the stage of landscape evolution along the OF as well.

4.2.3 Channel Steepness (ksn) and Concavity Indıces (Ɵ)

The analyses of longitudinal profiles are also used to establish the mathematical relations of steady-state equilibrium channel parameters (generally using power functions). Since the uplifting and erosion rates are equal in fluvial systems in steady state equilibrium, the height of the river bed will be constant and therefore the longitudinal profile will be smooth and concave in its shape (Hack, 1973). The resulting situation indicates a specific relationship between the local flow gradient and the stream length (Hack, 1957) or between the local channel slope and the upstream drainage area (Flint, 1974). Thus, evolution of river profiles, effect of bedrock lithology and erosional stage are described by deviations from slope-area relationship (Perron and Royden, 2013; Whipple and Tucker, 1999). Therefore, the incompatible relationship between the channel gradient and the upstream drainage area can be explained by active tectonics. In this study, the region was evaluated based on the power law function proposed by Flint (1974) on the drainage networks along the OF. As a result of these empirical studies on the longitudinal profiles, it has been shown that there is a power law function between the local channel gradient (S) and the upstream drainage area (A) (Flint, 1974; Hack, 1957, 1973).

$$S=k_{sn} A^{-\theta} \quad (4.2)$$

where k_{sn} and θ normalized channel steepness and concavity, respectively. θ is the ratio of the channel gradient, which is known as the concavity index (Snyder et al., 2000; Kirby & Whipple, 2001; Whipple and Tucker, 1999). The θ is independent from the erosional processes and it is generally in a narrow range between 0.35 and 0.6 (Whipple and Tucker, 1999, Seidl and Dietrich, 1992) and 0.5 ± 0.2 (Burbank and Anderson, 2001). We used 0.45 for θ_{ref} in order to calculate the normalized steepness index (k_{sn}) (Whipple, 2004). The steepness index increases with higher uplift rates, whereas decrease for weak rocks or more erosion (Burban and Anderson, 2001).

My interest is on knickpoints, which are generated teconically. Logslope-logarea projection is useful to look for separating of reaches by knickpoints.

The whole DEM coverage for the study region is used for the determination of steepness, whereas concavity values are calculated from individual DEM files for each DBs by using the Topotoolbox code for determining the regression line of drainage area and channel slope (Schwanghart and Kuhn, 2010; Schwanghart and Scherler, 2014) in Matlab.

4.2.4 Valley floor width-to-height ratio

The Valley floor width-to-height ratio quantifies the valley shape and formulates the distinction between V- and U-shaped valleys (Bull and McFadden, 1977; Keller and Pinter, 1996). The Vf is calculated by:

$$Vf=2Vfw/[(Eld-Esc)+(Erd-Esc)] \quad (4.3)$$

where the Vfw is the width of the valley, Eld and Erd are elevations of valley's left and right divides, and Esc is the elevation of the valley floor.

This index differenciates the type of valley as broad canyons with relatively high values of and V- shape valleys with relatively low Vf values (Keller and Pinter, 1995). The U shaped valleys with high values is mainly related with the low uplift rates however V- shape valleys, which indicates deep valleys associated with tectonically active uplift.The calculation of the Vf values of many basins in front of the mountain front is used to understand spatial distribution of incision and uplift rate of the region.

We measured Vf index within 300 m from the mountain front of main trunk system of drainage basins along the Ovacık Basin. Topographic profiles are extracted from the digital elevation model by ArcGIS Desktop 10.3.1 and all parameters are calculated from these profiles

4.2.5 Mountain front sinuosity (Smf)

The usage of the mountain front sinuosity (Smf) is first suggested by Bull (1977) to characterize the balance between the erosional and tectonic forces along a fault bounded basin margin. The Smf is calculated as:

$$Smf=Lmf/Ls \quad (4.4)$$

where Lmf is the total length of the mountain front and Ls is the length of a straight-line, connecting the two tips along the same frontal margin of a basin (Bull, 1977; Keller and Pinter, 1996). This index generally is usefull to compare the relative avtivity of mountain fronts.

Young mountain fronts generally have low Smf values due to the lack of range front erosion, which makes a straighter (linear) mountain front. On the other hand, higher values imply nontectonic or erosional processes dominated basin margins based on older or lower tectonic uplift, where we usually observe a sinusoidal geometry (Topal et al., 2016). We applied the Smf only to the margins of the Ovacık Basin in order to

understand this single basin has a tectonic control whether on its single side or on its both margins (Smf1, Smf2, Smf3, Smf4 in Fig. 4.1). We used high resolution DEM (2m), which are produced by aerial photos, along the Ovacık Basin. After the determination the exact location of the mountain front by vertical profiles to the basin, we measured the straight and sigmoidal length of the mountain front along the northern and southern boundary of the OB by using ArcGIS Desktop 10.3.1 software. A comparision of Smf values with Vf values for each mountain front is usefull to qualify the relative order of mountain front activity and quantify the uplift rate (Rockwell et al., 1984). with TANDEM-X data to measure the straight and total sigmoidal length of the mountain fronts of the Ovacık Basin.

4.3 Results and Interpretation

All results are first classified to the geometric segments of the fault and then these classes are correlated among each other in order to have a better understanding on the distribution of deformation along the different segments of the OF. The complete list of our DBs is provided in Table 4.1

For the fs1 segment, drainage basins, which are 1, 2, 3, 4, 5, 6, 7, have high hypsometric integral (HI) values, ranging from 0.477 to 0.616. DBs of 8, 9, 10, 11 and 12, generally have high HI between 0.314 and 0.572 along the fs2 (Fig. 4.2). However, DBs of the fs3 segment (13), the fs4 segment (14, 15, 16, 17, 18) and the fs9 (30, 31, 32, 33, 34, 35, 36) show wide range of HI that includes both high and low values from 0.330 to 0.659. On the other hand, the fs5 (DBs 22, 23, 24), the fs6 (DBs 19, 20, 21) and the fs8 (DBs 29, 33) have S-shaped hypsometric curves and yield HI values, which are between 0.381 and 0.560. The DBs 25, 26, 27, 28 of the fs7 segment have high HI values, ranging from 0.574 to 0.690 (Fig. 4.2). In summary, apart from fault segmentation, the DBs 1234, 35 have lowest HI values of, 0.314, 0.346 and 0.330, whereas the highest HI values of, 0.659, 0.690 and 0.673 are calculated for DBs, 15, 26 and 25, respectively (Fig. 4.2).

The shapes of the longitudinal river profiles are classified into three groups; concave, concave-convex and convex curves. DBs of the fs1 segment (basins from 1 to 7) show mainly concave shaped long profiles (Fig. 4.3). However, DBs 4 and 5 have convex shape particularly for the same segment. In fs2, the profiles of DBs 8 to 12 have relatively combination of concave-convex shapes. While DBs 8 and 12 show convex

Table 4.1 : Hypsometric Integral, Concavity and basin sizes for all extracted drainage basins.

DBs	HI	Concavity	Basin size (km2)	DBs	HI	Concavity	Basin size (km2)
1	0.616	0.512	87	19	0.56	0.333	12
2	0.527	0.473	9	20	0.459	0.223	260
3	0.533	0.445	5	21	0.509	0.627	17
4	0.511	0.477	11	22	0.387	0.391	97
5	0.477	0.514	8	23	0.423	0.493	49
6	0.566	0.391	5	24	0.55	0.399	87
7	0.562	0.382	4	25	0.673	0.4	23
8	0.448	0.413	13	26	0.69	0.319	41
9	0.466	0.34	18	27	0.621	0.364	36
10	0.572	0.56	29	28	0.574	0.446	14
11	0.544	0.282	54	29	0.466	0.341	246
12	0.314	0.455	38	30	0.565	0.28	30
13	0.649	0.3	55	31	0.468	0.388	26
14	0.476	0.329	243	32	0.343	0.432	87
15	0.659	0.466	42	33	0.381	0.313	943
16	0.453	0.284	16	34	0.346	0.492	253
17	0.428	0.271	28	35	0.33	0.242	350
18	0.496	0.314	47	36	0.354	0.281	293

shape, the DB 9 is S-shaped, on the other hand DBs 10 and 11 have concave shape of

longitudinal profile. Along the fs3 (DB 13) have concave-convex shapes, whereas DBs 14, 15, 16, 17 and 18 are in the range between S-shaped to concave shape for fs4 segment. DBs 19, 20, 21, 22, 23, 24, show S-shaped profiles for fs5 and fs6 segments (Fig. 4.3). On the other hand, DBs of fs7 segments (25, 26, 27 and 28) have smooth convex shaped longitudinal profiles. DBs in fs8 segments (29, 33) and a number of DBs (30, 31) of the fs9 segment have mainly concave shapes, while DBs 32, 34, 35 and 36 show convex geometry along the fs9. We also observe many knickpoints along the most of the long profiles. Especially, knickpoints within DBs of, 10, 13, 20, 21, 30 and 33 are the most remarkable ones (Fig. 4.3).

Calculated normalized steepness values are represented in four groups, which are classified according to their magnitudes (Fig. 4.5 and 4.7). The rivers along the fs1, fs2 and to the south of fs3 segments indicate low steepness values (<100). However, drainage pattern to the north of the fs3 and the Ovacık Basin reflects steepness values higher than 350 at the Munzur Mountains. Although surrounding regions of the fs4, fs5 and fs6 mainly have low steepness values, the drainage of the DB 38 that is cut by fs6 has relatively higher steepness value (from 100 to 350). The Karasu River, which is cut by fs7, shows high steepness all throughout its valley. On the other hand, drainage pattern around the fs8 and fs9 has low steepness values, but in places the calculated values are high, especially close to the middle reach of the DB 35 (south of fs8) and lower reaches of the DBs 34, 35 and 45 (Viran and Kozlu rivers) (Fig. 4.5).

The general range for the concavity index is between 0.3 and 0.6. Drainage basins 3, 10, 11, 13, 30, 31, 36, 38, 46, 47, 49 and 52 have lower values from 0.129 to 0.294 whereas DBs 2 and 27 represent higher values (0.784, 0.627).

The extent of palaeoglacial activity and wide-spread karstification, which is common in the eastern Munzur Mountains, have almost none or very limited control in this west/south-western parts of our study region (Akçar et al., 2007; Akçar et al., 2017; Yeşilyurt et al., 2015). We also did not observe any evidence of palaeoglacial activity and/or strong karstification during our field studies in the Kemaliye Region. In this region, incipient karstic voids at the valley walls suggest relatively fast uplifting of the region rather than the surroundings, whereas in the eastern Munzur Mountains vertical karstic morphology is more spread. The absence of no or limited palaeoglacial activity, karstification and the similar strength lithologies within the limits of the DBs 25, 26, 27 and 28 suggest that the tectonic uplift is the main control for Kemaliye and the

nearby region (Fig. 4.7). The reason for relative uplifting around Kemaliye region can be result of (a) the existence of a high convergence zone, which cuts the EASZ and

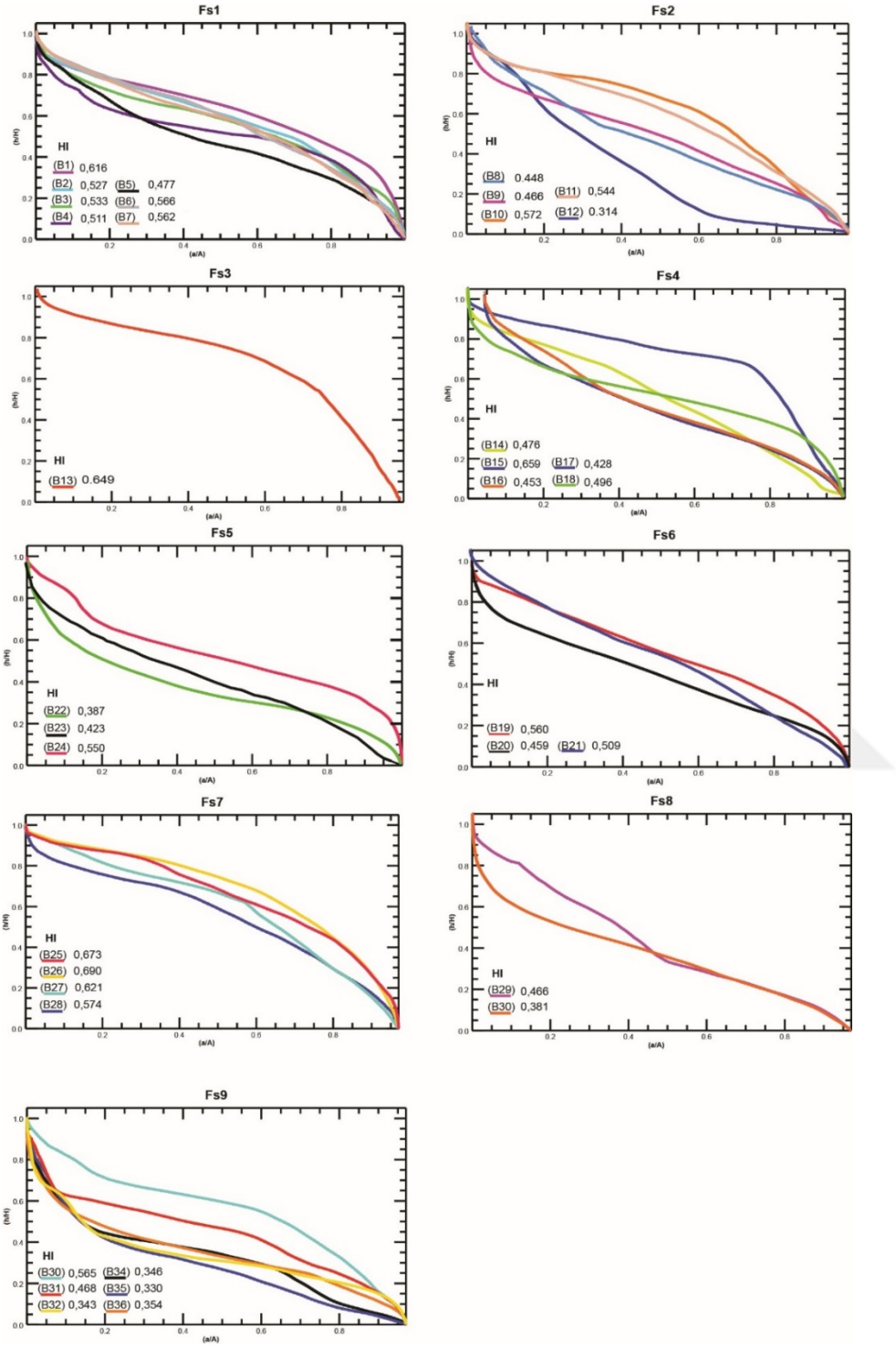

Figure 4.3 : Hypsometric curves and Hypsometric integral values for all different segment of the OF.

penetrates into Anatolia (Şengör et al., 1985) or (b) the interaction of the sinistral Malatya Fault (MF) and the OF.

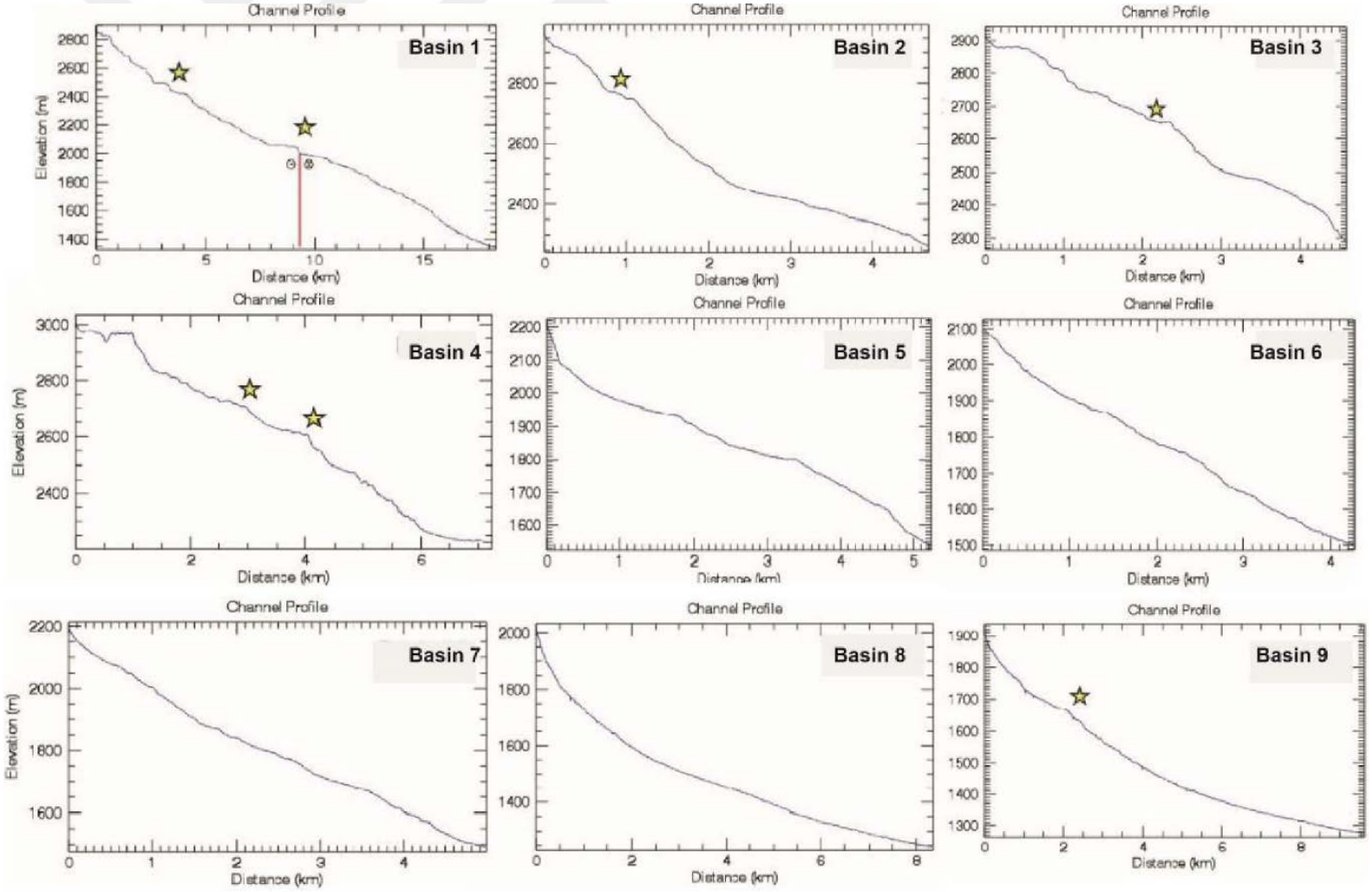

Figure 4.4 : Longitudinal channel profiles of drainage basins. Yellow stars mark some knick points. Position of the segments of the OF is also marked by red solid line on some of the profiles

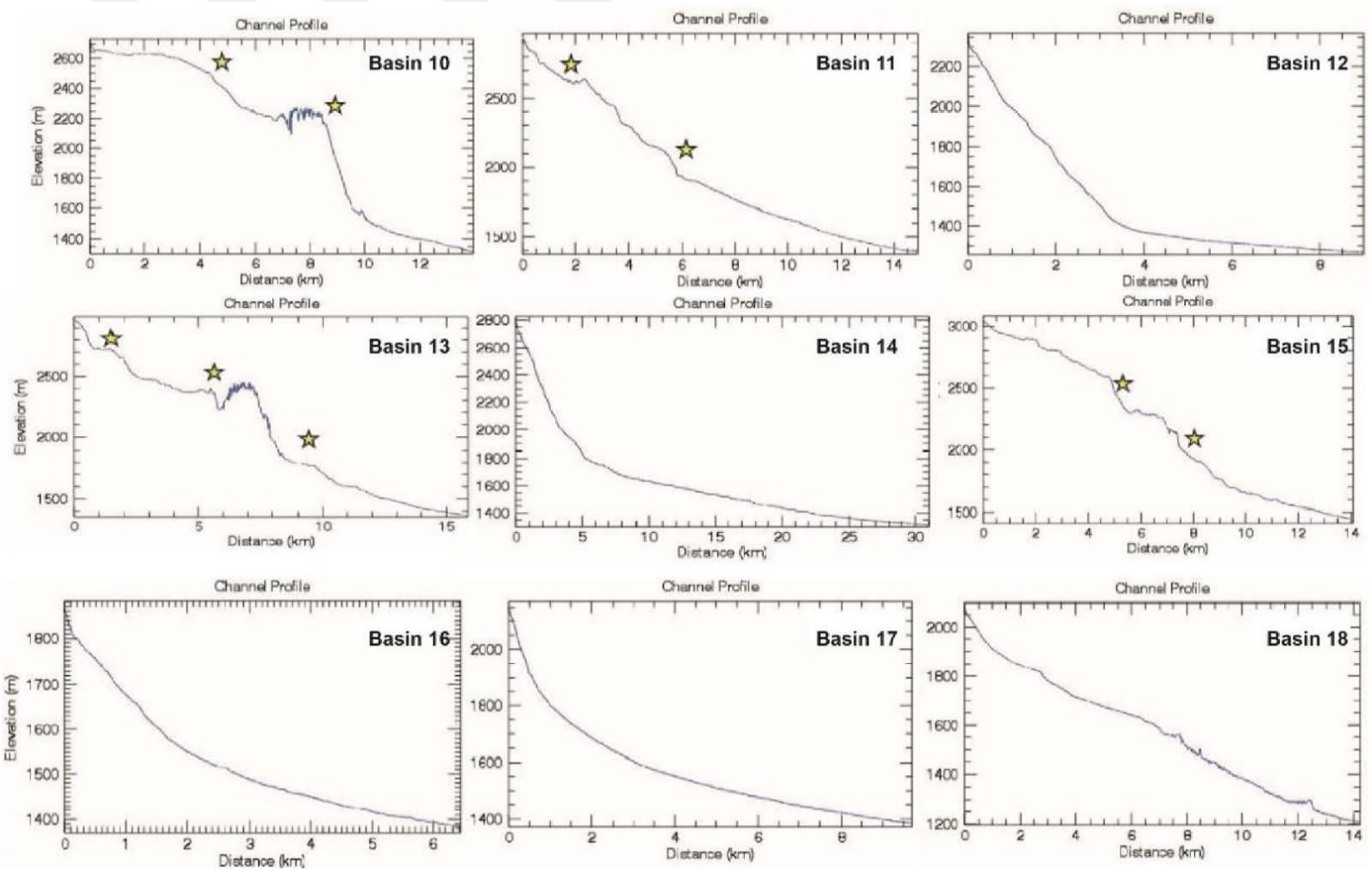

Figure 4.4. (Continue): Longitudinal channel profiles of drainage basins. Yellow stars mark some knick points. Position of the segments of the OF is also marked by red solid line on some of the profiles

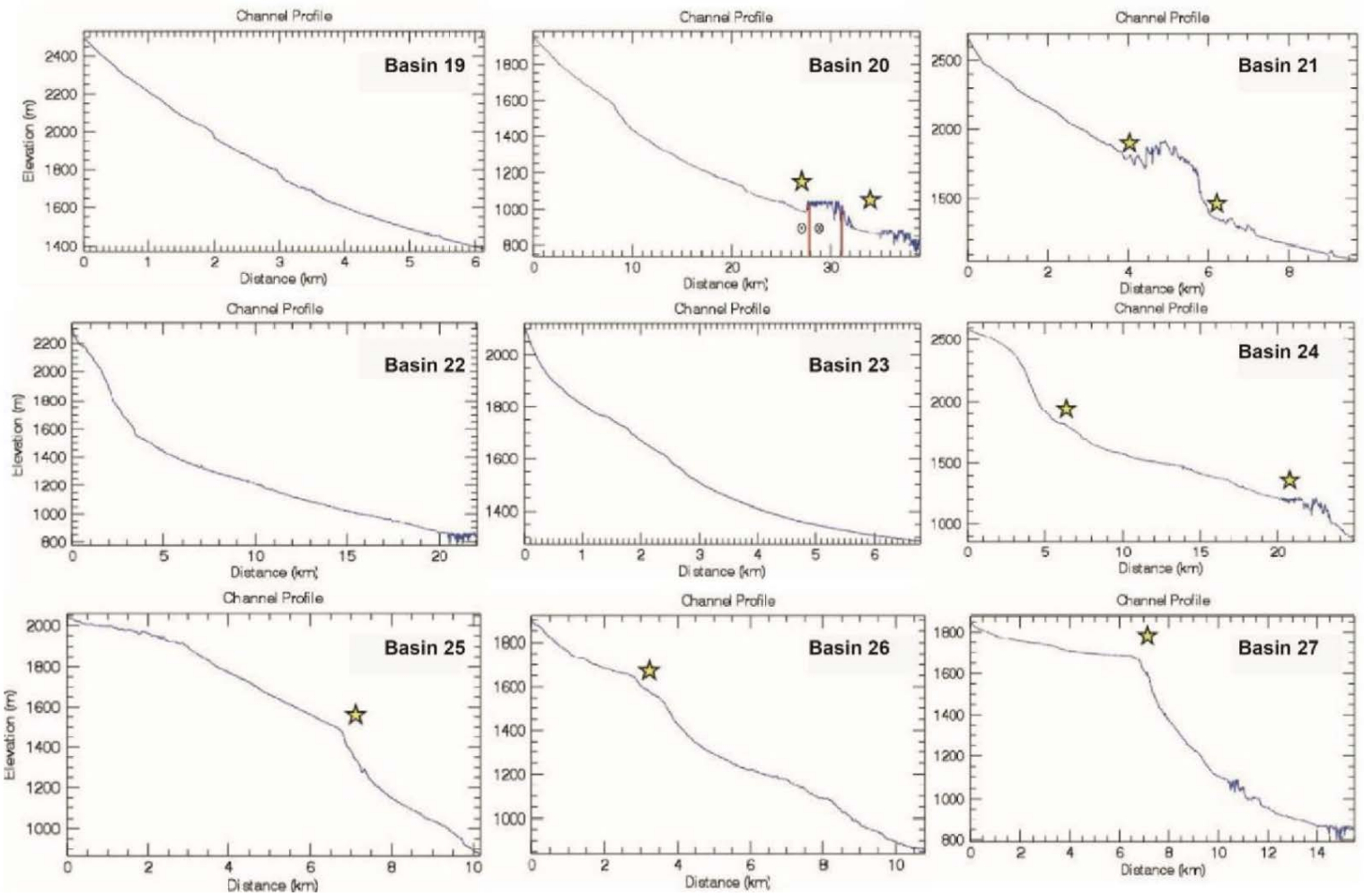

Figure 4.4 (continue): Longitudinal channel profiles of drainage basins. Yellow stars mark some knick points. Position of the segments of the OF is also marked by red solid line on some of the profiles

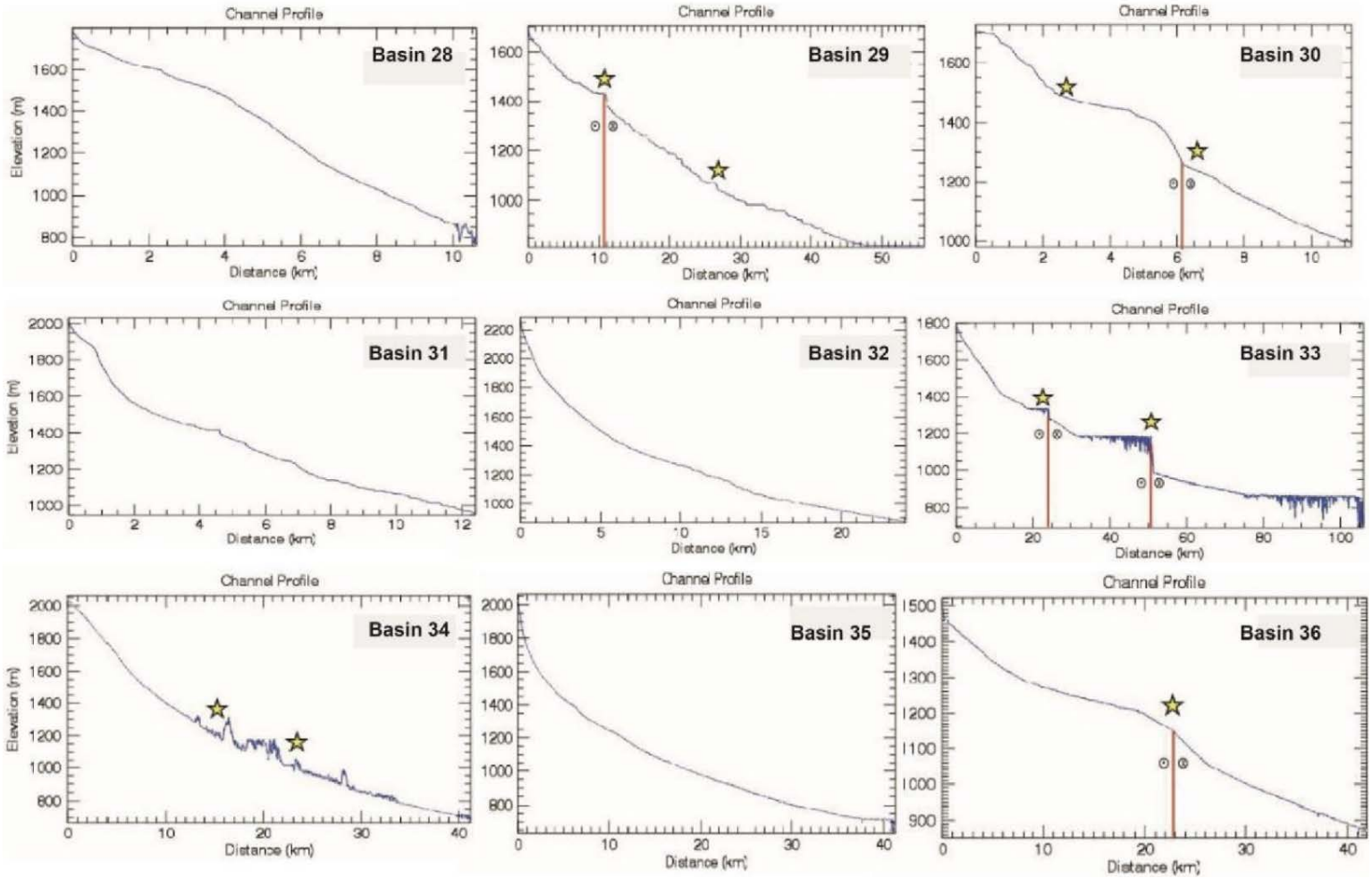

Figure 4.4 (continue): Longitudinal channel profiles of drainage basins. Yellow stars mark some knick points. Position of the segments of the OF is also marked by red solid line on some of the profiles

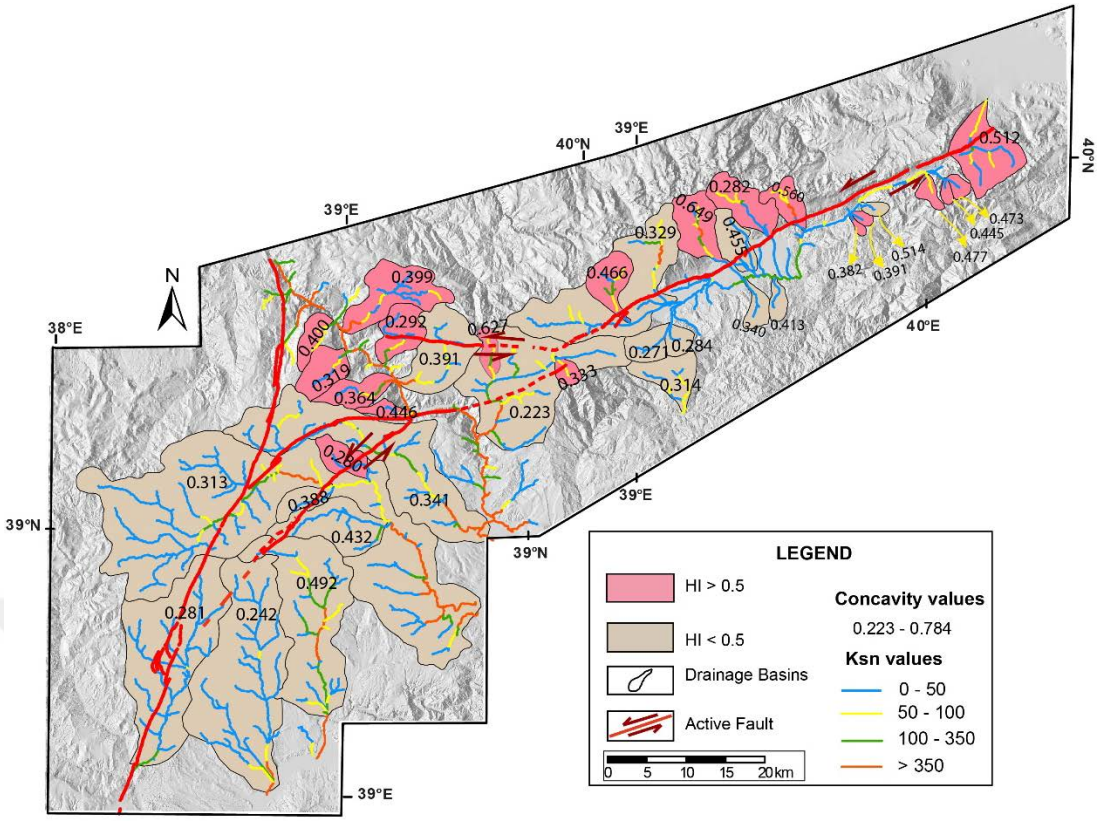

Figure 4.5 : The map shows the concavity and hypsometric integral (HI) values of the DBs, and normalized channel steepness (Ksn) of draneges along the OF.

To understand the relative tectonic activity of the Ovacık Basin Smf and Vf values are evaluated together, where the proportion of the Vf values (Vfmean) and Smf values can be used to determine the tectonic activity of mountain fronts (Rockwell et al., 1984; Silva et al., 2003). The average Vf and Standart deviation (σn-1) for each front is calculated and they show perfect correlation between Vmean and Smf with R2= 0. 99. Calculated Smf values for Sm1, Sm2, Sm3, and Sm4 are 1.13, 1.08, 2.61, 1.55 respectively. According to the classification of the Rockwell et al., 1984, Sm1 and Sm2 indicates that uplift rate for these fronts is at least 0.5 mm/yr (Fig. 4.6). The Sm3 and Sm4 from the southern margin of the Ovacık Basin indicates a low uplft rate < 0.05 mm/yr and moderate uplift 0.5 – 0.05 mm/ yr respectively (Fig. 4.6). In general, high values of hypsometric integral and the shape of the curve and steepness indices suggest that the morphology is in the 'young age' stage. Altough this stage mainly used to infer tectonically active regions, the same pattern can be seen also in glaciated landforms. If we compare the results of the indices and expectations, there is quite fit at the region along the Kemaliye region, between MF and the fs5 (Fig. 4.7).

The high HI and steepness values are also consentrated along the Munzur Mountains,

the north of the OB. However, considering the effect of the glacials on that regions complicates to make an interpretation. High-resolution aerial photos and some profiles of the valleys can help to understand and observe differences between the Kemaliye region and the Munzur Mountains (Fig. 4.8). Morphology on the Munzur Mountains shows existence of various sizes of cirques and morains (Fig. 4.8a). The valley of the Munzur Mountains shows generally U- type, which is an evidence for glacial erosion. The walls of the valley are more rubbed by glacials. However, the aerial photo and profiles of a drainage in the Kemaliye region suggest the opposite (Fig. 4.8b). Absence of any trace of glaciation and V-shape valley indicate that fluvial processes rather than glacials effect the region. Also formation of the horizontal karst are clearly visible on the aerial photo.

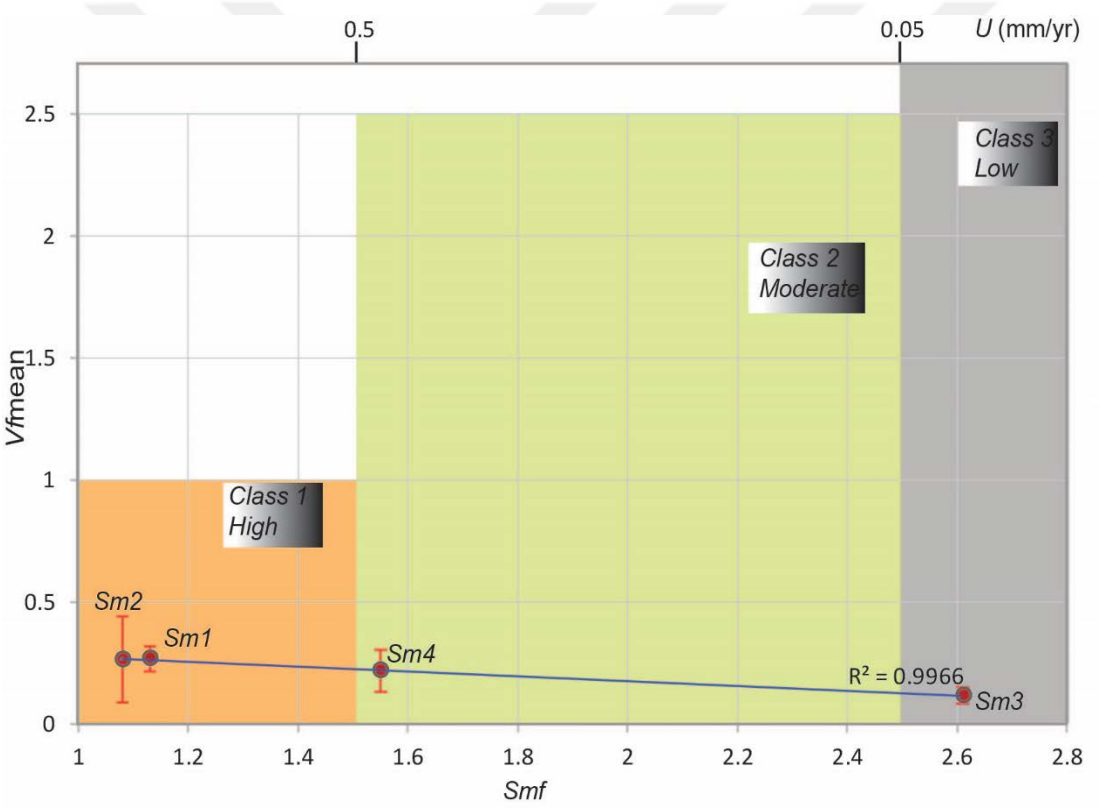

Figure 4.6 : A graph shows the Smf and Vfmean for the mountain fronts of each segment and inferred activity classes. Vertical bars show the standard deviation (σn-1) for Vf values. Numbers at the top indicate inferred uplift rates U (mm/yr) which are classified into three classes from Rockwell et al. (1984).

In general, the localised deformation zone of the OF at its north-eastern parts becomes wider to the southwest, especially around the Karasu River, where there is a good correlation between the transpressional fault geometry and our morphometric results (high HI and steepness values, knickpoints along longitudinal channel profiles in the Kemaliye Region).

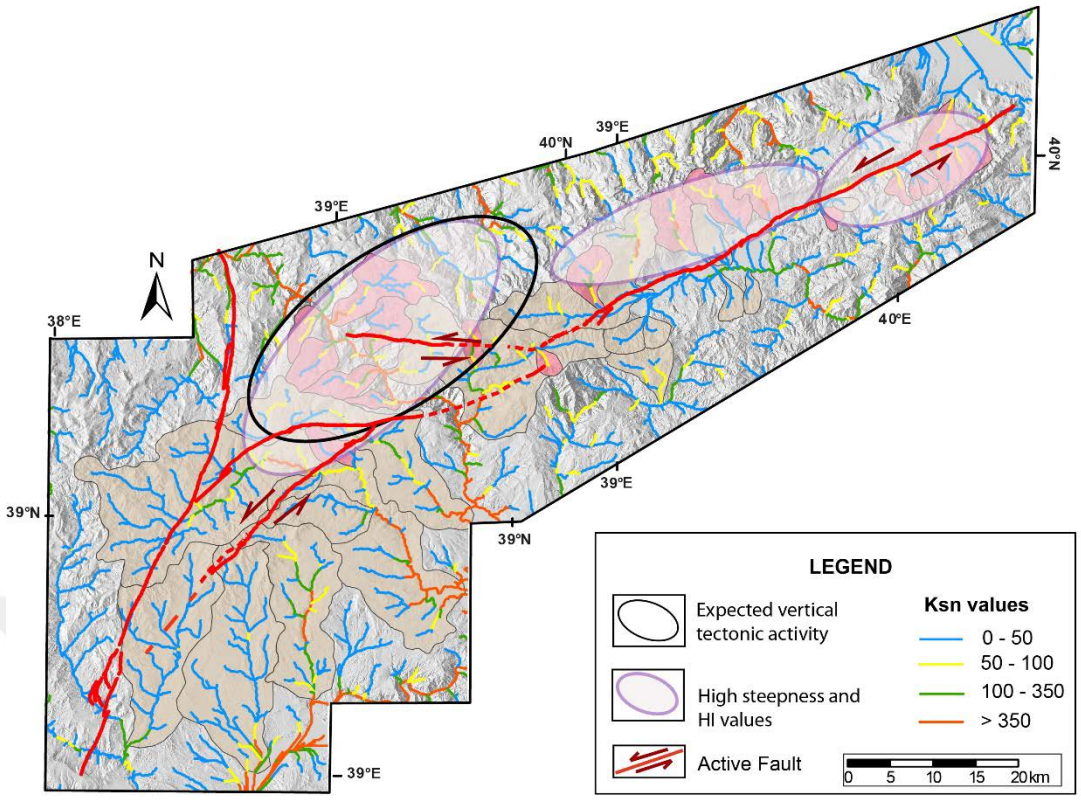

Figure 4.7 : The comparing figure of the expected vertical tectonic activity and calculated high values of geomorphic indices.

The vertical component of motion increases from east to west, which is also defined in our geomorphic analyses, especially around the complex faulting at the south-western parts of the OF. The Kemaliye Region, to the north of the fs7 shows a significant tectonic uplifting. The reason for the uplift can be because of two inter-related mechanisms; (a) the change of faults' geometry and interaction with MF, forming a transpressional region or (b) the existence of a high convergence strain zone that was suggested by Şengör et al. (1985). The first calculated vertical uplift is along the fs2 and fs3 segments show that the uplift rate is calculated at least 0.5 mm/yr.

According to tectonic geomorphology, the deformation is localized at the north-eastern parts of the OF and becomes wider to the southwest, especially around the Karasu River, where there is a good correlation between the transpressional fault geometry and our morphometric results (high HI and steepness values, knickpoints along longitudinal channel profiles).

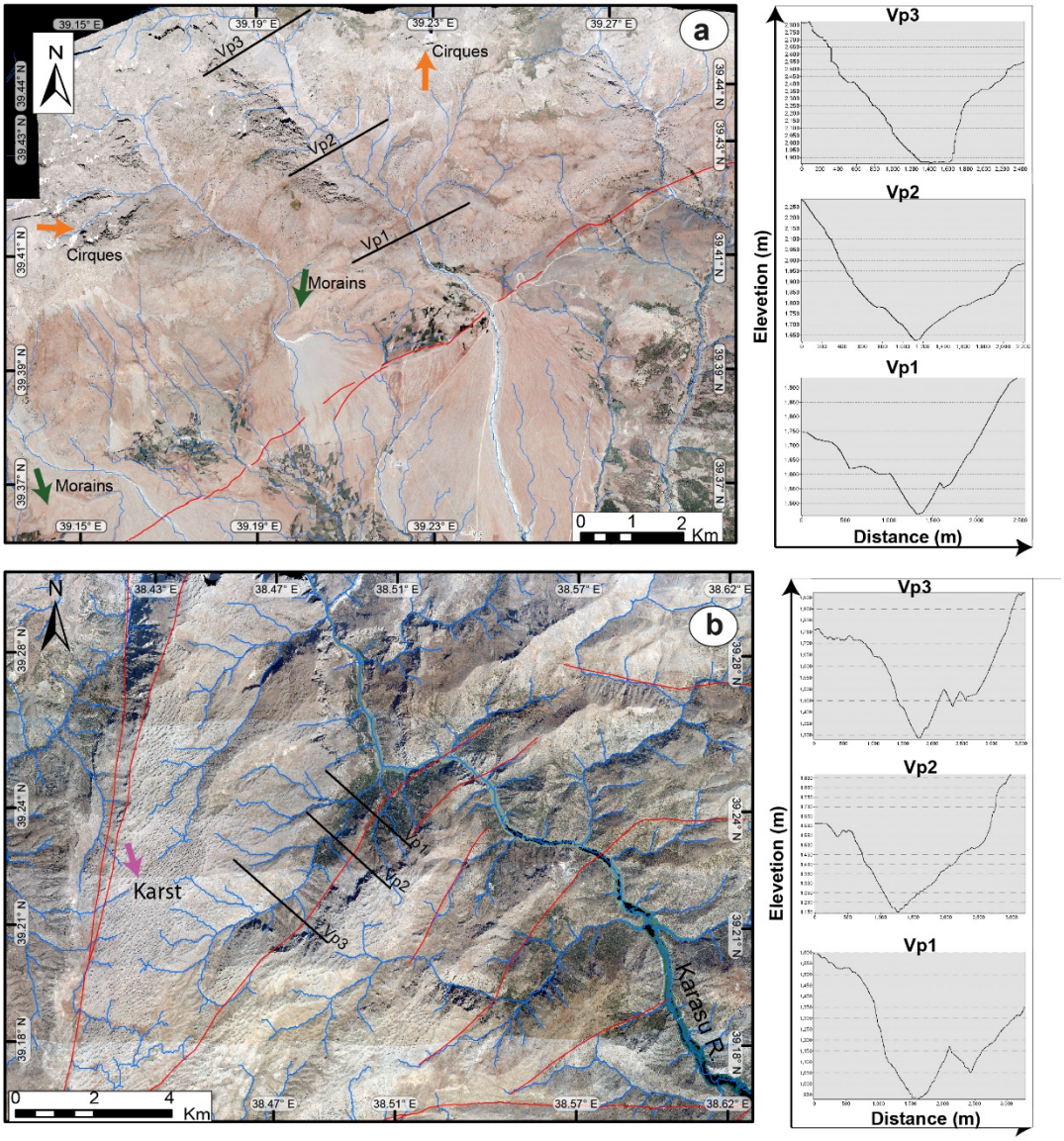

Figure 4.8 : Aerial photos of the regions (a) the Munzur Mountains (north of the OB) and (b) Kemaliye region (east of the MF). (a) shows glaciated morphology in both aerial photos and valley profiles (Vp1, Vp2,Vp3), whereas the Kemaliye region shows the dominance of fluvial processes.

5. PALAEOSEISMOLOGY

Understanding the timing, the magnitude, and the location of an earthquake provide an invaluable information about the seismic risk of a region. Moreover, the investigation of earthquakes also allows us to understand the dynamic structure of the earth. The instrumental seismicity represents spatially a detailed, but only a screenshot of the earth's dynamics when we consider the long history of faults. Therefore, any data about palaeoearthquakes provide a temporal control on the behaviour of active tectonic structures. For example, a palaeoseismological study in the New Madrid Seismic Zone, which is the plate interior in the North America, provides a catalogue of Late Holocene earthquakes with five dated palaeoearthquake events (A.D. 1811–1812, 1450 ± 150, 900 ± 100, 300 ± 200 years, and 2350 B.C. ± 200 (Guccione, 2005). Additionally, a study of Meghraoui et al. (2000) shows deformation in stable plate interiors by studing Bree Fault in Lower Rhine graben, which has 0.1 to 0.007 mm/yr of uplift rate and 15 kya reccurance period of large earthquakes. On the other hand, palaeoseismological studies in the Anatolian Block are also important to understand the deformation mechanism of plate interiors. Akyüz et al., 2013, indicates that a segment of the CAFZ, which is a sinistral strike slip fault of the Central Anatolian province, has 4500 years time span to produce surface rupturing earthquakes. Moreover, activity of the Tuz Gölü fault, which it's slip rate is 0.0536 mm/yr from Lower Pliocene to present with evidence of two earthquakes during the last 10.500 years, is discovered by palaeoseismological study (Kürçer and Gökten, 2012)

Trenching is one of the most common methods in the study of palaeoearthquakes, in which direct or indirect data on palaeoevents are exposed by digging the Quaternary (mostly Holocene) deposits (McCalpin, 2009). Location of the trench is differing according to purpose of the study. The best sites to find recurrence interval of earthquakes are local fault zone depressions which are filled with fine grain and organic sediments to date the palaeoearthquake levels. A type of trench can also change with purpose of the study. Generally, fault-perpendecular trenches often used to locate, define the faults and palaeoearthquakes whereas fault parallel trenches are defining offsets of piercing points. After digging of the trech in the best site, trench walls must be cleaned to remove soil that smeared on walls during excavation. After

cleaning, a reference grid for logging must be constructed. A grid is composed of horizontal and vertical lines of low-stretch nylon string, spaced 1m apart to each other. Especially, checking of horizontality by line level is curicial. Then, the trench wall is ready to give informations about its earthquake history. There are two types of defining the units in the trench wall. In subjective logging, a logger just defines the primarly geological features of the trench such as location of the fault which gives disadvantage to alternative intepretations of earthquake history of the trench. On the other hand, an objective logging gives lots of detail for all physical features of the trench with lots of alternative inteprateations. To define mappable units is generally defined by its lithology and weathering characteristics. Typical lithological descriptions should include colour, grain size, amount of clasts, shape and sorting of clasts, matrix grain size, bedding thickness, sedimentary structures, weathering, deformation and fossils. After lithological units are differentiated faults should be marked to identify the earthquake horizons. Faults or fault zones are charectirized by different features such as a fault gouge, tectonic mixing, or clay rich zones show different fabric from adjacent stratas. By the manuel mearument method, contacts are measured in relation to reference grid with a tape measure, all features of the trench is logged after all contacts have been marked. Photographs taken from the trench wall with 60% overlap to construct a photomosaic with stereo effect, which allow us to digitilize the trench wall.

Lastly, samples, which bound the earthquake event layers from above and below should be collect in order to find time span for eachearthquake layers. This study represents results of the first palaeoseismic study for the poorly known Ovacık Fault. A single slot trench was excavated at the Yukarı Yuvacık Site (38.563˚E – 39.164˚N; Fig. 5.2). I identified and dated a total of three palaeoearthquake events. My results are modelled using OXCAL (Ramsey and Lee, 2013), with the calibration curves of (Reimer et al., 2013), and I searched available earthquake catalogues (Ambraseys, 2009; Guidoboni, 1994; Guidoboni ve Comastri, 2005) for any possible correlation. Each detail is provided in relevant sections.

5.1 Historical Earthquakes of the Ovacık Fault

The records of historical earthquakes usually document effects of these natural hazards on man-made constructions and directly on human lives. Thus, the existence of a settlement is mandatory in case of documenting a historical earthquake.

In the study region, historical earthquakes are mostly recorded by Armenian and Ottoman historians (especially by priests). The history of settling goes back to the 10th century BCE along the OF and the surrounding region, especially in Arapgir (Malatya). Although there is a long history of records for the region, it is easy to make a mistake in assigning a historical earthquake to a specific fault due to existence of multiple fault zones, including the major plate boundary structure the NASZ.

I scanned multiple earthquake catalogues (Ambraseys, 2009; Guidoboni, 1994; Guidoboni ve Comastri, 2005), but I managed to find the spatially-refined and -classified information only in Ambraseys (2009) for my study region. There are only three records for possible surface rupturing events, which had an effect on settlements along or close to the OF (Table 5.1 and Fig. 5.1). These historical records are presented below with available information.

14 March 1779 Melitene (Malatya) Earthquake;

For this destructive earthquake in Central Anatolia, a report, written in Armenian towards the end of the 18th century, is the most important source.

"There is an earthquake, which damaged many settlements in Divriği and Malatya and many people were trapped in the wreckage. In the same year, an earthquake in the east has happened."(Hakobyan, 1951, ii.464).

A lot of houses and a church were destroyed in the Ağın and Arapgir. Many casualties were reported in most affected regions, Kızık and Hopik, which are located in the Ovacık Basin (Riggs, 1909).

A document dated to September 1779 indicates that the earthquake that happened on March 14, 1779 destroyed the Gazi Sinan Paşa Mosque in Malatya. The time of the Melitene Earthquake is dated according to this document.

16 January 1856 Ovacık Earthquake

On January 16, 1856, there was an earthquake that completely ruined the villages in Dersim and Harput. The greatest destruction has been in Varto, Hopik villages in the valley of Ovacık and Harput, which resulted in the relocation of many Armenian families from these regions (Ambraseys, 2009)

A note about this earthquake:

"At around 10:00 am on January 16, 1856, a very strong earthquake struck Harput and continued at regular intervals during the day and night. The most violent shaking was

in Kazin village of Ağın, where the mosque domes with one and two-roomed houses completely collapsed”

21 April 1896 Arapgir Earthquake

There is no any explanation for this earthquake except the shaking of the ground around Arapgir at 05.21 am.

Two of three historical earthquake records from the catalogue damage villages along the OF. The 1856 Ovacık Earthquake destroyed settlements at the southern part of the study region. Particularly, it caused a huge damage in Harput, which is close to the East Anatolian Shear Zone (EASZ); thus, this event is most probably related with the EASZ.

The Fig. 5.1 and Table 5.1 represents historical and instrumental earthquakes (Tan vd. (2008) ve Tapırdamaz (2011)), which have magnitude larger than 6.5 or have no information about this parameter. The spatial distribution of these events clearly shows that many of these large earthquakes are related with the NASZ or the EASZ.

Table 5.1 : . List of historical and instrumental earthquakes with magnitude larger than 6.5 and no data around the OF and the nearby regions (Tan vd. (2008) ve Tapırdamaz (2011)).

Latitude	Longitude	Magnitude	Year
38.1	38.6	7	499
39.7	39.5	6.5	802
38.5	39.5	No Data	995
39	40	7	995
39.7	39.5	6.5	1011
39.7333	39.5	8.1	1045
39	40	7.9	1046
39.75	39.5	No Data	1047
39.75	39.5	No Data	1068

Table 5.2 : Table 5.1.(continue): List of historical and instrumental earthquakes with magnitude larger than 6.5 and no data around the OF and the nearby regions (Tan vd. (2008) ve Tapırdamaz (2011)).

Latitude	Longitude	Magnitude	Year
38.5	37.83	7.5	1121
39.75	39.5	No Data	1236
39.7333	39.5	7.5	1254
39.75	39.5	No Data	1281
39.7333	39.5	6.9	1287
39.75	39.5	No Data	1289
39.75	39.5	No Data	1290
39.75	39.5	No Data	1345
39.75	39.5	No Data	1356
39.75	39.5	No Data	1366
39.7333	39.5	6.6	1419
39.75	39.5	No Data	1422
39.75	39.5	No Data	1433
39.75	39.5	No Data	1456
39.75	39.5	No Data	1482
39.75	39.5	No Data	1576
39.75	39.5	No Data	1583
40	39	6.6	1584
39.7	39.5	7.5	1666
38.3	38.3	6.5	1759

Table 5.1.(continue). List of historical and instrumental earthquakes with magnitude larger than 6.5 and no data around the OF and the nearby regions (Tan vd. (2008) ve Tapırdamaz (2011))

Latitude	Longitude	Magnitude	Year
39.75	39.5	No Data	1787
39	40	7.1	1789
38.4	39.4	No Data	1866
38.5	39.5	7.2	1874
38.5	39.5	6.8	1875
39.75	39.5	No Data	1888
38.7	39.9	No Data	1889
39.9	38.8	No Data	1890
38.35	38.3	No Data	1890
38.3	38.5	7.1	1893
38.4	38.3	No Data	1895
38.12	38.63	6.9	1905
39.85	39.6	6.6	1939
39.8	39.4	7.9	1939
39.6	38.1	No Data	1939
39.7	39.7	No Data	1939
39.7	39.7	No Data	1939
39.7	39.7	No Data	1939
39.6	38.1	No Data	1940
39.6	38.1	No Data	1940
39.7	39.7	No Data	1940
39.7	39.7	No Data	1940

Table 5.1.(continue). List of historical and instrumental earthquakes with magnitude larger than 6.5 and no data around the OF and the nearby regions (Tan vd. (2008) ve Tapırdamaz (2011)).

Latitude	Longitude	Magnitude	Year
39.6	38.1	No Data	1940
38.9	39.4	No Data	1940
39	38	No Data	1941
38.9	39.4	No Data	1942
40	39	No Data	1960
40	39.5	No Data	1960

After extensive usage of seismometers has been started, many earthquakes are recorded by seismometers, which are located all around the world. In Turkey AFAD and Kandilli Observatory are places to record the seismic activity of Turkey. From the microseismicity, which is taken from AFAD and Kandilli, shows limited earthquakes has happened around the OF. (Table 5.1 and Fig. 5.1)

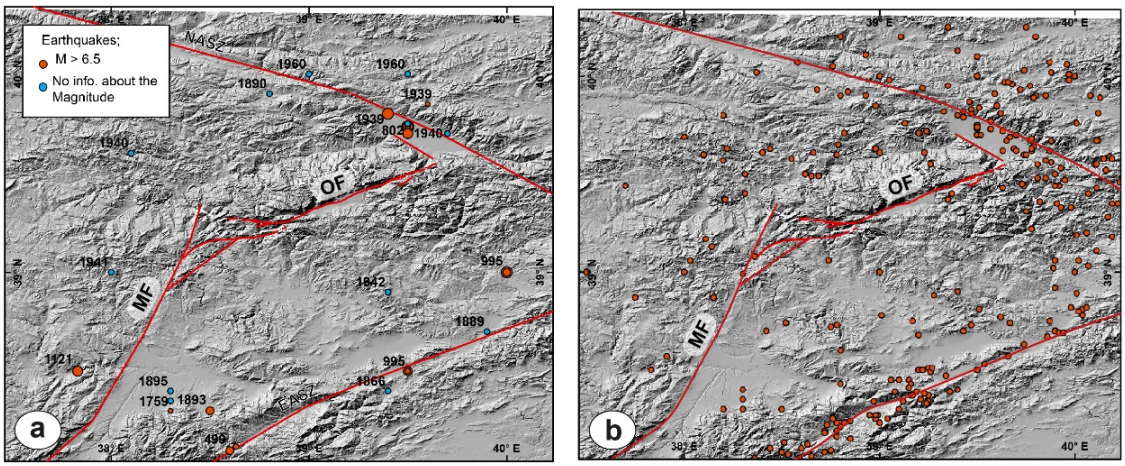

Figure 5.1 : Historical earthquakes in the study and the nearby region (Tan et al., 2008; Tapırdamaz, 2011). Estimated earthquakes' epicentres are generally located along the NASZ and the EASZ. (a) earthquake magnitudes > 6.5 and (b) includes all historical earthquakes. Faults revised from Emre et al., (2012a; 2012b).

5.2 Trench Study

There is no any previous trench based palaeoseismological study on the OF. Therefore, this study provides the first palaeoseismic records and first ideas on the seismic behaviour of this fault system.

A single trench was excavated near the Yukarı Yuvacık Site, close to the western end of the fs7 segment. This north-south striking fault perpendicular trench, is about 1.5 m-wide and 18 m-long, whereas the deepest parts reach hardly down to 2.5 m due to the high water level. Unfortunately, the high-water level had a negative effect on the stability of trench and almost all of the western wall and partially the eastern wall of the trench was collapsed. Therefore, only the first 8 metres of the eastern wall was studied in detail in the Yukarı Yuvacık Site. Almost 200 photos of the trench wall are used to produce the photomosaic image of the trench site by using the method of Reitman et al. (2015) (Fig. 5.4a). All photos were shot by a Nikon D5300 without recording location info into their EXIF data. Two different sets of photographs were subclassified according to their angles, distance and the time of shot (the daylight effect).

The studied wall was cleaned in order to remove soil smeared on during excavation. A reference grid 1 x 1 m spacing the first 8 metres of the trench wall was constructed. Due to absence of fault related stratigraphy and structure, just 8 meters of the 18 m long trench wall was logged. Logging of the trench is made by objective logging method. Different lithologies were marked, faults according to their colour, grain size, amount and size of clasts and level of weathering. By the manuel measurment method, the log was completed. Based on the interprated log, 20 samples for age determination were collected. However, 16 of them are analysed. Photographs taken from the trench are processed by using the Agisoft PhotoScan Professional software. GPS coordinates of each level is taken and plotted as ground control points in the software. A photomosaic of the trench wall is produced with 70.000 key points and 1.000 tie points (Fig. 5.4a).

5.2.1 Location and Geomorphology of the trench site

Absence of continuous and modern sediments complicates to find a suitable trench site in the study region. However, by using aerial photos, high resolution digital elevation models, and detailed field observations, Yukarı Yuvacık Site is chosen for

the trench study. Moreover, the absence of any nearby settlement, which eliminates any anthropogenic effect and continuous sedimentation make this place ideal for a palaeoseismological study.

The Yukarı Yuvacık Site is located approximately 25 km southwest of the Kemaliye region, situated in a fault related linear valley where a seasonal river channel exist, the Karşıbağ and Dörtsöğüt creeks (Fig. 5.2). The valley walls are made of marbles of the Keban metamorphics. However, the valley floor is filled by the Eocene fossiliferous limestone and the modern channel deposits. Fine clastic sediments are also deposited in the fault-related small depressions. The Karşıbağ and Dörtsöğüt creeks connect with other creeks to the west and all drain to the Karasu River. The Karşıbağ creek drains at the bottom of the valley, which lies almost east-west direction, whereas Dörtsöğüt Creek flows to the southwest from the hillslope to the valley where the Karşıbağ Creek stretches out (Fig. 5.2). The morphology of the site is not only characterized with this fluvial system and its two terrace treads, but also with an alluvial fan as well (Fig. 5.2). Sediments of the Dörtsöğüt Creek feed this small alluvial fan, which is partly eroded by the modern channel system. A gentle terrace riser separates two terraces, T1 and T0 from older to younger respectively, from each other. The fs7 segment of the OF bounds the southern margin of the valley, which is also the border of Keban marbles and T0 terrace level. Moreover, the existence of dry and wet regions along the fs7 indicates that the Yukarı Yuvacık Site is an ideal place for trenching (Fig. 5.2).

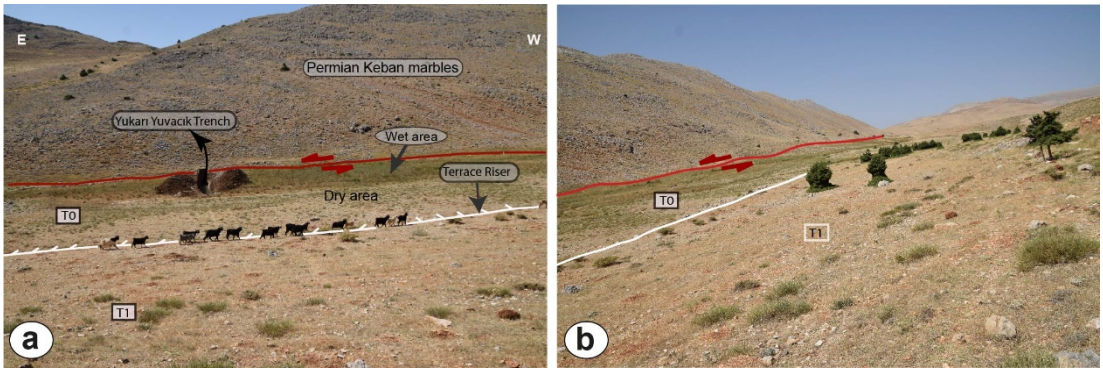

Figure 5.2 : (a) Photograph of the trench site and (b) the western continuation of the linear valley. The Yukarı Yuvacık Trench is composed of the Keban marbles, slope derived deposits and modern sediments of the T0 terrace tread. Difference between wet and dry area reflects the location of the fault (solid red line with arrows showing the sense of motion) as well. Two different terrace levels (T0 and T1) are seperated from each other by gentle scarp, which is indicated with white lines with hachures and goats.

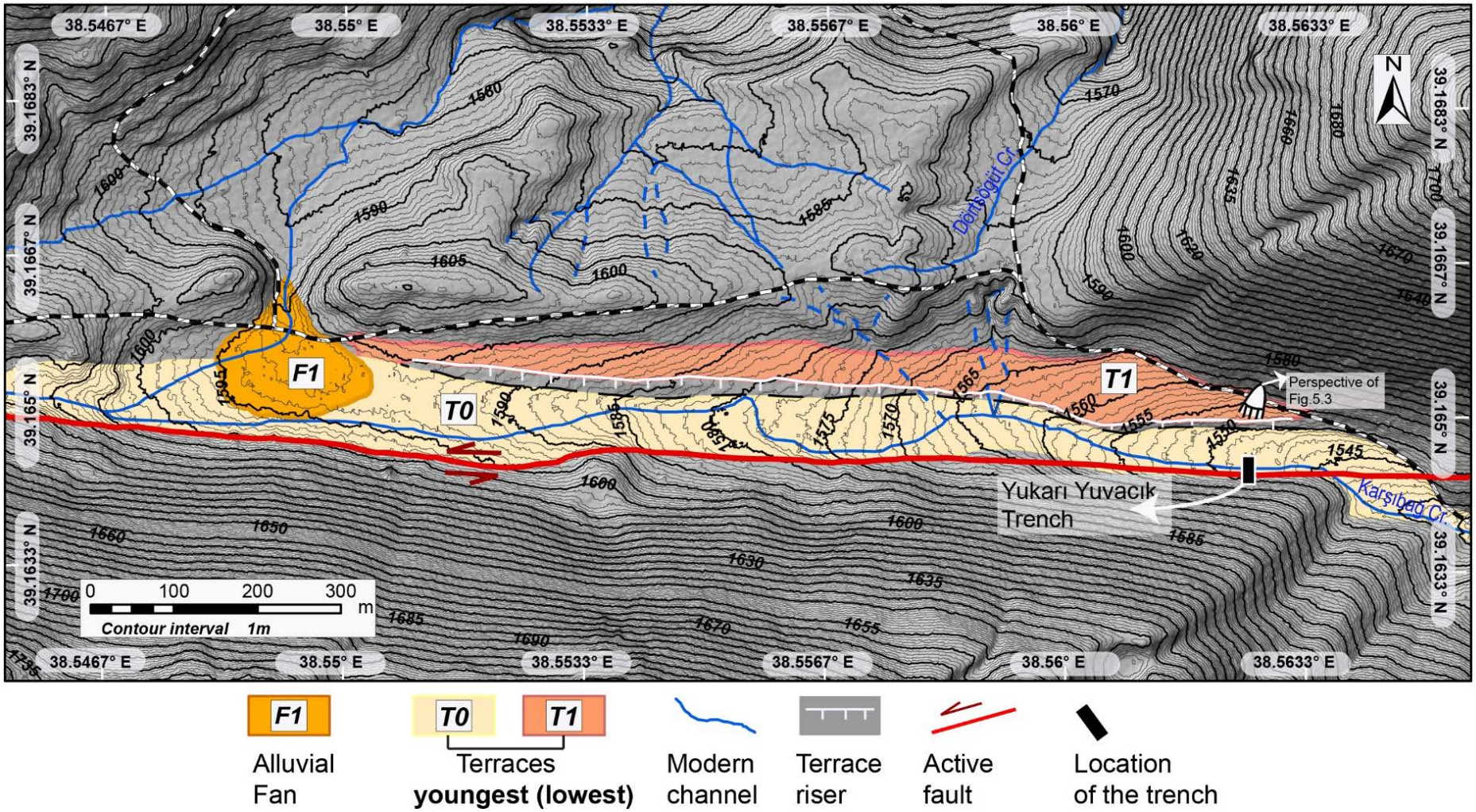

Figure 5.3 : The morphotectonic map of the Yukarı Yuvacık Trench site.

5.2.2 Stratigraphy of the Trench

In addition to the scarp derived colluvium, which occupies almost most upper part of the trench wall at the most southern part of the trench, there are three main sedimentary packages; altered bedrock, fine grain clastic sediments and coarse-to-medium grain clastic sediments. These sequences are of predominantly fine to medium-grained clastic sediments (mostly clay, silt and sand) with some caliches and gravels. The composition, colour, amount of caliche, distribution of gravels and structural relationships were used to identify the stratigraphy and palaeoseismic history of the trench. The brief information about the layers from younger to older is given in Table 5.2.

The dark brown altered rock, which is exposed between 1-2 (unit a) and 7-8 m (unit aa), is composed of crushed marbles of the Keban metamorphics (Fig. 5.4b). The exposed thickness of this unit (a) exceeds 1 metre at the southern tip of the trench (between 7 and 8 m), however it is less than half a metre between 1-3 m where the aa wedges out to the north. An infill of this altered bedrock (a1) is interpreted to happen as the result of faulting between 6.5-8 m.

The sequence of fine grain sediments is exposed at the middle of the trench between 2.5-7 m. Various colours, changing from brown to green, and a complex distribution due to multiple faulting events, characterize this sequence. The bottom of the sequence starts with white clay and silt (unit p) as a non-continuous layer in lateral direction (Fig. 5.4). This non-continuity in lateral direction is controlled by two structural elements (F6 and F8-X). Above the “unit p”, the greenish to white clay rich unit (n) exposes in relatively a small and narrow area, which is controlled by two faults, F6 and FZ8). The sheared internal structure of the “unit n” suggest that this unit is a fault clay. The yellowish white sandy clay of the “unit m-1”, and “m-2” including pebbles, are delimited from units “p” and “n” by the F6. The “unit m” is occupies relatively a wider space than units “p” and “n”. A yellowish white silty clay “unit k” is also limited by F5-Y in the north and F5-X in the south of the trench into a very narrow zone. The middle section of the sequence is composed of greyish white clay and silt (unit j) and continues upward to greenish grey clay (unit h). The “unit h” includes high amount of caliches, which lie parallel to layering. The light brown silty clay with high amount of caliches (unit g), is divided into two sub-units (g1 and g2) according to their compositions and colours. The “g1” is very narrow and made of sheared green clay within the “unit g”, whereas the “g2” is white clay with an irregular layering. The dark

brown clay “unit f” with a cobble of altered bedrock wedges out toward the north where it is limited by F4 and is overlain stratigraphically by light brown silt unit (unit e). The “unit d”, in which the bottom horizon of the unit is represented by dark brown and sheared silt (sub-unit d1), is the thickest unit of the sequence. The d is composed of dark brown clay with a few amount of silt and high amount of caliches which are white in colour. All layers from “unit j” to the “unit d” are tilted to the south of about 20 degrees. A dark brown clayey sand, “unit c”, overlies the “unit d”. The “unit c”, however, most possibly was formed by bioturbation or other processes. The top unit of this sequence is light brown colour clay-silt material (unit b), which includes small amounts of caliches and it has light brown infill sediments without any caliche (sub-unit b1). Coarse grain sequences are mainly located at the northern part of the trench. The bottom of the sequence is represented by light brown sand with various sizes of sorted gravels of a channel deposits (ch3) and continue upward to a successive layer of yellowish brown sand (t, s, r, from older to younger respectively) with very few amount of pebbles “t” at the bottom to calishe rich greenish brown colour sand “r”. A light brown sandy channel deposits (ch2) includes poorly sorted and rounded pebbles in the northern part of the layer. All of these units are unconformably overlain by a dark brown colluvium (Col), which includes gravels of marbles in a brown sandy matrix. Moreover, the angular shape and poorly sorted texture of Col imply that it is close to the source. The thick unit of Col wedges out to north where it becomes distant from its source and is cut by the modern channel deposits (ch1) including brown sands with fine grain sorted pebbles A thin layer of dark brown soil represents the top of the trench (Table 5.2 and Fig. 5.4b).

Table 5.3 : The brief explanation of the units of the trench.

Unit	Feature
Soil	Brown colour organic rich silt
	Coarse grain sediments
ch1	Reddish sand with clay, limited amount semi rounded pebbles
Col	Dark brown sand with weathered bed rock poorly sorted pebbles
ch2	Dark brown clay with various size of pebles

Table 5.2. (Continue): The brief explanation of the units of the trench

Unit	Feature
r	Greenish brown clayish sand with few caliches
s	Ligth brown silty sand without any calishe
t	Yellowish brown colour sand with few amount of sorted pebbles
ch3	Dark brown clayed sand with weathered bed rock pebles
	Fine grain clastic sediments
b	Light brown sheared clayish silt with caliches, (b1) infill deposits
c	Dark colour clayish sand most probably related with bioturbation
d	Grayish brown clay with lots of elongated caliches, (d1) Light brown silt
e	Beige colour silt with few caliche
f	Dark greenish gray clay with the block of bedrock and its weathered fragments
g	Silty clay with calishes, (g1) sheared greenish clay and (g2) beige colour clay
h	Greenish gray clay with elongated caliches
j	Beige color silt with weathered pebbles of the bed rock
k	Sheared fault zone yellowish white colour silty clay
m	(m-1) Light brown clay, (m-2) yellowish white clay with pebbles
n	Sheared fault zone greenish clay
p	Yellowish white clayish silt with few caliche
	Alterated bedrock
a	Weathered bed rock (a), (a1) Infill deposits,
aa	Weathered bed rock

5.2.3 Structural relationship of the Yukarı Yuvacık Trench

The Yukarı Yuvacık Trench displays several fault strands, which deform the exposed stratigraphy. Faults are distributed along the trench, therefore we named fault strands starts from the 8th to the 1st metre as FZ1 to F8, respectively.

The FZ1 is made of many bifurcated and sub-parallel fault strands within the exposed bedrock. This fault zone leads to the shearing of the altered bedrock (unit a) and separates units “a” and “b” as well (Fig. 5.5). The FZ1 connects with F2, which is almost parallel to the FZ1. At this junction F2 is bifurcated into two sub-parallel brances, all which climb up to the bottom of the Col. The bifurcated sections of both the FZ1 and the F2 is well defined with a sheared infill material (a1 and b1). The F2 is the structural boundary between the unit b in one side and unit c and d on the other side, whereas the “unit d” is structurally separated from the “unit e” by the F3 in the 6th metre of the trench. The F3 delimits some part of the boundary between units “d” and “e”, then it goes up within the “unit d” again until the bottom boundary of the Col. The “unit f” wedges out toward the north where it is laterally truncated by the F4. The F4, which starts as a single strand and bifurcates into two subparallel strands, makes the structural contact between units “e”, “f” and “g”. When it laterally cuts the “unit f”, it starts to deform the “unit e” with its two subparallel strands. Two strands of the F4 are well defined by abrupt vertical separation of the contact between units “d” and “e”. To the north, units “e”, “g”, “h” and “j” from the southern block and the units “m-1”, “m-2” and “r” from the northern block are cut by the F5 in the 3rd metre of the trench. The F5 has two strands parallel to each other as F5-a at the northen part and F5-b at the southern part. From 3rd to 8th metres, almost all fault strands dip to the south except a few ones within the FZ1. Moreover, at this section of the trench, Col overlies all of these faults and related layers; thus, I interpreted the bottom contact of this unit as the youngest event (YUV-1) of the Yukarı Yuvacık trench (Fig. 5.4b).

The F6 starts climbs up parallel to the F5, but it does not reach to the bottom the Col and terminates under the unit “r”. Another termination of a fault strand (F8-a and F8-b) under the same horizon is observed at the ~2. metre. The F6 delimits the unit “m” in the south and “n” and “p” at the north, whereas the F7-x bounds the unit “p” from the north and F7-b delimits the unit “ch3” from the south. Moreover, they climbs up to bottom contact of units “t”, “s” and “t”, which is interpreted as second palaoerthquake event of the trench (YUV-2)

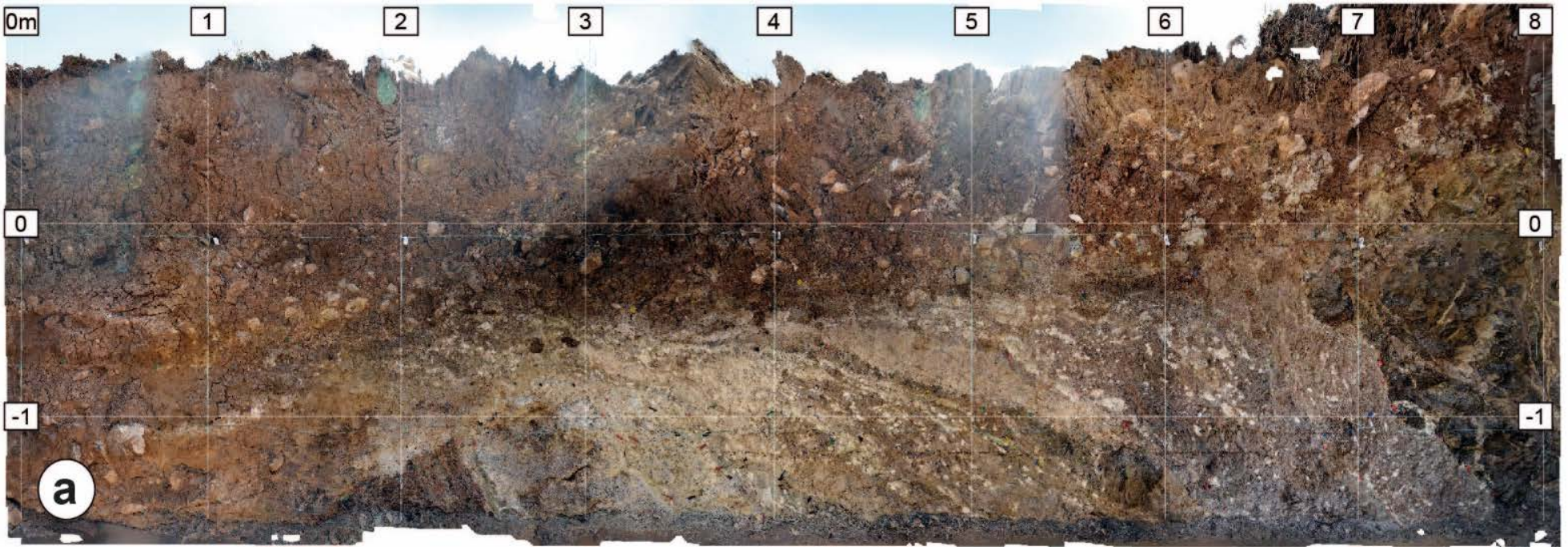

Figure 5.4 : The eastern wall of the Yukarı Yuvacık Trench. (a) the photomosaic of the trench wall withour any interpretation, (b) geological and structural interpratetion of the wall.

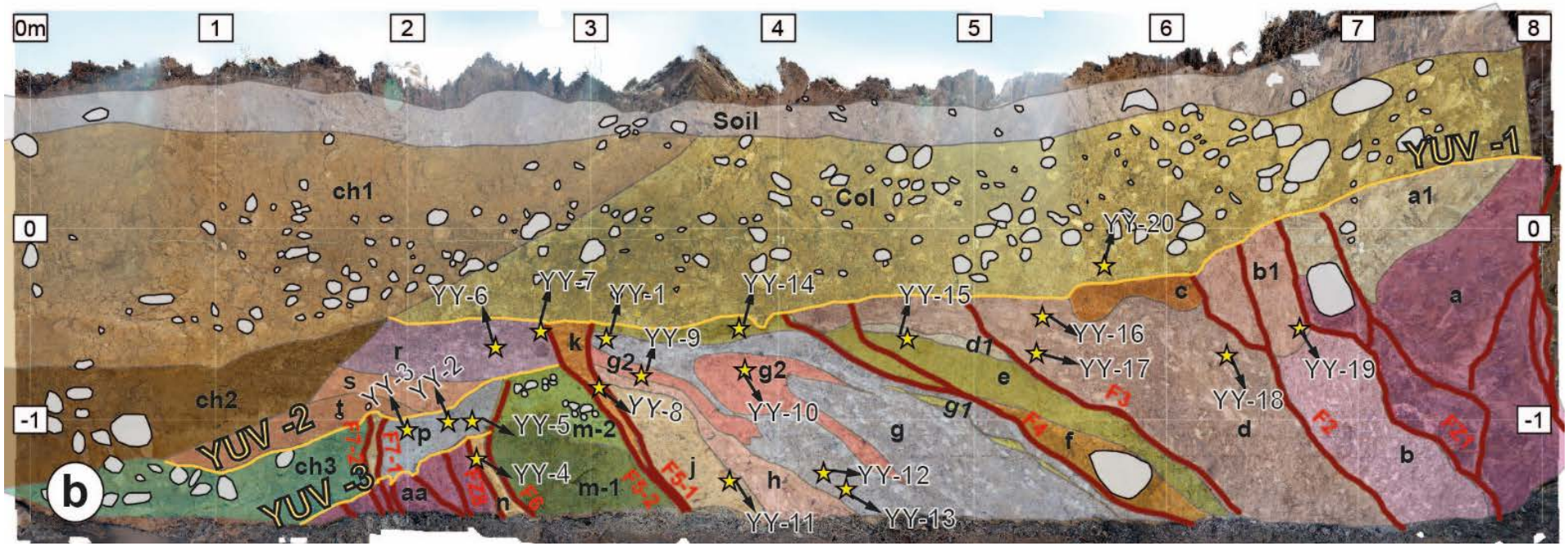

Figure 5.4. (continue): The eastern wall of the Yukarı Yuvacık Trench. (a) the photomosaic of the trench wall withour any interpretation, (b) geological and structural interpratetion of the wall.

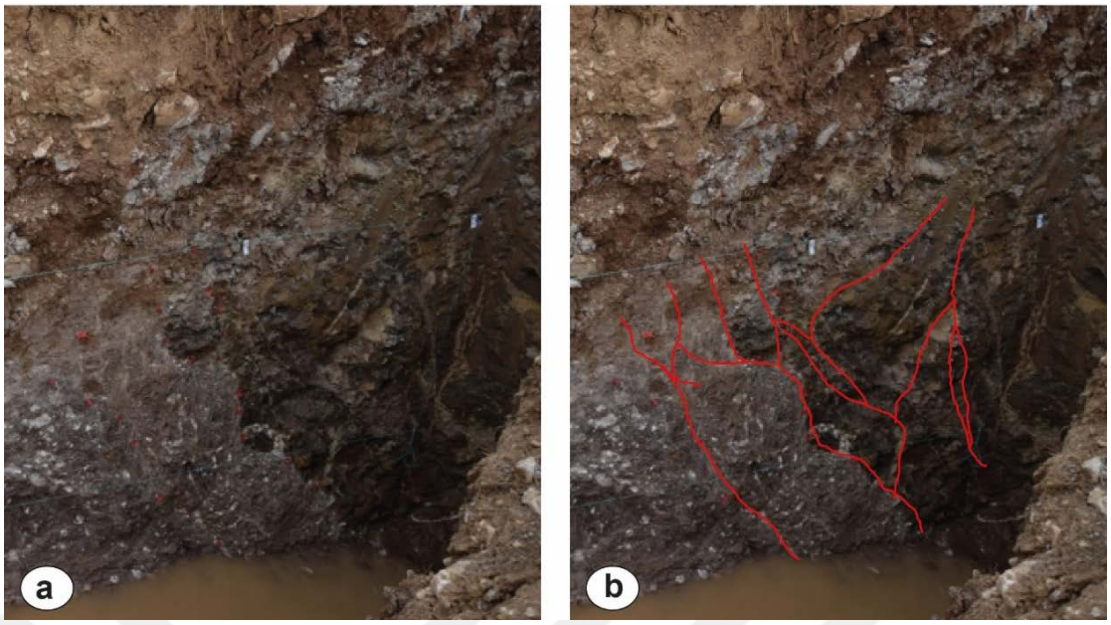

Figure 5.5 : The photo showing the 6th to 8th metres of the trench's eastern wall. (a) the raw version, (b) interpretated photo of structures. The Fault Zone (FZ1), which is well defined with sharp lateral discontinuties and light colour faults clays, are developed within the shear planes.

The units "n" and "aa" are delimited from each other by the FZ8, which is very closely spaced parallel strand to the F6. The F6 and the FZ8 are well defined with a fault clay that constitutes the unit n. The FZ8 laterally truncates the unit aa.

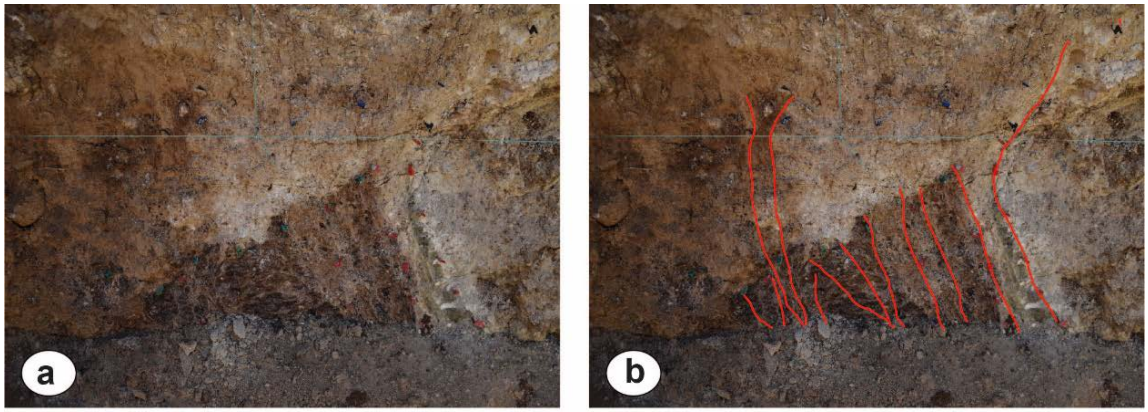

Figure 5.6 : The apperiance of the FZ8 in the trench (a) and its tectonic interpretation. (b) Within the unit aa, FZ8 has many strands that constitutes the aa as an fault rock

The last fault is the FZ8, which composed of many subparallel fault strands and all of them buried within the weathered bedrock unit "aa" (Fig. 5.6). This unit is sheared by 7 different branches of the FZ8 that cause vertical displacement of the contact between the "aa" and overling units (p and ch3). Therefore, the upper limit of the "aa" refers to the oldest event horizon YUV-3 (Fig. 5.4b).

5.2.4 Palaeoearthquakes of the Yukarı Yuvacık Trench

The Yukarı Yuvacık trench presents evidence of three different palaeoearthquakes as a result of stratigraphic and structural relations of units. The YUV-1 horizon constitutes the youngest event, which bounds the colluvium (Col) from the rest of the units and represented by the bottom of the colluvium (Col) (Fig. 5.4b).

The second event horizon is YUV-2 that delimits mainly coarse grain sediments from the fine grain sediments and “ch3”. The YUV-2 event horizon is defined by the bottom contact of the “t”, “s”, “r” (Fig. 5.4a) and top of “ch3”, “p”, and “m-2”. The F7-b that laterally truncates the unit ch3 and the F7-a delimits the “p” from the north. The deformation on the F7 does not affect the “t” and younger units, where the bottom of the “t” infers the second palaeoearthquake event horizon of the trench.

The oldest event that is caused by FZ8 and their strands, which lead to shearing and uplifting of the bedrock (aa). These strands of the FZ8 lead to offsets along the contact of the “aa” and the “p” units. Therefor, the upper limit of the unit “aa” gives the event horizon for the YUV-3.

Altough 16 radiaocarbon ages were determined for the trench, just 6 of them can be used, which are coherent with the stratigraphy of the trench. Table 5.3 summarized the age range for the samples and the palaeoearthquake events (Fig. 7).

Table 5.4 : The radiocarbon age results of all 16 collected samples

Sample	Radiocarbon age (B.P.)	Calendar Calibration	Probability (σ2)
YY-20	3470 ± 30	B.C.E. 1884 -1734	91.50%
		B.C.E. 1717-1694	8.50%
YY-19	2110 ±30	B.C.E. 203-46	100%
YY-18	5850 ±30	B.C.E. 4793-4653	95.10%
		B.C.E. 4639-4617	4.90%

Table 5.3.(Continue): The radiocarbon age results of all 16 collected samples

Sample	Radiocarbon age (B.P.)	Calendar Calibration	Probability (σ2)
YY-16	2130 ±30	B.C.E. 349-311	10.40%
		B.C.E. 209-53	89.60%
YY-15	2740 ±30	B.C.E. 971-960	2.10%
		B.C.E. 936-816	97.90%
YY-14	3300 ±30	B.C.E. 1643-1504	100%
YY-13	8890 ±40	B.C.E. 8238-7938	98.40%
		B.C.E. 7922-7920	0.10%
		B.C.E. 7891-7870	1.20%
		B.C.E. 7854-7848	0.30%
YY-10	2560 ±30	B.C.E. 804-747	70.10%
		B.C.E. 685- 666	7.50%
		B.C.E. 642-554	22.40%
YY-9	3710 ±30	B.C.E. 2200-2158	15.10%
		B.C.E. 2155-2025	84.90%
YY-8	4180 ±30	B.C.E. 2887-2835	22.70%
		B.C.E. 2817-2665	76.80%
		B.C.E. 2643-2649	0.50%

Table 5.3.(Continue): The radiocarbon age results of all 16 collected samples.

Sample	Radiocarbon age (B.P.)	Calendar Calibration	Probability (σ2)
YY-7	3360 ±30	B.C.E. 1742-1710	10.70%
		B.C.E. 1700-1606	83.50%
		B.C.E. 1583-1558	4.80%
		B.C.E. 1554-1546	1%
YY-6	4910 ±30	B.C.E. 3762-3738	6.30%
		B.C.E. 3735-3725	2.10%
		B.C.E. 3715-3642	91.50%
YY-5	4370 ±30	B.C.E. 3088-3056	9.80%
		B.C.E. 3031-2907	90.20%
YY-4	5860 ±30	B.C.E. 4822-4820	0.10%
		B.C.E. 4800-4677	97.40%
		B.C.E. 4674-4670	0.30%
		B.C.E. 4636-4618	2.30%
YY-3	3810 ±30	B.C.E. 2397-2385	1.20%
		B.C.E. 2346-2189	88.40%
		B.C.E. 2182-2141	10.40%
YY-1	3730 ±30	B.C.E. 2205-2032	100%

Table 5.5 : Chronology of the samples, which are used for age modelling and event horizons.

Sample	Radiocarbon age B.C.E.	δ13C	Type of Material
YUV-1 (after 56 B.C.E)			
YY-19	203 - 46	-22.6	Bulk
YY-16	209 - 53	-22.6	Charcoal
YY-10	807 - 747	-23.4	Charcoal
YY-7	1700 - 1606	-23.7	Charcoal
YUV-2 (2950 - 1600 B.C.E.)			
YY-5	3031 - 2907	-22.5	Charcoal
YUV-3 (4700 - 3022 B.C.E)			
YY-4	4800 - 4677	-24.3	Charcoal

The probability density function from the six ages presents the time interval for both samples and event horizons (Fig. 5.7 and Table 5.3). The bulk samples of the YY-19 (203-46 BCE with 100%; 2σ probability) and the YY-16 (209-53 BCE with 89.6%; 2 σ probability) were taken from the upper part of the unit b, and d in order, which are represent the lower limit for the YUV-1 (Youngest event) (Fig. 5.7). However, absence of age from the unit "Col" prevents to confine it from the above. Taking into account of this situation, the time interval for the YUV-1 can be calculated by its lower boundary. Therefore, from the density function time of the youngest event (YUV-1) is after the 56 B.C. with the absence of upper limit. Altoug the time interval for the YUV-1 is high, the YUV1 can be interpreted as surface rupture of two mentioned historical earthquake (Fig. 5.7).

The YY-10 gives an age 804- 747 BCE with 70.1%; 2 σ probability, whereas older age comes from the YY-7 as 1700- 1606 BCE with 83.5%; 2σ probability. The penultimate event YUV-2 is limited with the YY-5 from the below and the YY-7, YY-

10, YY-16 and YY-19 from the above. The age of the YY-7 sample (1700-1606 BCE with 83.5%; 2σ probability) is the upper limit of the event whereas the YY-5 3031-2907 BCE (09.2 %; 2σ probability) bounds the YUV-2 from the below. From the density function and probability calculation it can be found that the age of the YUV-2 is 2950- 1600 BCE.

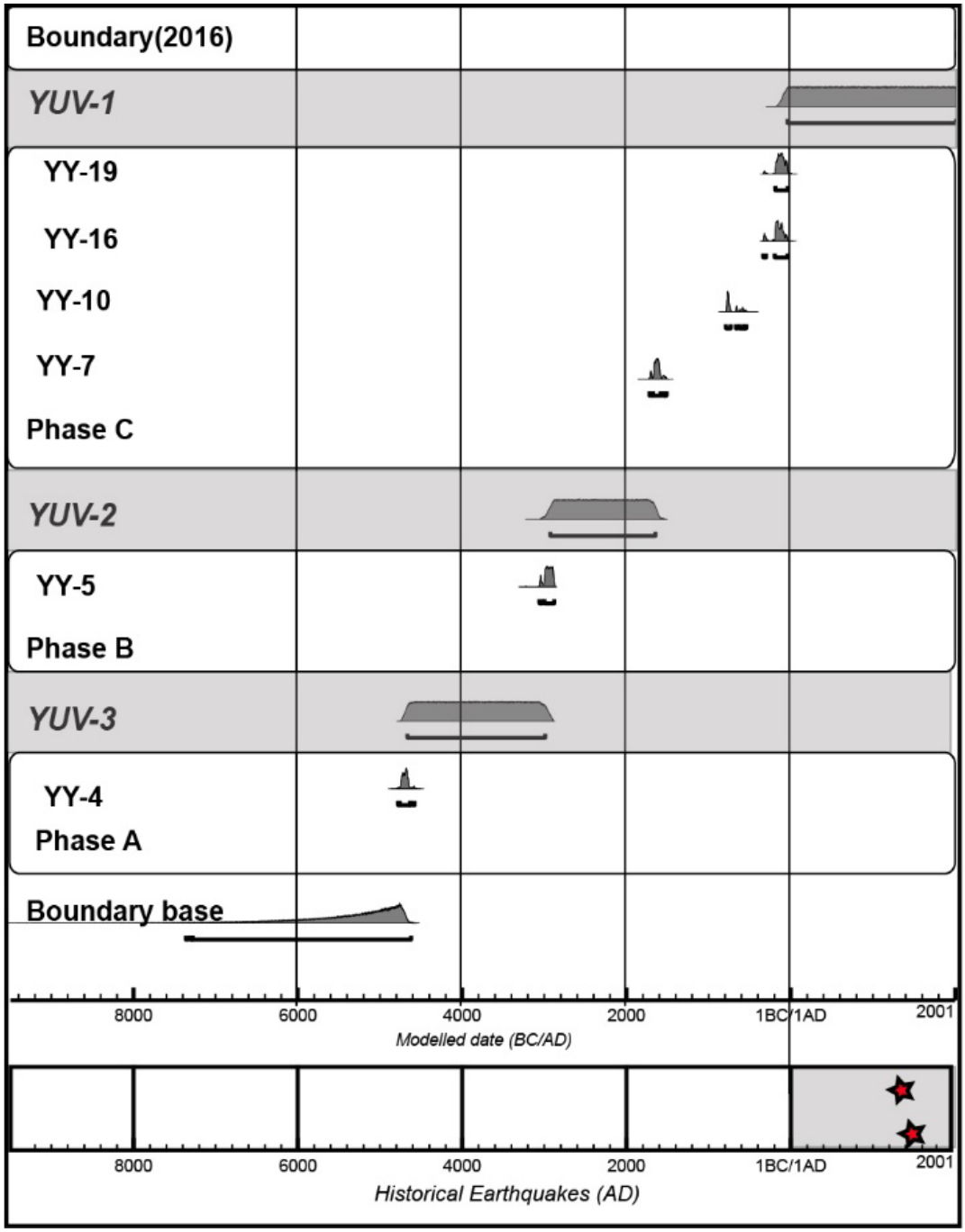

Figure 5.7 : The OxCal calibration probability age modelling for the samples. The two red starts indicate possible historical earthquakes related with the OF (1779 Melitene and 1896 Ovacık earthquakes).

The oldest event YUV-3 is constrained by the YY-5 from the above and YY-4 from

the below. So, it can be assumed that the oldest event has happened before the 3031-2907 BCE (YY-5) and after 4800-4677 BCE as an age of the YY-4 (97.4%; 2σ probability). From the age modelled stratigraphy, time interval for the oldest earthquake event (YUV-3) is 4700- 3022 B.C.E.

The probability curve for the ages of the trench gives an idea to reoccurance interval of earthquake, which can create surface rupture. From the probability model, reoccurrence interval of an earthquake that generates surface rupture is calculated as 2400 ± 765 years (Fig. 9 and Table 3).

6. DISCUSSIONS

Earthquakes on plate boundaries, which are mainly large and periodic for long intervals, are recorded by historically and instrumentally. However, earthquakes especially in continental intra-plate regions are episodic, clustered and migrating (Li et al., 2009). The historical and instrumental records usually do not represent the seismic activity in the intra-plate region where the rate of seismic activity is relatively low and recurrence interval of surface rupturing earthquakes are long. Therefore, palaeoseismologic studies provide valuable data, which extends the time coverage of historical records to thousands, even to tens of thousands, of years, to understand the earthquake behaviour of active faults in 'stable'plate interiors. Palaeoseismological studies make available to increase the knowledge of magnitude of events, their geometries, migration of earthquakes, slip rates and recurrence rates for surface in intra-plate regions (Meghraoui et al., 2000). Intra-plate earthquakes especially in continental crust show occurrence in temporal clusters on faults that remain active for some time and then have long quiescent period ((Camelbeeck et al., 2007; Crone et al., 2003).

The Ovacık Fault, which is one of the sinistral strike slip intra-plate fault of the Anatolian Block, shows very limited activity in the historical records (Fig. 5.1). Although looking the historical and instrumental records it seems that it is not an active seismogenic fault, the palaeoseismic study in this thesis clearly show multiple palaeoearthquakes on the OF in the last 5 ka.

The OF starts from the north-eastern end as a single strand until the south-western end of the Ovacık Basin (to the west / southwest of 38.83°E). After this location, it bifurcates into several branches with different strikes, which generates a wider deformation zone between the fs5 and fs9 segments. The region, between the fs5 and fs8, represents a transpressional setting due to the fault geometry, restraining bending, and also interaction of the OF with the MF. This region is sliced into many pieces by different fault segments and tectonic lineaments, few of which follow the pre-weakness zone of the palaeothrust boundary between the Munzur Limestone and Kemaliye Formation.

Geomorphic indices, showing high steepness and hypsometric integral values at the Kemaliye Region, between the fs5 and fs8 segments and at the Munzur Mountains, yield tectonic uplift. The Kemaliye Region, where there is no glacial and karstic effect, these high values are directly referring to a sudden tectonic uplift. However, glaciation and karstification at the Munzur Mountains affect results of geomorphic indices. Therefore, these high values cannot directly relate to the tectonic uplift at the Munzur Mountains.

The extent of palaeoglacial activity and wide-spread karstification, which is common in the eastern Munzur Mountains, have almost none or very limited control in this west/south-western parts of our study region (Akçar et al., 2007; Akçar et al., 2017; Yeşilyurt et al., 2015). We also did not observe any evidence of palaeoglacial activity and/or strong karstification during our field studies in the Kemaliye Region. In this region, incipient karstic voids at the valley walls suggest relatively fast uplifting of the region rather than the surroundings, whereas in the eastern Munzur Mountains vertical karstic morphology is more spread. The absence of no or limited palaeoglacial activity, karstification and the similar strength lithologies within the limits of the DBs 25, 26, 27 and 28 suggest that the tectonic uplift is the main control for Kemaliye and the nearby region (Fig. 10). The reason for relative uplifting around Kemaliye region can be result of (a) the existence of a high convergence zone, which cuts the EASZ and penetrates into Anatolia (Şengör et al., 1985) or (b) the interaction of the sinistral Malatya Fault (MF) and the OF.

Furthermore, we also tried to understand the fault control on the formation of the Ovacık Basin. The differential lithology, which is metamorphic and young sedimentary rocks of the southern part and the limestone on the northern part of the Ovacık Basin, can affect the sinuosity of the mountain front. Not only easily erodible limestone in the northern part, but also palaeoglacial and alluvial fan activity can be attributed to its Smf value. However, four measurements from the four different mountain fronts (Sm1 and Sm2 in the north, Sm3 and Sm4 in the south) indicate that sinuosity of the mountain front increases from Sm3, Sm4, Sm1 to Sm2 respectively. The plot of Smf and Vfmean values indicates that the relatively most tectonically active mountain front is related with the fs3 segment and then followed by the fs2 segment. These values also prove the location of the fault scarp that interpreted as a fault-controlled nature, while the southern boundary is mainly dominated with erosional processes. The first calculated vertical uplift is along the fs2 and fs3

segments show that the uplift rate is calculated at least 0.5 mm/yr along the northern margin of the OF. This is also well supported by almost all available active fault maps of the region (Arpat and Şaroğlu, 1975; Emre et al., 2012a, 2012b, 2012c; Şaroğlu et al., 1992), which do not show any active tectonic structure along the southern margin of the Ovacık Basin.

On the other hand, NW-striking normal faults on the fs8 and the fs9 were observed segments in the Tertiary cover deposits and the Yamadağ Volcanic Complex (Fig. 3.22). This normal faulting is observed at the region between two sinistral strike slip faults, which leads to extentional setting. Moreover, existence of Yamadağ Volcanic Complex also proofs the extentional setting to emplacement of the magmatic bodies.

The cumulative deflection of the Karasu River is measured approximately as 14.7 ± 0.5 km, which is accumulated along the different branches of the OF (Fig. 3.28). The age of the Karasu River, a main branch of Euphrates, assumed as younger than Pliocene (5.3ka) according to its youngest deposits in the Eastern Anatolia (Avşin; Erinç, 1953). Therefore, the very long-term slip rate is calculated to be 2.6 mm/yr by using the cumulative offset of the Karasu River and its age, which is compatible with short-term slip rate estimate of Zabcı et al. (2017), which is constrained in the Ovacık Basin of about 50 km to the east/northeast. Moreover, the slip rate site of Zabcı et al. (2017) is located on the single strand section of the fault, which suggests that the rate of slip does not change along the strike of the fault, but it is distributed to multiple sub-parallel fault segments at the southwestern part of the Ovacık Fault.

Studies on the CAFZ and TZF show that the southern part of faults are under the extentional setting which is mainly effected by Western Anatolia Extentional province (Higgins et al.), or combination effect of tectonic escape towasd the west and upwelling asthenosphere that heats the crust and leads to extentional deformation (Yıldırım et al., 2016). However, to the eastern part of the Central Anatolia, compressional setting become dominant rather than the extensional regime. These tectonic features are components of a single diffuse deformation system, which is bounded by NASZ and EASZ and covers the whole Anatolian Block. Triggered factor for this deformation related with the transmission of from the boundary zone especially from the NASZ.

One of the most important impact of this study is the first palaeoseismic result for the poorly known Ovacık Fault. The Yukarı Yuvacık Trench shows data beyond the

general expectation. Founding of three different palaeoevents indicate that this seismologically unknown fault has higher potential to produce earthquakes than previous assumptions (Westaway andArger, 2001a). Although, there is limited number of age results, I constructed the best age modelling with the available data. The analysis of the stratigraphy and their structural positions indicate that six of the ages for layers can be used for age modelling. The obtained ages for events from the trench, indicates that four different event occurred on this particular fault since about 5 ka. After Oxcal calibration model the time interval for the events are calculated with statistically reoccurrence period of 2400 ± 765 years for the fs7 segment.

7. CONCLUSIONS

The purpose of this graduate thesis is to understand the deformation history of the Ovacık Fault and surroundings. With this aim, two geological map, one is 1: 400.000 scale along the whole strike of the OF (App. A1) that is mainly complied by previous studies and Landsat images, and a 1:200.000 scale geological map of the western part of the Karasu River (App. A2), mainly from personal field observations and previous studies were produced.

In the studied area, the Keban Metamorphics constitute the basement of the region that consist of marble and schist, which is uncomfortably overlaid by the Kemaliye Formation. The allocthonous Munzur Limestone thrusted over the older units. Moreover, the Munzur Limestone overlaid by the Cretaceous ophiolitic melange by south vergence thrusting. The Tertiary cover deposits unconformably underlain by all these Mesozoic units. All of these units are intruded by the Çöpler granitoid and then unconformably overlain by the Yamadağ Volcanic Complex. The Quaternary deposits, which are alluvial fans, morains, debris flows and alluviums constitute the top of the stratigraphic column.

Structural data of the paleo tectonic units show dominance of folding plunging to E-NE in the western part of the Karasu River. This result indicates that western part of the study region is tectonically uplifted, which is also confirmed by geomorphic indices.

Examination of aerial photographs, digital elevation models, Landsat images and field observations are tools, which are used in this study, to determine the morphotectonic structures of the OF. Geomorphic indices are used to characterize the deformation along the OF. The hypsometric curve and integral, normalized steepness and concavity index, channel profiles, valley floor height-width ratio and mountain front sinuosity may indicate that the relatively young morphology, which is related with tectonic activity. The Kemaliye Region, which does not show glacial morphology, is mostly considered as a sudden tectonic uplift between sinistral fs5, fs8 and the MF. The interaction of these three fault

branches should lead to clockwise rotation, which is also indicated by tectonic lineaments at the Kemaliye Region. The first calculated vertical uplift is along the fs2 and fs3 segments show that the uplift rate is calculated at least 0.5 mm/yr.

The first palaeoseismological study at the Yukarı Yuvacık site, on the fs7 segment, indicates the occurence of three different paleoearthquakes on this particular segment. A recurrence scenario of earthquakes, which is produced by date of related stratigraphic sequence, is interpreted as 2400 ± 765 years, which is very close to MF (Sancar et al., 2018). This significant result of paleoseismological study clearly show that the OF is a seismogenic fault within the Anatolian Block.

To be conclusive about the deformation and its distubution on the OF, additional paleoseismological studies are necessary on the different segments of the OF.

REFERENCES

Afad. (2013). **URL-1** https://www.afad.gov.tr/tr/3017/Son-48-Saatte-48-Deprem

Akçar, N., Yavuz, V., Ivy-Ochs, S., Kubik, P. W., Vardar, M., Schlüchter, C., 2007. Cosmogenic exposure dating of snow-avalanche ridges Eastern Black Sea Mountains, NE Turkey. Quaternary International, 167–168(0), 4-11.

Akçar, N., Yavuz, V., Yeşilyurt, S., Ivy-Ochs, S., Reber, R., Bayrakdar, C., Kubik, P. W., Zahno, C., Schlunegger, F., Schlüchter, C., 2017. Synchronous Last Glacial Maximum across the Anatolian peninsula. Geological Society, London, Special Publications, 433(1), 251.

Aksoy, E. (1996). Ovacık Fay Zonunun Arapgir - Keban Baraj Gölü Arasındaki Kesiminde Tektonik İncelemeler. Fırat Üniversitesi, Fen ve Müh. Bilimleri Dergisi, 8(1), 1 - 20.

Aktuğ, B., Dikmen, Ü., Doğru, A. &Özener, H. (2013a). Seismicity and strain accumulation around Karliova Triple Junction (Turkey). Journal of Geodynamics, 67(0), 21-29. doi: http://dx.doi.org/10.1016/j.jog.2012.04.008

Aktuğ, B., Parmaksız, E., Kurt, M., Lenk, O., Kılıçoğlu, A., Gürdal, M. A. &Özdemir, S. (2013b). Deformation of Central Anatolia: GPS implications. Journal of Geodynamics, 67, 78-96.

Aktuğ, B., Parmaksız, E., Kurt, M., Lenk, O., Kılıçoğlu, A., Gürdal, M. A. &Özdemir, S. (2013c). Deformation of Central Anatolia: GPS implications. Journal of Geodynamics, 67(0), 78-96. doi: http://dx.doi.org/10.1016/j.jog.2012.05.008

Akyuz, H. S., Altunel, E., Karabacak, V. &Yalciner, C. C. (2006). Historical earthquake activity of the northern part of the Dead Sea Fault Zone, southern Turkey. Tectonophysics, 426(3-4), 281-293.

Akyuz, H. S., Ucarkus, G., Altunel, E., Dogan, B. &Dikbas, A. (2013). Paleoseismological investigations on a slow-moving active fault in central Anatolia, Tecer Fault, Sivas. Annals of Geophysics, 55(5).

Aleksandrowski, P. (1985). Graphical determination of principal stress directions for slickenside lineation populations: an attempt to modify Arthaud's method. Journal of Structural Geology, 7(1), 73-82.

Arpat, E. &Şaroğlu, F. (1975). Türkiye'de Bazı Önemli Genç Tektonik Olaylar. Türkiye Jeoloji Bülteni, 18(1-2), 91-101.

Avagyan, A., Sosson, M., Karakhanian, A., Philip, H., Rebai, S., Rolland, Y. .Davtyan, V. (2010). Recent tectonic stress evolution in the Lesser Caucasus and adjacent regions. Geological Society, London, Special Publications, 340(1), 393-408.

Avşin, N.n.d**.** Karasu Nehri Vadisinin Morfotektonik Gelişiminde Tiltlenme Etkisi.

Barka, A. A. (1992). The North Anatolian fault zone. Annales Tectonicae, 6, 164-195.

Barka, A. A. &Kadinsky-Cade, K. (1988). Strike-Slip Fault Geometry in Turkey and Its Influence on Earthquake Activity. Tectonics, 7(3), 663-684.

Bayrakdar, C., Çılğın, Z., Döker, M. F., Canpolat, E., 2015. Evidence of an active glacier in the Munzur Mountains, eastern Turkey. Turkish Journal of Earth Sciences, 24(1), 56-71.

Bilgiç, T., 2008. Geological map of Turkey at 1:100000 scale, no. 86, 87, 84, Divrigi- J40, Divrigi- J41, and Erzincan-I42. Mineral Research and Exploration Institute (MTA) of Turkey publications (in Turkish with English abstract), Ankara

Bilgin, T., 1972. Munzur Dağları doğu kısmının glasiyal ve periglasiyal morfolojisi, İstanbul Üniversitesi Yayınları No: 1757, Coğrafya Enstitüsü Yayınları No: 69

Bilham, R. &King, G. (1989). Slip distribution on oblique segments of the San Andreas fault, California: Observations and theory. US Geol. Surv. Open-File Rept. 89, 315, 80-93.

Bird, P. (2003). An updated digital model of plate boundaries. Geochemistry, Geophysics, Geosystems, 4(3), n/a-n/a. doi: 10.1029/2001GC000252

Blackett, M. (2014). Early analysis of Landsat-8 thermal infrared sensor imagery of volcanic activity. Remote Sensing, 6(3), 2282-2295.

Bozkurt, E. (2001). Neotectonics of Turkey; a synthesis. Geodinamica Acta, 14(1-3), 3-30.

Braile, L. W., Keller, G. R., Hinze, W. J. &Lidiak, E. G. (1982). An Ancient Rift Complex and its relation to contemporary seismicity in the New Madrid Seismic Zone. Tectonics, 1(2), 225-237. doi: 10.1029/TC001i002p00225

Brocklehurst, S. H., Whipple, K. X., 2004. Hypsometry of glaciated landscapes, Earth Surface Processes and Landforms, 29(7), 907-926.

Bull, W.B., 1977. The alluvial-fan environment. Progress in Physical Geography: 1, 222-270.

Bull, W. B., McFadden, L. D., 1977. Geomorphology in arid regions. Geomorphology in arid regions.

Burbank, D.W., Anderson RS., 2011. Tectonic geomorphology. John Wiley & Sons.

Burke, K. &Sengör, C. (1986). Tectonic escape in the evolution of the continental crust. Reflection seismology: the continental crust, 41-53.

Camelbeeck, T., Vanneste, K., Alexandre, P., Verbeeck, K., Petermans, T., Rosset, P. et al .Stein, S. (2007). Relevance of active faulting and seismicity studies to assessments of long-term earthquake activity and maximum magnitude in intraplate northwest Europe, between the Lower Rhine Embayment and the North Sea. SPECIAL PAPERS-GEOLOGICAL SOCIETY OF AMERICA, 425, 193.

Castillo, M., Muñoz-Salinas, E., Ferrari, L., 2014. Response of a landscape to tectonics using channel steepness indices (ksn) and OSL: A case of study from the Jalisco Block, Western Mexico. Geomorphology, 221, 204-214.

Chen, Y.C., Sung, Q., Cheng, K.Y., 2003. Along-strike variations of morphotectonic features in the Western Foothills of Taiwan: tectonic implications based on stream-gradient and hypsometric analysis. Geomorphology: 56, 109-137.

Chorowicz, J., Dhont, D. &Gündoğdu, N. (1999). Neotectonics in the eastern North Anatolian fault region (Turkey) advocates crustal extension: mapping from SAR ERS imagery and Digital Elevation Model. Journal of Structural Geology, 21(5), 511-532.

Chorowicz, J., Luxey, P., Rudant, J. P., Lyberis, N., Yürür, T. &Gündoğdu, N. (1995). Slip-motion estimation along the Ovacik fault near Erzincan (Turkey) using ERS-1 radar image: Evidence of important deformation inside the Turkish plate. Remote Sensing of Environment, 52(1), 66-70. doi: http://dx.doi.org/10.1016/0034-4257(95)00014-R

Clark, D., McPherson, A. &Van Dissen, R. (2012). Long-term behaviour of Australian stable continental region (SCR) faults. Tectonophysics, 566, 1-30.

Clark, M.K., Schoenbohm, L.M., Royden, L.H., Whipple, K.X., Burchfiel, B.C., Zhang, X., Tang, W., Wang, E., Chen, L., 2004. Surface uplift, tectonics, and erosion of eastern Tibet from large-scale drainage patterns. Tectonics: 23, TC1006. DOI:10.1029/2002TC001402.

Crone, A. J., De Martini, P. M., Machette, M. N., Okumura, K. &Prescott, J. R. (2003). Paleoseismicity of two historically quiescent faults in Australia: implications for fault behavior in stable continental regions. Bulletin of the Seismological Society of America, 93(5), 1913-1934.

Çılğın, Z., 2013. Ovacık ovası (Tunceli) ve Munzur dağlarının güneybatı aklanının jeomorfolojisinde buzullasmaların etkisi. Sosyal Bilimler Dergisi, 3(6), 103-122.

Çılğın, Z., Bayrakdar, C., Oliphant, J. S., 2014. An example of polygenetic geomorphologic development (Karst-Glacial-Tectonics) on Munzur Mountains: Kepir Cave-Elbaba spring karstic system, Journal of Human Sciences, 11(1), 89-104

Demets, C., Gordon, R. G. &Vogt, P. (1994). Location of the Africa-Australia-India triple junction and motion between the Australian and Indian Plates: Results from an aeromagnetic investigation of the central Indian and Carlsberg ridges. Geophysical Journal International, 119(3), 893-930.

Dewey, J. F. &Şengör, A. M. C. (1979). Aegean and surrounding regions: Complex multiplate and continuum tectonics in a convergent zone. Geological Society of America Bulletin, 90(1), 84-92. doi: 10.1130/0016-7606(1979)90<84:aasrcm>2.0.co;2

Dhont, D., Chorowicz, J. &Luxey, P. (2006). Anatolian escape tectonics driven by Eocene crustal thickening and Neogene-Quaternary extensional collapse in the eastern Mediterranean region. SPECIAL PAPERS-GEOLOGICAL SOCIETY OF AMERICA, 409, 441.

DiBiase, R. A., Whipple, K. X., Heimsath, A. M., Ouimet, W. B., 2010. Landscape form and millennial erosion rates in the San Gabriel Mountains, CA. Earth and Planetary Science Letters, 289(1-2), 134-144.

Dietz, R. S. (1961). Continent and ocean basin evolution by spreading of the sea floor. Nature, 190(4779), 854-857.

Duman, T. Y. &Emre, Ö. (2013). The East Anatolian Fault: geometry, segmentation and jog characteristics. Geological Society, London, Special Publications, 372.

Duvall, A., Kirby, E., Burbank, D., 2004. Tectonic and lithologic controls on bedrock channel profiles and processes in coastal California. Journal of Geophysical Research: Earth Surface, 109(F3).

Egholm, D. L., Nielsen, S. B., Pedersen, V. K., Lesemann, J. E., 2009. Glacial effects limiting mountain height, Nature, 460(7257), 884.

Ekici, T., Alpaslan, M., Parlak, O., Temel, A., 2007. Geochemistry of the Pliocene basalts erupted along the Malatya-Ovacik fault zone (MOFZ), eastern Anatolia, Turkey: Implications for source characteristics and partial melting processes. Chemie der Erde – Geochemistry: 67, 201-212.

Ekström, G., Nettles, M. &Dziewoński, A. M. (2012). The global CMT project 2004–2010: Centroid-moment tensors for 13,017 earthquakes. Physics of the Earth and Planetary Interiors, 200–201(0), 1-9. doi: http://dx.doi.org/10.1016/j.pepi.2012.04.002

Emre, Ö., Duman, T.Y., Kondo, H., Olgun, Ş., Özalp, S., Elmacı, H., 2012a. 1:250000 ölçekli Türkiye Diri Fay Haritası serisi, Erzincan (NJ37-3) Paftası, Seri No 44. Maden Tetkik ve Arama Genel Müdürlüğü, Ankara.

Emre, Ö., Duman, T.Y., Olgun, Ş., Elmacı, H., Özalp, S., 2012b. 1:250000 Türkiye Diri Fay Haritası serisi, Divriği (NJ37-2 Paftası), Seri No: 41. Maden Tetkik ve Arama Genel Müdürlüğü, Ankara.

Emre, Ö., Duman, T.Y., Olgun, Ş., Elmacı, H., Özalp, S., 2012c. 1:250000 Türkiye Diri Fay Haritası serisi, Malatya (NJ37-6 Paftası), Seri No: 41. Maden Tetkik ve Arama Genel Müdürlüğü, Ankara.

England, P., Molnar, P., 1990. Surface uplift, uplift of rocks, and exhumation of rocks. Geology: 18, 1173-1177.

Erinç, S. (1953). Doğu Anadolu Coğrafyası: İstanbul Üniversitesi Coğrafya Enstitüsü.

Faccenna, C., Bellier, O., Martinod, J., Piromallo, C. &Regard, V. (2006). Slab detachment beneath eastern Anatolia: A possible cause for the formation of the North Anatolian fault. Earth and Planetary Science Letters, 242(1-2), 85-97.

Faccenna, C., Becker, T.W., Jolivet, L., Keskin, M., 2013. Mantle convection in the Middle East: Reconciling Afar upwelling, Arabia indentation and Aegean trench rollback. Earth and Planetary Science Letters: 375, 254-269.

Flint, J. J., 1974. Stream gradient as a function of order, magnitude, and discharge. Water Resources Research, 10(5), 969-973.

Gawad, A. E. A., Donia, A. M. A. &Elsaid, M. (2016). Processing of Landsat 8 Imagery and Ground Gamma-Ray Spectrometry for Geologic Mapping and Dose-Rate Assessment, Wadi Diit along the Red Sea Coast, Egypt. Open Journal of Geology, 6(08), 911.

Gordon, R. G. (1998). The plate tectonic approximation: Plate nonrigidity, diffuse plate boundaries, and global plate reconstructions. Annual Review of Earth and Planetary Sciences, 26(1), 615-642.

Görür, N., Şengör, A. M. C., Sakınç, M., AKkok, R., Yiğitbaş, E., Oktay, F. Y. et al .Aykol, A. (1995). Rift formation in the Gökova region, southwest Anatolia: implications for the openning of the Aegean Sea. Geological Magazine, 132, 637-650. doi: 10.1017/S0016756800018884

Guccione, M. J. (2005). Late Pleistocene and Holocene paleoseismology of an intraplate seismic zone in a large alluvial valley, the New Madrid seismic zone, central USA. Tectonophysics, 408(1-4), 237-264.

Gupta, R. P. (2017). *Remote sensing geology*: Springer.

Hack, J. T., 1957. Studies of longitudinal stream profiles in Virginia and Maryland (Vol. 294). US Government Printing Office.

Hack, J.T., 1973. Stream-profile analysis and stream-gradient index. Journal of Research of the US Geological Survey: 1, 421-429.

Hall, J., Aksu, A.E., Elitez, I., Yaltırak, C., Çifçi, G., 2014. The Fethiye-Burdur Fault Zone: A component of upper plate extension of the subduction transform edge propagator fault linking Hellenic and Cyprus Arcs, EasternMediterranean. Tectonophysics: Vol. 635, 80-99

Higgins, M., Schoenbohm, L.M., Brocard, G., Kaymakci, N., Gosse, J.C., Cosca, M.A., 2015. New kinematic and geochronologic evidence for the Quaternary evolution of the Central Anatolian fault zone (CAFZ). Tectonics: 34, 2118-2141.

Higgins, M., Schoenbohm, L. M., Gosse, J. C. 2013. Tectonic Geomorphology and 36Cl geochronology of the Camardi Alluvial Fan Complex, Central Anatolia:

Implications for Neotectonic activity of the Central Anatolian Fault Zone (CAFZ)

Holbrook, J., Schumm, S. A., 1999. Geomorphic and sedimentary response of rivers to tectonic deformation: a brief review and critique of a tool for recognizing subtle epeirogenic deformation in modern and ancient settings. Tectonophysics, 305(1), 287-306.

Howard, A.D., Dietrich, W.E., Seidl, M.A., 1994. Modeling fluvial erosion on regional to continental scales. Journal of Geophysical Research: Solid Earth: 99, 13971-13986.

Hall, J., Aksu, A. E., Elitez, I., Yaltırak, C. &Çifçi, G. (2014). The Fethiye–Burdur Fault Zone: A component of upper plate extension of the subduction transform edge propagator fault linking Hellenic and Cyprus Arcs, Eastern Mediterranean. Tectonophysics, 635(0), 80-99. doi: http://dx.doi.org/10.1016/j.tecto.2014.05.002

Isacks, B., Oliver, J. &Sykes, L. R. (1968). Seismology and the new global tectonics. Journal of Geophysical Research, 73(18), 5855-5899.

Kadinsky-Cade, K. &Barka, A. A. (1989). Effects of restraining bends on the rupture of strike-slip earthquakes. Fault Segmentation and Controls of Rupture Initiation and Termtnation, US Geol. Surv. Open File Rep, 89(315), 181-192.

Kalafat, D., Kekovalı, K., Güneş, Y., Yılmazer, M., Kara, M., Deniz, P. &Berberoğlu, M. (2009). Türkiye ve çevresi faylanma–kaynak parametreleri (MT) kataloğu (1938–2008). Turkey: Boğaziçi Üniversitesi Yayınevi.

Kalafat, D., Kekovalı, K., Kılıç, K., Güney, Yılmazer, M., Ögütçü, Z., Kara, M., Güngör, A., Küsmezer, A., Çomoglu, M., Deniz, P., Berberoglu, A., Kılıçer Bekler, F., Berberoglu, M.,Gümüş, H., Altuncu, S., Suvarıklı, M., Kepekçi, D.,Gül, M., Çok, Ö., Polat, R., 2008. An Earthquake Cataloque for Tukey and Surrounding Area (M>=3.0; 1900-2008,Kandilli Observatory

Kaymakçı, N., İnceöz, M. &Ertepınar, P. (2006). 3-D Architecture and Neogene Evolution of the Malatya Basin: Inferences for the Kinematics fof the Malatya and Ovacık Fault Zone. Turkish Journal of Earth Sciences, 15, 123-154.

Keller, E. A. &Pinter, N. (1996). Active tectonics (Vol. 1338): Prentice Hall Upper Seddle River, NJ, USA.

Kirby, E., Johnson, C., Furlong, K., Heimsath, A., 2007. Transient channel incision along Bolinas Ridge, California: Evidence for differential rock uplift adjacent to the San Andreas fault. Journal of Geophysical Research: Earth Surface: 112, F03S07. DOI:10.1029/2006JF000559.

Kirby, E., Whipple, K. 2001. Quantifying differential rock-uplift rates via stream profile analysis. Geology, 29(5), 415-418.

Kirkbride, M., Mathews, D., 1997. The role of fluvial and glacial erosion in landscape evolution: The Ben Ohau Range, New Zealand: Earth Surface Processes and Landforms , v. 22p. 317–327.

Kirby, E., Whipple, K., 2001. Quantifying differential rock-uplift rates via stream profile analysis. Geology: 29, 415-418.

Kirby, E., Whipple, K.X., Tang, W., Chen, Z., 2003. Distribution of active rock uplift along the eastern margin of the Tibetan Plateau: Inferences from bedrock channel longitudinal profiles. Journal of Geophysical Research: Solid Earth: 108, B4, 2217.DOI:10.1029/2001JB000861.

Koçyiğit, A. &Beyhan, A. (1998). A new intracontinental transcurrent structure: the Central Anatolian Fault Zone, Turkey. Tectonophysics, 284(3-4), 317-336. doi: Doi: 10.1016/s0040-1951(97)00176-5

Koçyiğit, A., Yusufoğlu, H. &Bozkurt, E. (1999). Evidence from the Gediz graben for episodic two-stage extension in western Turkey. Journal of the Geological Society, 156(3), 605-616.

Kürçer, A., Gökten, Y.E., 2012. Paleoseismological three dimensional virtual photography method; a case study: Bağlarkayası-2010 trench, Tuz Gölü Fault Zone, Central Anatolia Turkey. in: Sharkov, E. (Ed.). Tectonics - Recent Advances. InTech: 201-228.

Kürüm, S., Önal, A., Boztuğ, D., Spell, T., Arslan, M., 2008. 40Ar/39Ar age and geochemistry of the post-collisional Miocene Yamadağ volcanics in the Arapkir area (Malatya Province), eastern Anatolia, Turkey. Journal of Asian Earth Sciences: 33, 229-251.

Le Pichon, X. (1968). Sea-floor spreading and continental drift. Journal of Geophysical Research, 73(12), 3661-3697.

Le Pichon, X. &Angelier, J. (1979). The hellenic arc and trench system: A key to the neotectonic evolution of the eastern mediterranean area. Tectonophysics, 60(1-2), 1-42. doi: 10.1016/0040-1951(79)90131-8

Le Pichon, X., Chamot-Rooke, N., Lallemant, S., Noomen, R. &Veis, G. (1995). Geodetic determination of the kinematics of central Greece with respect to Europe: Implications for eastern Mediterranean tectonics. Journal of Geophysical Research: Solid Earth, 100(B7), 12675-12690. doi: 10.1029/95JB00317

Le Pichon, X. &Kreemer, C. (2010). The Miocene-to-Present Kinematic Evolution of the Eastern Mediterranean and Middle East and Its Implications for Dynamics. Annual Review of Earth and Planetary Sciences, 38, 323-351. doi: doi:10.1146/annurev-earth-040809-152419

Li, Q., Liu, M. &Stein, S. (2009). Spatiotemporal complexity of continental intraplate seismicity: insights from geodynamic modeling and implications for seismic hazard estimation. Bulletin of the Seismological Society of America, 99(1), 52-60.

Liu, M., Stein, S. &Wang, H. (2011). 2000 years of migrating earthquakes in North China: How earthquakes in midcontinents differ from those at plate boundaries. Lithosphere, 3(2), 128-132.

McCalpin, J. P. (Ed.). (2009). *Paleoseismology* (2nd ed.). Amsterdam: Academic Press.

McKenzie, D. (1972a). Active Tectonic of the Mediterranean Region. The Geophysical Journal of the Royal Astronomical Society, 30, 109-185.

McKenzie, D. (1978). Active Tectonics of the Alpin-Himalayan Belt: the Aegean Sea and the surrounding regions (Tectonics of the Aegean region). Geophys. J. R. Astron. Soc., 55, 217-254.

McKenzie, D. P. &Parker, R. L. (1967). The North Pacific: an example of tectonics on a sphere. Nature, 216(5122), 1276.

Meghraoui, M., Camelbeeck, T., Vanneste, K., Brondeel, M. &Jongmans, D. (2000). Active faulting and paleoseismology along the Bree Fault, Lower Rhine Graben, Belgium. Journal of Geophysical Research, 105(B6), 13,809-813,841.

Miller, S.R., Baldwin, S.L., Fitzgerald, P.G., 2012. Transient fluvial incision and active surface uplift in the Woodlark Rift of eastern Papua New Guinea. Lithosphere: 4, 131-149.

Molin, P., Pazzaglia, F.J, Dramis, F., 2004. Geomorphic expression of active tectonics in a rapidly-deforming forearc, Sila massif, Calabria, southern Italy. American Journal of Science: 304, 559-589

Morgan, W. J. (1968). Rises, trenches, great faults, and crustal blocks. Journal of Geophysical Research, 73(6), 1959-1982.

Mwaniki, M. W., Moeller, M. S. &Schellmann, G. (2015). A comparison of Landsat 8 (OLI) and Landsat 7 (ETM+) in mapping geology and visualising lineaments: A case study of central region Kenya. The International Archives of Photogrammetry, Remote Sensing and Spatial Information Sciences, 40(7), 897.

Norton, K. P., Abbühl, L. M., Schlunegger, F., 2010. Glacial conditioning as an erosional driving force in the Central Alps. Geology, 38(7), 655-658.

Nyst, M. &Thatcher, W. (2004). New constraints on the active tectonic deformation of the Aegean. Journal of Geophysical Research: Solid Earth, 109(B11).

Ouimet, W. B., Whipple, K. X., Granger, D. E., 2009. Beyond threshold hillslopes: Channel adjustment to base-level fall in tectonically active mountain ranges. Geology, 37(7), 579-582

Özener, H., Arpat, E., Ergintav, S., Doğru, A., Çakmak, R., Turgut, B. &Doğan, U. (2010). Kinematics of the eastern part of the North Anatolian Fault Zone. Journal of Geodynamics, 49(3-4), 141-150. doi: 10.1016/j.jog.2010.01.003

Özeren, M. S. &Holt, W. E. (2010). The dynamics of the eastern Mediterranean and eastern Turkey. Geophysical Journal International, 183(3), 1165-1184.

Özgül, N., Turşucu, A., Özyardımcı, N., Şenol, M., Bingöl, İ., Uysal, Ş., 1981. Munzur Dağlarının Jeolojisi. MTA Temel Araştırmalar Dairesi Proje Raporu, No: 6995, Ankara.

Pérez-Peña, J.V., Azañón, J.M., Azor, A., Tuccimei, P., Della Seta, M., Soligo, M., 2009. Quaternary landscape evolution and erosion rates for an intramontane Neogene basin (Guadix–Baza basin, SE Spain). Geomorphology: 106, 206-218.

Pérez-Peña, J.V., Azor, A., Azañón, J.M., Keller, E.A., 2010. Active tectonics in the Sierra Nevada (Betic Cordillera, SE Spain): Insights from geomorphic indexes and drainage pattern analysis. Geomorphology: 119, 74-87.

Perron, J. T., Royden, L., 2013. An integral approach to bedrock river profile analysis. Earth Surface Processes and Landforms, 38(6), 570-576.

Philip, H., Cisternas, A., Gvishiani, A. &Gorshkov, A. (1989). The Caucasus: an actual example of the initial stages of continental collision. Tectonophysics, 161(1–2), 1-21. doi: http://dx.doi.org/10.1016/0040-1951(89)90297-7

Prasicek, G., Larsen, I. J., Montgomery, D. R., 2015. Tectonic control on the persistence of glacially sculpted topography, Nature communications, 6

Ramsey, C. B. &Lee, S. (2013). Recent and planned developments of the program OxCal. Radiocarbon, 55(2), 720-730.

Reilinger, R., McClusky, S., Vernant, P., Lawrence, S., Ergintav, S., Cakmak, R. et al .Stepanyan, R. (2006). GPS constraints on continental deformation in the Africa-Arabia-Eurasia continental collision zone and implications for the dynamics of plate interactions. Journal of Geophysical Research: Solid Earth, 111(B5).

Reimer, P. J., Bard, E., Bayliss, A., Beck, J. W., Blackwell, P. G., Ramsey, C. B. et al .Friedrich, M. (2013). IntCal13 and Marine13 radiocarbon age calibration curves 0–50,000 years cal BP. Radiocarbon, 55(4), 1869-1887.

Reitman, N. G., Bennett, S. E., Gold, R. D., Briggs, R. W., DuRoss, C. B. 2015. High-resolution trench photomosaics from image-based modeling: Workflow and error analysis. Bulletin of the Seismological Society of America, 105(5), 2354-2366.

Rockwell, T. K., Keller, E. A., Johnson, D. L., 1985. Tectonic geomorphology of alluvial fans and mountain fronts near Ventura, California. In Tectonic

Geomorphology. Proceedings of the 15th Annual Geomorphology Symposium. Allen and Unwin Publishers, Boston, MA (pp. 183-207).

Sağlam Selçuk, A., 2016. Evaluation of the relative tectonic activity in the eastern Lake Van basin, East Turkey. Geomorphology: 270, 9-21

Sanders, C. O. (1989). *Fault segmentation and earthquake occurrence in the strike-slip San Jacinto fault zone, California*.

Sarıkaya, M.A., Yıldırım, C., Çiner, A., 2015. No surface breaking on the Ecemiş Fault, central Turkey, since Late Pleistocene (~64.5 ka); new geomorphic and geochronologic data from cosmogenic dating of offset alluvial fans. Tectonophysics: 649, 33-46.

Sarp, G., 2015. Tectonic controls of the North Anatolian Fault System (NAFS) on the geomorphic evolution of the alluvial fans and fan catchments in Erzincan pull-apart basin; Turkey. Journal of Asian Earth Sciences, 98, 116-125.

Saroglu, F., Emre, O. &Kuscu, I. (1992). Active fault map of Turkey. General Directorate of Mineral Research and Exploration, Ankara.

Schoenbohm, L.M., Whipple, K.X., Burchfiel, B.C., Chen, L., 2004. Geomorphic constraints on surface uplift, exhumation, and plateau growth in the Red River region, Yunnan Province, China. Geological Society of America Bulletin: 116, 895-909

Scholz, C. H., Aviles, C. A. &Wesnousky, S. G. (1986). Scaling differences between large interplate and intraplate earthquakes. Bulletin of the Seismological Society of America, 76(1), 65-70.

Schwanghart, W. &Kuhn, N. J. (2010). TopoToolbox: A set of Matlab functions for topographic analysis. Environmental Modelling & Software, 25(6), 770-781.

Schwanghart, W. &Scherler, D. (2014). TopoToolbox 2-MATLAB-based software for topographic analysis and modeling in Earth surface sciences. Earth Surface Dynamics, 2(1), 1.

Searle, M. P., Chung, S.-L. &Lo, C.-H. (2010). Geological offsets and age constraints along the northern Dead Sea fault, Syria. Journal of the Geological Society, 167(5), 1001-1008.

Seidl, M. A., Dietrich, W. E., 1992. The problem of channel erosion into bedrock. Functional geomorphology, 23, 101-124.

Seyitoğlu, G. &Scott, B. (1991). Late Cenozoic crustal extension and basin formation in west Turkey. Geological Magazine, 128, 155-166.

Seyitoğlu, G. &Scott, B. C. (1992). The Age of the Buyuk Menderes Graben (West Turkey) and Its Tectonic Implications. [Note]. Geological Magazine, 129(2), 239-242.

Shaw, B. &Jackson, J. (2010). Earthquake mechanisms and active tectonics of the Hellenic subduction zone. Geophysical Journal International, 181(2), 966-984.

Silva, P.G., Goy, J.L., Zazo, C., Bardají, T., 2003. Fault-generated mountain fronts in southeast Spain: geomorphologic assessment of tectonic and seismic activity. Geomorphology: 50, 203-225.

Snyder, N.P., Whipple, K.X., Tucker, G.E., Merritts, D.J., 2000. Landscape response to tectonic forcing: Digital elevation model analysis of stream profiles in the Mendocino triple junction region, northern California. Geological Society of America Bulletin: 112, 1250-1263.

Sternai, P., Herman, F., Fox, M. R., Castelltort, S., 2011. Hypsometric analysis to identify spatially variable glacial erosion, Journal of Geophysical Research: Earth Surface, 116(F3).

Stock, J. D., and Montgomery, D. R., 1999. Geologic constraints on bedrock river incision using the stream power law. Journal of Geophysical Research: Solid Earth, 104(B3), 4983-4993

Storti, F., Holdsworth, R. E. &Salvini, F. (2003). Intraplate strike-slip deformation belts. Geological Society, London, Special Publications, 210(1), 1-14.

Strahler, A.N., 1952. Hypsometric (Area-Altitude) Analysis Of Erosional Topography. Geological Society of America Bulletin: 63, 1117-1142.

Şaroglu, F., Emre, Ö., Kuscu, I., 1992. Active fault map of Turkey, General Directorate of Mineral Research and Exploration. Ankara

Şengör, A. M. C. (1979). The North Anatolian transform fault; its age, offset and tectonic significance. Journal of the Geological Society of London, 136, Part 3, 269-282.

Şengör, A. M. C. (1980). *Türkiye'nin neotektoniğinin esasları (Principles of the Neotectonism of Turkey)* (Vol. 2). Ankara: Türkiye Jeoloji Kurumu Konferans Serisi.

Şengör, A. M. C. (1987). Cross-faults and differential stretching of hanging walls in regions of low-angle normal faulting: examples from western Turkey. Geological Society, London, Special Publications, 28(1), 575-589.

Şengör, A. M. C., Görür, N. &Şaroğlu, F. (1985a). Strike-slip faulting and related basin formation in zones of tectonic escape: Turkey as a case study.

Şengör, A. M. C., Görür, N. &Şaroğlu, F. (1985b). Strike-slip faulting and related basin formation in zones of tectonic escape: Turkey as a case study. In K. T. Biddle &N. Christie-Blick (Eds.), *Strike-slip Deformation, Basin Formation, and Sedimentation, Soc. Econ. Paleontol. Spec. Publ.* (Vol. 37, pp. 227-264). Oklahoma: Society of Economic Paleontologists and Mineralogists.

Şengör, A. M. C., Grall, C., İmren, C., Le Pichon, X., Görür, N., Henry, P. et al .Siyako, M. (2014). The geometry of the North Anatolian transform fault in the Sea of Marmara and its temporal evolution: implications for the development of intracontinental transform faults1. Canadian Journal of Earth Sciences, 51(3), 222-242. doi: 10.1139/cjes-2013-0160

Şengör, A. M. C., Özeren, M. S., Keskin, M., Sakınç, M., ÖzbakIr, A. D. &Kayan, I. (2008a). Eastern Turkish high plateau as a small Turkic-type orogen: Implications for post-collisional crust-forming processes in Turkic-type orogens. Earth-Science Reviews, 90(1-2), 1-48. doi: DOI: 10.1016/j.earscirev.2008.05.002

Şengör, A. M. C., Özeren, M. S., Keskin, M., Sakınç, M., Özbakır, A. D. &Kayan, I. (2008b). Eastern Turkish high plateau as a small Turkic-type orogen: Implications for post-collisional crust-forming processes in Turkic-type orogens. Earth-Science Reviews, 90(1-2), 1-48.

Şengör, A. M. C., Tüysüz, O., Imren, C., Sakınç, M., Eyidoğan, H., Görür, N. et al .Rangin, C. (2005). The North Anatolian fault: A new look. Annu. Rev. Earth Planet. Sci., 33, 37-112.

Şengör, A. M. C. &Yılmaz, Y. (1981). Tethyan evolution of Turkey; a plate tectonic approach. Tectonophysics, 75(3-4), 181-241.

Şengör, A. M. C. l. (1990). Plate tectonics and orogenic research after 25 years: a Tethyan perspective. Earth-Science Reviews, 27(1-2), 1-201.

Tapponnier, P., Peltzer, G., Le Dain, A. Y., Armijo, R. &Cobbold, P. (1982). Propagating extrusion tectonics in Asia: New insights from simple experiments with plasticine. Geology, 10(12), 611-616.

Tarhan, N., 2008. Geological map of Turkey at 1:100000 scale, no. 68, Erzincan-I43. Mineral Research and Exploration Institute (MTA) of Turkey publications (in Turkish with English abstract).

Tarı, U., Tüysüz, O., 2016. The effects of the North Anatolian Fault on the geomorphology in the Eastern Marmara Region, Northwestern Turkey. Geodinamica Acta: 28, 139-159.

Tatar, O., Poyraz, F., Gürsoy, H., Cakir, Z., Ergintav, S., Akpınar, Z. et al .Hastaoğlu, K. Ö. (2012). Crustal deformation and kinematics of the Eastern Part of the North Anatolian Fault Zone (Turkey) from GPS measurements. Tectonophysics, 518, 55-62.

Topal, S., Keller, E., Bufe, A., Koçyiğit, A., 2016. Tectonic geomorphology of a large normal fault: Akşehir fault, SW Turkey. Geomorphology, 259, 55-69

Tuttle, M. P., Schweig, E. S., Sims, J. D., Lafferty, R. H., Wolf, L. W. &Haynes, M. L. (2002). The earthquake potential of the New Madrid seismic zone. Bulletin of the Seismological Society of America, 92(6), 2080-2089.

Walcott, R.C., Summerfield, M.A., 2008. Scale dependence of hypsometric integrals: An analysis of southeast African basins. Geomorphology: 96, 174-186.

Westaway, R. &Arger, J. (2001). Kinematics of the Malatya–Ovacık Fault Zone. Geodinamica Acta, 14(1–3), 103-131. doi: http://dx.doi.org/10.1016/S0985-3111(00)01058-5

Westaway, R., Demir, T. &Seyrek, A. (2008). Geometry of the Turkey-Arabia and Africa-Arabia plate boundaries in the latest Miocene to Mid-Pliocene: the role of the Malatya-Ovacık Fault Zone in eastern Turkey. eEarth, 3(1), 27-35. doi: 10.5194/ee-3-27-2008

Westaway, R., Demir, T., Seyrek, A. &Beck, A. (2006). Kinematics of active left-lateral faulting in SE Turkey from offset Pleistocene river gorges: improved constraint on the rate and history of relative motion between the Turkish and Arabian plates. Journal of the Geological Society, 163(1), 149-164.

Whipple, K. X., 2004. Bedrock rivers and the geomorphology of active orogens. Annu. Rev. Earth Planet. Sci., 32, 151-185.

Whipple, K.X., Tucker, G.E., 1999. Dynamics of the stream-power river incision model: Implications for height limits of mountain ranges, landscape response timescales, and research needs. Journal of Geophysical Research: Solid Earth: 104, 17661-17674.

Whitney, B.B., Hengesh, J.V., 2015. Geomorphological evidence of neotectonic deformation in the Carnarvon Basin, Western Australia. Geomorphology: 228, 579-596.

Whittaker, A. C., 2012. How do landscapes record tectonics and climate?. Lithosphere, 4(2), 160-164.

Wobus, C., Whipple, K. X., Kirby, E., Snyder, N., Johnson, J., Spyropolou, K., Crosby B., Sheehan, D., 2006. Tectonics from topography: Procedures, promise, and pitfalls. Special papers-geological society of america (editor Willett, S. D), 398, 55.

Wiens, D. A., Stein, S., Demets, C., Gordon, R. G. &Stein, C. (1986). Plate tectonic models for Indian Ocean “intraplate” deformation. Tectonophysics, 132(1-3), 37-48.

Wilson, J. T. (1965). A new class of faults and their bearing on continental drift. Nature, 207(4995), 343.

Yazici, M., Zabci, C., Sançar, T., Sunal, G. &Natalin, B. A. (2016, 2016). Preliminary results on the tectonic activity of the Ovacik Fault (Malatya-Ovacik Fault Zone, Turkey): Implications of the morphometric analyses.

Yeşilyurt, S., Akçar, N., Doğan, U., Yavuz, V., Ivy-Ochs, S., Vockenhuber, C., Schluchter, C., 2015. Extensive ice fields in eastern Turkey during the Last

Glacial Maximum, paper presented at INQUA XIX, Nagoya, Japan, pp. T00993.

Yıldırım, C., 2014. Relative tectonic activity assessment of the Tuz Gölü Fault Zone; Central Anatolia, Turkey. Tectonophysics: 630, 183-192

Yıldırım, C., Sarıkaya, M. A. &Ciner, A. (2016). Late Pleistocene intraplate extension of the Central Anatolian Plateau, Turkey: Inferences from cosmogenic exposure dating of alluvial fan, landslide, and moraine surfaces along the Ecemiş Fault Zone. Tectonics, 35(6), 1446-1464.

Zabcı, C., Sançar, T., Tikhomirov, D., Ivy-Ochs, S., Vockenhuber, C., Friedrich, A. M. et al .Akçar, N. (2017, 2017). Geodynamics, active deformation, GPS, active fault, paleoseismology.

Zoback, M. D., Hamilton, R. M., Crone, A. J., Russ, D. P., McKeown, F. A. &Brockman, S. R. (1980). Recurrent intraplate tectonism in the New Madrid seismic zone. Science, 209(4460), 971-976.

APPENDICES

APPENDIX A1: The Geological Map along the Ovacık Fault.

APPENDIX A2: The Geological Map of the south-western part of the Ovacık Fault.

CURRICULUM VITAE

Name Surname **: Müge Yazıcı**

Place and Date of Birth **: Samsun, 29.10.1991**

E-Mail **: yazicimug@itu.edu.tr**

Education

2005-2009 Yeşilkent Anadolu Lisesi, Samsun (High School)

2010-2015 İstanbul Technical University, Geological Engineering (BSc)

2015- Istanbul Technical University, Graduate School of Science Engineering and Technology (MSc continue)

Professional Experience

2016-2017 Visiting Student, Ludwig Maximillians Universitat München (6 months)

2017- Research assistant, Istanbul Technical University, Faculty of Mines

Experience in Education

2017 - Assistant, Istanbul Technical University, Department of Geology, Field Geology Course, Gökçeada camp

2017 - Teaching Assistant (General Geology, Structural Geology, Tectonics, Field Geology, Neotectonics)

Field Experience

2011 Internship, Burdur-Fethiye, Field Study (July, 2011)

2013 Field Geology camp, Nallıhan, Ankara (June)

2014-2015 Field Study, Strandja Mountains (BSc)

2014 Internship, Hasan Mountain, Field Study, volcanology (July-August, 2014)

2015 Researcher, Malatya, Paleoseismology and Tectonic Geomorphology (July-August, 2015)

2016 Researcher, Paleoseismology and Tectonic Geomorphology, Malatya – Erzincan, Malatya-Ovacık Fault Zone, MSc Thesis (June-September, 2016)

2017 Researcher, Australian Alps Field Trip, (October 2017)

2017 Researcher, Paleoseismology and Tectonic Geomorphology, Muğla, Muğla Fault (July- 2017)

Membership in Societies

2015-2017 American Geophysical Union (Student member)

2015-2017 Geological Society of America (Student member)

2015-2017 Seismological Society of America (Student member)

2010-present Türkiye Jeoloji Mühendisleri Odası (Chamber of Geological Engineers of Turkey) (Student member)

Honors and Awards

1. High Honor List, Istanbul Technical University, Department of Geology, BSc program, 2013-2014 Spring
2. 1nd price, Graduation at ITU, Geology, BSc degree (2015).
3. 3 nd Oral presentation, Active Tectonic Research Group of Turkey (ATAG), (October 2017)

Languages

Turkish, English

Projects

2014-2015 Schollarship researcher, Ovacık Fayı (Malatya-Ovacık Fay Zonu) üzerinde morfokronolojik ve paleosismolojik çalışmalar: Jeolojik kayma hızı ve eski deprem tarihçesinin araştırılması (The morhochronology and paleoseismology of the Ovacık Fault (Malatya-Ovacık Fault Zone, Turkey): The study of the geologic slip-rate and the paleoseismic history, TÜBİTAK 114Y227.

2015-2017 Researcher, Ovacık Fayı (Malatya-Ovacık Fay Zonu) üzerinde morfokronolojik ve paleosismolojik çalışmalar: Jeolojik kayma hızı ve eski deprem tarihçesinin araştırılması (The morhochronology and paleoseismology of the Ovacık Fault (Malatya-Ovacık Fault Zone, Turkey): The study of the geologic slip-rate and the paleoseismic history, TÜBİTAK 114Y227.

2017 – Researcher, Büyük doğrultu atımlı fayların zamansal ve mekansal atım tarihçesinin araştırılması: Kuzey Anadolu ve Ovacık faylarının morfokronoloji tmelli kayma hızları (Investigaiton of history of the temporal and spatial offsets along the big strike-slip faults: Slip rates of the North Anatolian and Ovacık Faults based on morphochronology, BAP, ITU.

Publications – International peer reviewed papers in preparation

- Zabcı, C., Sançar, T., Tikhomirov, D., Ivy-Ochs, S., Vockenhuber, C., Friedrich, M.A., **Yazıcı, M**., Akçar, N. Cosmogenic 36Cl geochronology of offset terraces along the Ovacık Fault (Turkey): Implications for the intraplate deformation of Anatolia (Submitted to Tectoncis).
- **Yazıcı, M.,** Zabcı, C., Sançar, T., Natalin, B. Morphological response to the internal deformation of the eastern Anatolia (Turkey): The Ovacık Fault and surrounding region as a case study (in preparation)

Publications – International abstracts

- Zabcı, C., Sançar, T., Tikhomirov, D., Ivy-Ochs, S., Vockenhuber, C., **Yazıcı, M**., Natalin, B., Akyuz, H.S., Akçar, N. 2015. Understanding the intraplate deformation of the Anatolian Scholle: Insights from the study of the Ovacık Fault (Eastern Turkey). *EGU General Assembly Conference Abstracts. Vol. 17.*
- **Yazıcı, M**., Natalin, B. Structural geology and sedimentology of the Sermat Quartzites, Strandja Massif, NW Turkey. 2015. *EGU General Assembly Conference Abstracts. Vol. 17.*
- **Yazici, M**., Zabci, C., Sançar, T., Sunal, G., Natalin, B. 2016. Preliminary results on the tectonic activity of the Ovacik Fault (Malatya-Ovacik Fault Zone, Turkey): Implications of the morphometric analyses. *EGU General Assembly Conference Abstracts. Vol. 18.*
- Sançar, T., Zabci, C., Akçar, N., Karabacak, V., **Yazici, M**., Akyüz, H. S., Önal, A. Ö., Ivy-Ochs, S., Christly, M., Vockenhuber, C. 2016. Preliminary results on the deformation rates of the Malatya Fault (Malatya-Ovacik Fault Zone, Turkey). *EGU General Assembly Conference Abstracts. Vol. 18*.
- Sançar, T., Zabci, C., Karabacak, V., **Yazici, M**., Akyüz, H. S. 2017. Paleoseismic history of the Malatya Fault (Malatya-Ovacik Fault Zone, Eastern Anatolian scholle) for the last 10 ka. *EGU General Assembly Conference Abstracts. Vol. 19.*
- Zabcı, C., Sançar T., Tikhomirov, D., Ivy-Ochs, S., Vockenhuber, C., Friedrich A., **Yazici, M.,** Akçar, N. Cosmogenic 36Cl Geochronology of Offset Terraces Along The Ovacık Fault (Malatya-Ovacık Fault Zone, Eastern Turkey): Implications for the Intra-plate Deformation of the Anatolian Scholle. 2017. *The International Conference on Astronomy and Geophysics, Ulaanbaata, Mongolia*.
- **Yazici, M**., Zabcı, C., Natalin, B., Akyüz, H.S., Paleoseismology of the Ovacık Fault (OF): Timing of palaeoevents and implications for the internal deformation of Anatolia, 2017, *5th International Colloquium Historical Earthquakes, Paleoseismology, Neotectonics and Seismic Hazard*. Hannover, Germany

Publications – National abstracts

- **Yazıcı M**., Zabcı, C., Sançar, T., Natalin, B. 2016. Ovacık Fayı'nın tektonik jeomorfolojisi: Jeomorfik indisler kullanılarak deformasyonun mekansal analizi. *ATAG-20*, Denizli, Vol:20
- Zabcı C., Sançar, T., **Yazıcı, M**., Tikhomirov, D., Ivy-Ochs, S., Vockenhuber, C., Akçar, N. 2016. Ovacık fayı'nın morfokronoloji temelli kayma hızı: Anadolu'nun ic deformastonu hakkında düşünceler. *ATAG - 20,* Denizli, Vol:20
- Kırkan, E., Akyuz, H.S., Zabcı, C., Basmenji, M., Akyüz, A.D., **Yazıcı, M**., Aksoy, E.M., Uçarkuş, G., Yakupoğlu, N. 2017. Milas Fayı'nın paleosismolojik, morfotektonik ve depremsellik özelliklerine dair ilk bulgular. *ATAG- 21,* Afyon, Vol.21
- Basmenji, M., Akyüz, H.S., Kırkan, E., Aksoy, E.M., Uçarkus, G., Zabcı, C., Yakupoğlu, N., Akyüz, A.D., **Yazici, M**. 2017. Yatağan Fayının Jeomorfolojik ve Paleosismolojik özellikleri hakkında ilk bulgular, *ATAG- 21,* Afyon, Vol: 21
- **Yazıcı, M**., Zabcı, C., Natalin, B., Sançar, T., Akyuz, H.S. 2017. Anadolu'nun iç deformasyon ürünü'Ovacık Fayı' : Paleosismoloji ve tektonik jeomorfolojisi hakkında bulgular. *ATAG-21,* Afyon, Vol:2